UC Irvine

UC Irvine Electronic Theses and Dissertations

Title

Glutamine deficiency in driving cancer development and modulating therapeutic response

Permalink

https://escholarship.org/uc/item/1zd6526c

Author

Tran, Thai Quan

Publication Date

2019

Peer reviewed|Thesis/dissertation

eScholarship.org Powered by the California Digital Library
University of California

UNIVERSITY OF CALIFORNIA,

IRVINE

Glutamine deficiency in driving cancer development and modulating therapeutic response

DISSERTATION

submitted in partial satisfaction of the requirements

for the degree of

DOCTOR OF PHILOSOPHY

in Biological Sciences

by

Thai Quan Tran

Dissertation committee:

Professor Mei Kong, Chair

Professor David A. Fruman

Professor Marian L. Waterman

2019

Portions of Chapter 2 © 2016 Nature Publishing Group

Portions of Chapter 3 © 2017 PLOS

Portions of Chapter 5 © 2017 AACR publication

All other material © 2019 Thai Quan Tran

DEDICATION

This dissertation is dedicated to my parents, Trinh and Nhung.

From whom I learn the power of sacrifice, perseverance, and understanding.

To my best friend, Nam

From whom I learn the value of service and humility.

To my friends, my mentors, and my critics.

From whom I learn to “differentiate” into myself.

TABLE OF CONTENTS

LIST OF FIGURES

ACKNOWLEDGEMENTS

This journey would not be possible with the support of so many people near and far. I would like to thank all friends and family members for believing in me and my pursuit of this career.

I would like to express my deepest gratitude to my adviser Mei Kong. Mei is always a caring and down-to-earth person inside and outside the lab. Her gentle yet potent guidance has helped me to realize my potentials, overcome my shortcomings, and learn to look at everything with an open mind from a big-picture perspective. I truly appreciate Mei for giving me the freedom to explore new ideas and believing in my capacities in pursuing my research. After almost five years in her lab, I am confident that I will head into the next phase of my life as a better scientist and a more complete person.

I have been very fortunate to have amazing lab mates around me. I would like to thank all the members of the Kong lab: Xazmin, Jenny, Mike, Eric, Mari, Kim, Min, Ying for creating a supportive and collaborative environment. We are always there for each other during time of need. I especially thank my lab neighbor Xazmin for her wittiness, her excessive decorations for my birthdays throughout the years, and her genuine friendship. I want to thank Eric for helping me with my manuscript and having confidence in my research. I also want to thank Ying for showing me how to persevere and to take small steps one at a time.

I would like to thank all my committee members: Drs. David Fruman and Marian Waterman at UCI and Drs. Jeremy Stark and Timothy O'Connor at City of Hope for their continuous support and guidance. I also appreciate the insights and advices from Drs. Christopher Hughes and Wenqi Wang who served on my advancement committee. I owe a great debt of gratitude to Dr. Fruman who has accepted me to work in his lab as a volunteer before graduate school and

introduced me to the world of cancer research. I am also grateful to Dr. Waterman for her support of my thesis project and for her immense knowledge and kindness.

Lastly, I want to thank the talented and diverse group of people that I have come across at UCI and City of Hope. These remarkable individuals have always inspired me to strive harder and to be better, not only in the pursuit of science but also in service to humanity.

CURRICULUM VITAE

Thai Q Tran

Education

UNIVERSITY OF CALIFORNIA, IRVINE Irvine, CA
Ph.D. in Biological Science 2019

UNIVERSITY OF CALIFORNIA, LOS ANGELES Los Angeles, CA
B.S. in Biochemistry 2012

Experience

City of Hope National Medical Center Duarte, CA 2013 to 2018
University of California, Irvine Irvine, CA 2018-Present
Graduate Researcher with Dr. Mei Kong

- Executed an independent project to investigate the impacts of metabolic stress on colon cancer development using 3D intestinal organoids and mouse models.
- Investigated how metabolic microenvironment alters epigenetics and cellular differentiation in colon cancer. Identified a new therapeutic direction to inhibit tumor growth using metabolite supplementation.
- Identified the crosstalk between cancer metabolism and DNA damage response leading to the identification of a novel drug synergy between glutaminase inhibitor and alkylating agents.
- Performed and validated drug screening for a novel glutaminase enzyme inhibitor.

University of California, Irvine Irvine, CA
Research assistant with Dr. David Fruman 2012 – 2013

- Examined the molecular mechanism of combination therapy of PI3K inhibitor and HDAC inhibitor for the treatment of lymphoblastic leukemia.
- Assisted with transgenic mouse model projects and performed genotyping in an immunology lab.

University of California, Los Angeles Los Angeles, CA
Researcher assistant with Dr. Juli Feigon 2011 - 2012

- Conducted and optimized a complete project in a structural biology laboratory involved in protein expression and purification of different human telomerase subunits.
- Performed biochemical assays and kinetic studies of telomerase and RNA complex.

Publications

Tran TQ, Habowski NA, Li H, Hanse EA, Gabra MB, Yang Y, Lowman XH, Ooi AM, Edwards RA, Waterman ML, Kong M. Metabolic control of Wnt signaling and cellular differentiation in colorectal cancer. Submitted.

Tran TQ, Ishak Gabra MB, Lowman XH, Yang Y, Reid MA, et al. Glutamine deficiency induces DNA alkylation damage and sensitizes cancer cells to alkylating agents through inhibition of ALKBH enzymes. PLOS Biology. 15(11): e2002810, Nov 2017 (Impact Factor-9.1)

Tran TQ, Lowman XH, Reid MA, Mendez C, Pan, M, Yang Y, and Kong M. Tumor-associated mutant p53 promotes cancer cell survival upon glutamine deprivation through p21 induction. Oncogene. doi: 10.1038/onc.2016.360, Oct 2016 (Impact Factor – 7.5)

Tran TQ, Kong M. Molecular Pathways: Metabolic control of histone methylation and gene expression in cancer. Clinical Cancer Research. 10.1158/1078-0432. CCR-16-2506, April 12 2017 (Impact Factor – 10.1)

Yang Y, Ishak Gabra MB, Hanse EA, Lowman XH, **Tran TQ**, Li H, Milman N, Liu J, Reid MA, Locasale JW, Gil Z and Kong M. MiR-135 suppresses glycolysis and promotes pancreatic cancer cell adaptation to metabolic stress by targeting phosphofructokinase-1. Nature Communication. 10-809, Feb 2019

Lowman XH, Hanse EA, Yang Y, Ishak Gabra MB, **Tran QT**, Li H, Kong M. p53 promotes cancer cell adaptation to glutamine deprivation by upregulating Slc7a3 to increase arginine uptake. Cell Report. 26, 3051–3060, Feb 2019.

Ishak Gabra MB, Ying Yang, Lowman XH, Reid MA, **Tran TQ** and Kong M. IKKβ activates p53 to promote cancer cell adaptation to glutamine deprivation. Oncogenesis. doi: 10.1038/s41389-018-0104-0, Nov 2018

Reid MA, Lowman XH, Pan M, **Tran TQ**, Warmoes MO, Ishak Gabra MB, Yang Y, Locasale JW, and Kong M. IKK promotes metabolic adaptation to glutamine deprivation via phosphorylation and inhibition of PFKFB3. Genes and Development. 10.1101/gad.287235.116, Sep 2016

Pan M, Reid MA, Lowman XH, Kulkarni RP, **Tran TQ**, Liu X, Yang Y, Hernandez-Davies JE, Rosales KK, Li H, Hugo W, Song C, Lo RS, Locasale JW, and Kong M. Regional glutamine deficiency in tumours promotes dedifferentiation through inhibition of histone demethylation. Nature Cell Biology 18, 1090-1101, Aug 2016

Mohanty S, Mohanty A, Sandoval N, **Tran, TQ**, Bedell V, Wu, J, Ngo, VN. Cyclin D1 depletion induces DNA damage in mantle cell lymphoma lines. Leukemia & Lymphoma. 1-13. doi: 10.1080/10428194.2016.1198958, Jun 2016

Rosales KR, Reid M, Yang Y, **Tran TQ**, Wang W, Lowman X, Pan M and Kong M. TIPRL inhibits protein phosphatase 4 activity and promotes H2AX phosphorylation in the DNA Damage Response. PLOS ONE. 10(12): e0145938, Dec 2015

Hernandez JE, **Tran TQ**, Reid MA, Rosales KR, Lowman XH, Pan M, Moriceau G, Yang Y, Wu J, Lo RS, and Kong M. Vemurafenib resistance reprograms melanoma cells towards glutamine dependence. Journal of Translational Medicine. 13:210, Mar 2015

Leadership experience

City of Hope National Medical Center Duarte, CA

Teaching Fellow – Fundamentals of Scientific Research graduate course Spring 2016

- Delivered a lecture pertaining to cancer metabolism, designed and graded written assignments.

Research mentor – Tumor Metabolism Laboratory 2014-2018

- Trained two undergraduate students and four graduate students on lab techniques.
- Designed and supervised research projects for the students.

Chair – Graduate Student Forum Committee 2017 -2018

- Invited speakers and organized monthly student seminars.

University of California, Irvine Irvine, CA

Research mentor – Tumor Metabolism Laboratory 2018 - Present

- Designed and supervised research projects for one graduate student and one undergraduate student

Awards

- H.N. & Frances Berger Fellowship, 2013-2014
- City of Hope Travel Grant
    - Keystone symposium, Integrating Metabolism and Tumor Biology, Vancouver, Canada, 2015
    - Keystone symposium, Understanding Tumor Metabolism, Banff, Canada, 2016
- Teaching Assistant Award, 2016
- First Place Poster Award, RSO Advance Conference, CA, 2016
- First Place Poster Award, Biomedical Research Graduate Student Symposium, City of Hope, 2017

ABSTRACT OF THE DISSERTATION

Glutamine deficiency in driving cancer development and modulating therapeutic response

By

Thai Quan Tran

Doctor of Philosophy in Biological Sciences

University of California, Irvine, 2019

Professor Mei Kong, Chair

Metabolic reprogramming is a hallmark of cancer that plays an essential role in tumor initiation and progression. Glutamine metabolism, due to its diverse role in central metabolism, signaling and epigenetics, has become the forefront of cancer metabolism research. In addition to the Warburg's effect, emerging evidence reveals that the "glutamine addiction" in human tumors play an important role in both tumorigenesis and therapeutic response. With enhanced glutamine uptake and poor vascularization at the tumor sites, it appears that most solid tumors will experience some degree of glutamine deficiency similar to the low oxygen conditions or hypoxia. While the role hypoxia in tumor biology is well established, the impact of intratumoral glutamine deficiency on cancer progression and therapeutic response remains largely unknown. This dissertation will explore potential effects of glutamine deficiency on various cellular processes in malignant cells including DNA damage response pathway, epigenetic reprogramming, oncogenic signaling, and drug response.

In chapter 1, I summarize recent progress in understanding the glutamine addiction in cancer and highlight clinical opportunities in targeting glutamine metabolism.

In chapter 2, we investigate the role of tumor-associated mutant p53 in cellular response to glutamine deprivation. We demonstrate that mutant p53 plays a major role in cellular adaptation to glutamine deprivation through the upregulation of pro-survival genes but not pro-death genes.

In chapter 3, we examine the crosstalk between glutamine metabolism and DNA damage repair pathway. We provide mechanistic insights by which glutamine deficiency inhibits the DNA repair activity of the *ALKBH* enzymes, leading to an accumulation of DNA alkylation damage and thereby increasing cellular sensitivity to alkylating agents.

In chapter 4, we study the effect of glutamine metabolism on oncogenic Wnt signaling pathway and colorectal cancer development. We reveal that glutamine/alpha-ketoglutarate axis through epigenetic modulations is a critical regulator of Wnt signaling and cellular differentiation in colon cancer. We further explore the potential impact of glutamine starvation on the adeno-carcinoma transition in colon cancer progression and the therapeutic potential of alpha ketoglutarate supplementation in colon cancer treatment.

In chapter 5, I discuss recent progress on the crosstalk between metabolism and epigenetic regulation in cancer. I will further discuss remaining questions, future directions and clinical implications derived from these findings.

Chapter 1

Introduction

Glutamine metabolism in cancer: glutamine addiction, survival strategy and therapeutic opportunities

Glutamine metabolism

Glutamine is one of the most abundant amino acids in the human body, with glutamine levels in circulation sustained at around 0.5 mM (1). Glutamine serves as a main source of carbon and nitrogen for the biosynthesis of different macromolecules, including amino acids, nucleotides, proteins and the antioxidant glutathione (2). Furthermore, glutamine metabolism participates in different biochemical processes including ammoniagenesis in the kidney, ammonia-trapping pathways, and gluconeogenesis in the liver, and glutamate production in the brain (3-6). Notably, glutamine serves as a critical oxidative fuel in fast proliferating cells, including lymphocytes of the immune system and enterocytes of intestinal tracts. While glutamine is a non-essential amino acid that can be synthesized by mammalian cells, certain fast-growing cells require excessive exogenous glutamine supply from the environment that supports the elevated bioenergetic demands (7). Furthermore, glutamine can be consumed rapidly upon a variety of stresses, including injury, infection, post-surgery, chemotherapy treatment, and infection; suggesting that glutamine can be an essential amino under certain physiological conditions (8, 9). For example, lymphocytes, once activated in response to infection, rapidly uptake exogenous protein to support rapid proliferation (8, 10). Therefore, glutamine is a vital and versatile nutrient that supports many biological and biochemical processes in the body, especially under stress. Furthermore, emerging evidence suggests that elevated glutamine dependency is also a feature of metabolic alterations in malignant cells (11, 12). Enhanced glutamine uptake and metabolism have been shown to play a critical role in the growth and survival of cancer cells, thereby directly contributing to tumor development and therapeutic response (13).

Altered glutamine metabolism in cancer

Metabolic reprogramming is an emerging hallmark of cancer. Many oncogenic signaling pathways alter cellular metabolism to support tumor initiation and progression. Unlike quiescent cells, cancer cells favor aerobic glycolysis to sustain uncontrolled proliferation (14). In particular, glucose is rapidly consumed by cancer cells at a surprisingly high rate, and the majority of glucose is converted into lactate despite available oxygen. This phenomenon is also known as the Warburg effect, which is believed to provide rapid energy generation and support macromolecule biosynthesis for cancer cells (15). Under this metabolic alteration, cancer cells often become dependent on glutamine as a major carbon and nitrogen source to generate new building blocks and maintain cell survival (16) (Figure 1).

In cancer cells, glutamine can be used to replenish the truncated the tricarboxylic acid (TCA) cycle, which is a result of the Warburg effect (17). Intracellular glutamine can be converted into glutamate by glutaminase enzymes. Subsequently, glutamate can be catabolized into TCA cycle intermediate alpha-ketoglutarate (aKG), which can be fed into the TCA cycle for energy production and other anabolic reactions (18). Thus, glutamine serves as a critical oxidative fuel in cancer cells. Moreover, glutamine also serves as a precursor for the biosynthesis of different amino acids and nucleotides to support biosynthetic requirements in cancer cells (19). In addition, glutamine also plays an important role in redox homeostasis by supporting the production of an important antioxidant, glutathione, that can protect cancer cells from reactive oxygen species (20, 21) (Figure 1). In addition to cellular metabolism, emerging evidence also suggests that intracellular glutamine levels contributes to many biological processes including the regulation of mTOR signaling, autophagy and epigenetics (22). Moreover, glutamine supports the biosynthesis of uridine diphosphate N-acetylglucosamine (UDP-GlcNAc), which

plays an important role in proper protein localization and folding in cells (23, 24). Therefore, glutamine is a vital nutrient that participates in many different cellular and metabolic processes, making it an "essential" amino acid in malignant cells.

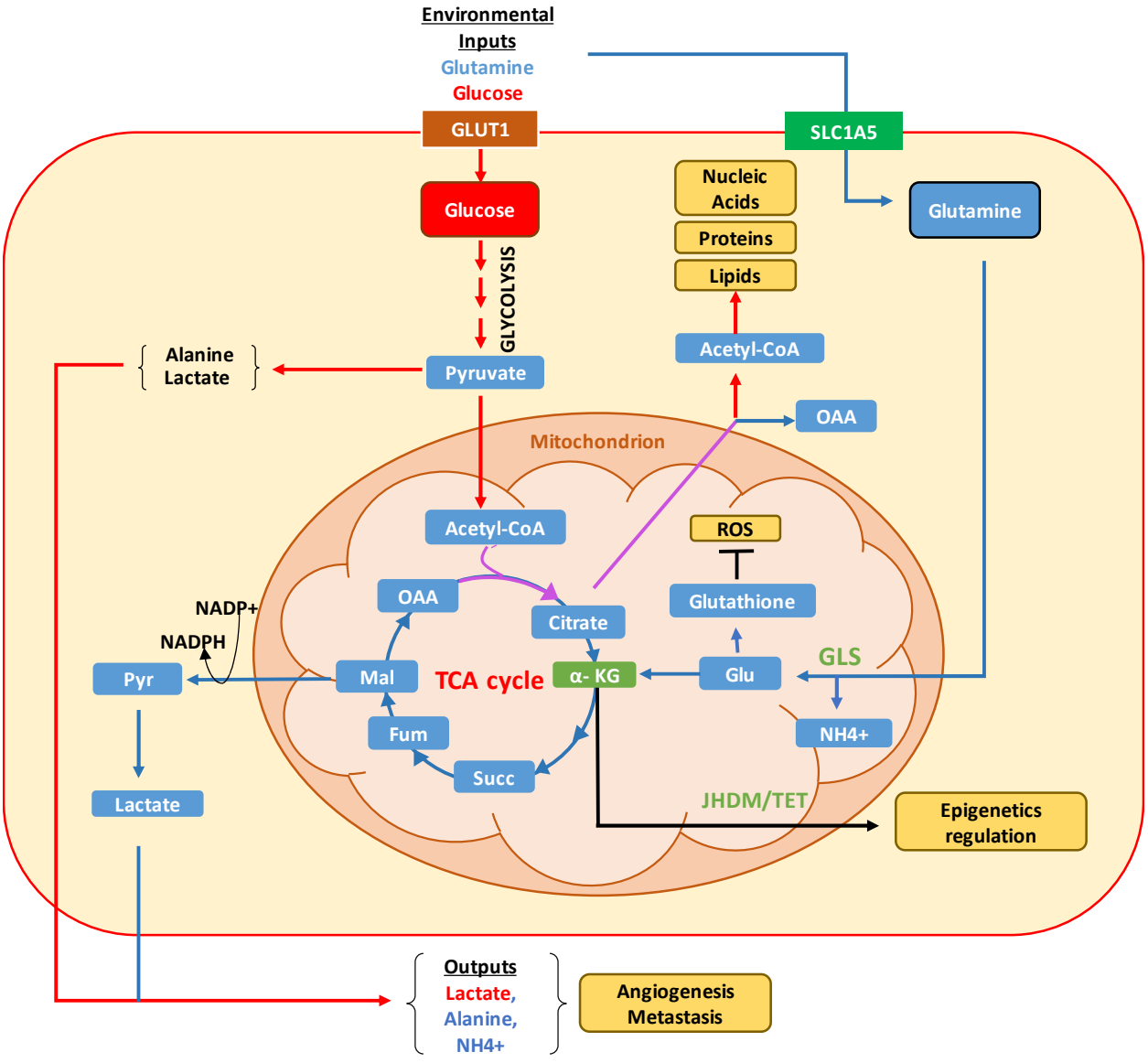

Figure 1: The crosstalk between glucose metabolism and glutamine metabolism in cancer cells. Under the Warburg effect, cancer cells uptake glucose at a surprisingly high rate for glycolysis. However, cancer cells convert glucose to pyruvate, and subsequently, to lactate rather

than oxidizing it completely despite available oxygen. Lactate in cancer cells is often secreted into the tumor microenvironment to facilitate metastasis and angiogenesis (red arrows). Glutamine is converted to glutamate by the metabolic enzyme glutaminase. Glutamate can be subsequently converted to aKG to replenish the truncated TCA cycle (blue arrows). Glutamate is important for the biosynthesis of glutathione, a potent antioxidant. aKG also plays an important role in the regulation of DNA and histone methylation. Fum, fumarate; GLS, glutaminase; Glu, glutamate; Lac, lactate; Mal, malate; NADPH, nicotinamide adenine dinucleotide phosphate; Pyr, pyruvate; Succ, succinate; TCA, tricarboxylic acid; a-KG, a-ketoglutarate.

Glutamine addiction: a hallmark of cancer metabolism

Cancer cells rapidly consume glutamine at a surprisingly high rate compared to normal cells in order to maintain uncontrolled proliferation and survival (25). It has been reported that many oncogenic signaling pathways not only promote rapid cell division but also directly reprogram glutamine metabolism to match with the bioenergetic demand of rapid cell division (26). For example, c-Myc amplification in many cancers upregulates the expression of glutamine transporters and glutaminase enzymes. Myc-induced metabolic alterations lead to enhanced glutamine uptake and glutaminolysis, ultimately resulting in glutamine addiction in cancer cells (27, 28). Similarly, activating K-Ras mutant in various cancers, including pancreatic tumors, drive the expression of metabolic enzymes Glud1 and Got1 to regulate glucose and glutamine metabolism (29, 30). Furthermore, androgen receptor (AR) signaling and mTOR signaling in prostate cancer promote the upregulation of many glutamine transporters including *SLC1A4* and *SLC1A5,* leading to enhanced glutamine metabolism in cancer (31).

In addition to oncogenic signaling pathways, emerging evidence suggests that environmental factors and drug treatments also contribute to glutamine addiction in tumors. For examples, nutrient starvation, such as glucose depletion, renders cancer cells dependent on glutamine for survival and growth (32, 33). Interestingly, BCL2 inhibitor treatment in blood cancer and mTOR inhibitor treatment in glioblastoma can lead to elevated dependency on glutamine metabolism to counteract mitochondrial apoptosis (34, 35). Similarly, melanoma cells that are resistant to a BRAF inhibitor treatment, Vemurafenib, exhibit enhanced glutamine dependency; and targeting glutamine metabolism to restore cellular sensitivity to the drug treatment (33).

The increased demand for glutamine driven by oncogenes or environmental factors often renders cancer cells dependent on exogenous glutamine supply from circulation. Consequently, cancer cells often deplete the local nutrient supply in the tumor microenvironment, leading to severe glutamine restriction. Indeed, this glutamine deficiency in solid tumors has been documented in multiple studies across different tumor types (36). Glutamine concentration in tumors fall to almost undetectable levels compared to healthy tissues in a report over 50 years ago (37). Recent studies using metabolomics analysis also reveal that glutamine is one of the most depleted nutrients within the tumor microenvironment of pancreatic cancer (38). This glutamine starvation is remarkably severe in the core region of solid tumors or tumor sites with poor vascularization compared to cells at the peripheral sites (39, 40). Moreover, it also appears that tumors with K-Ras mutation or Myc amplification are more addicted to glutamine than cancer cells without these genetic alterations (28, 30). Thus, many additional factors including tumor sizes, the tissue of origin, and oncogenic drivers dictate the severity of glutamine starvation experienced by cancer cells in the tumor microenvironment.

Cancer cell adaptation to glutamine deprivation

Increased glutamine uptake coupling with the poor vasculatures of the tumor sites often results in periods of glutamine deprivation which can induce cell cycle arrest and cancer cell death. Interestingly, cancer cells often adapt to the nutrient limitation via various stress response pathways. These survival pathways not only promote cancer cell survival and expansion under the nutrient-poor microenvironment, but also promote resistance to cancer therapies that inhibit glutamine metabolism (41). Thus, with a better understanding of these survival strategies employed by cancer cells under glutamine deprivation, we will be able to effectively target glutamine metabolism for the treatment of cancer and minimize side toxicities.

Tumor suppressor p53, commonly mutated in the majority of human tumors, is a major regulator of cellular response to various stresses ranging from hypoxia to genotoxic agents (42). p53 can be activated through phosphorylation by various stress sensors including AMPK, ATM, p38, Chk2 (43). p53, once activated, acts as a transcription factor that induces the expression of different genes involved in cell cycle arrest, apoptosis, DNA damage repair, differentiation and metabolism (44). Traditionally, p53 activation in response to DNA damage or chemotherapy drug treatment exhibits tumor suppressive function by inducing cell cycle arrest and cellular death (45). However, emerging evidence suggests that p53 is also a major sensor and effector of metabolic stress (46, 47). The activation of p53 under metabolic stress such as glucose or amino acid starvation not only activates cell cycle arrest, but also directly reprograms cellular metabolism to promote cellular adaptation (48). For example, p53 under metabolic stress upregulates the expression of TP53-induced glycolysis and apoptosis regulator (Tigar) which blocks glycolysis and favors the pentose phosphate shunt (49, 50). In addition, the activation of p53 also modulates glutamine metabolism through the induction of glutaminase and glycolysis

through Sco2 regulation (50). Surprisingly, unlike the DNA-damage induced p53 activation which likely induces apoptosis, p53 activation plays an important survival role in response to mild metabolic stresses including glutamine deprivation (51). Thus, it appears that p53 can mediate cellular proliferation and tumor growth under the condition of moderate and temporary nutrient deprivation. The ability of p53 to induce cell cycle arrest, block apoptosis effectors, and promote metabolic reprograming allows cancer cells to adapt and grow in glutamine restricted environment (51, 52). In addition to p53, recent studies also demonstrate different mechanisms used by cancer cells to survive under glutamine deprivation including p63, peroxisome proliferator-activated receptor gamma coactivator-1 (PCG-1), the protein phosphatase PP2A, AMPK and IκB kinase β (46, 51, 53, 54).

Glutamine deficiency alters histone methylation to drive drug resistance in cancer

Cancer cells favor aerobic glycolysis to sustain chronic proliferation (14). Because most glucose is often diverted to lactate production, glutamine can be converted to glutamate which is subsequently converted to αKG to replenish the TCA cycle in many cancers. For example, metabolic flux analysis in Ras-transformed cells suggests that glutamine is rapidly converted into αKG in the TCA cycle to support oxidative phosphorylation and ATP production (55). Therefore, cancer cells also depend on glutamine to make αKG to replenish the TCA cycle (56). Interestingly, oncogenic signaling, including c-Myc and K-Ras, drive excessive uptake and metabolism of glutamine to support cancer cell growth and survival (27, 30). However, glutamine addiction coupled with poor vascularization within the tumor microenvironment depletes the local supply of glutamine. Indeed, metabolomic analyses revealed that glutamine

reaches undetectable levels in tumors compared to healthy tissue (38, 57). Interestingly, the tumor also displays differential glutamine levels in intratumoral regions, and glutamine levels are extremely low in the core of tumors compared to peripheral regions (40, 51). The glutamine deficiency in the tumor microenvironment, especially the core region of solid tumors, leads to depletion of αKG levels, which is a critical cofactor for histone demethylases. The low glutamine levels inhibit the JmjC-KDM leading to histone hypermethylation in the tumor core. Specifically, hypermethylation at histone H3K27 represses the expression of melanocyte differentiation genes, such as *PMEL, KIT*, and *GJB1*, ultimately resulting in a block to cell differentiation (Figure 1). Importantly, the alteration in histone methylation and gene expression upon glutamine depletion promotes drug resistance of melanoma cancer cells to BRAF inhibitor treatment both *in vitro* and *in vivo* (40).

Targeting glutamine metabolism in cancer treatment

While normal cells can synthesize glutamine via de novo pathways, some cancers also become dependent on exogenous glutamine and cannot grow in the absence of glutamine (58). Thus, glutamine metabolism has become an attractive target in cancer treatment. Indeed, inhibition of glutamine metabolism can inhibit cancer growth and malignant transformation both in cell culture and animal studies (18, 59). Importantly, malignant cells driven by K-Ras and C-Myc are more dependent on glutamine for cellular growth and survival, thus they are more responsive to molecules that target glutamine metabolism (60, 61).

Many compounds have been developed to target glutamine metabolism in cancer cells (62). Cellular uptake of glutamine can be inhibited with L-γ-glutamyl-p-nitroanilide, which is an

inhibitor of glutamine transporter SLC1A5 (63). Alternatively, L-asparaginase can be used to break down glutamine to glutamic acid and ammonia, thus lowering blood glutamine concentration (64). While these compounds can reduce glutamine concentration in tumor cells, they remain as preclinical tools due to high toxicity and the lack of specificity. Inhibition of glutaminase *GLS* with an allosteric inhibitor is the most effective strategy to inhibit glutamine metabolism for cancer therapy so far. Inhibition of glutaminase blocks the conversion of glutamine into glutamate and aKG resulting in dramatic response in some cancer cell lines (2). 6-diazo-5-oxo-L-norleucine (L-DON), isolated from Streptomyces, was found to inhibit glutamine metabolism and exert potent anticancer effects in cancer cell lines (65). However, L-DON is not an ideal glutaminase inhibitor due to off-target toxicities. Bis-2-(5-phenylacetamido-1,2,4-thiadiazol-2-yl) ethyl sulfide (BPTES) and compound 986 are specific inhibitors of glutaminase that have been developed recently. BPTES treatment not only results in a robust cellular response in vitro but also prolongs survival in genetically engineered mouse models of lymphoma (66). While BPTES has been shown to inhibit tumor growth in multiple animal studies, clinical studies with these compounds were discontinued due to serious side effects. A newly developed glutaminase inhibitor, CB-839, is shown to be well tolerated in patients and exhibit a potent antitumor effect in preclinical studies with breast cancer and blood cancer (65, 67). The compound is currently in phase II clinical trial for the treatment of different cancers.

Combination therapy with glutaminase inhibitor

It is worth mentioning that glutaminase inhibitor treatments often result in cell cycle arrest and rarely induces apoptosis at lower concentrations in preclinical studies. Thus, it is crucial to

identify potential drugs that can be used in conjugant with glutaminase inhibitor in clinical settings to improve efficacy and minimize toxicity. To maximize the therapeutic effect of glutaminase inhibitor, the following factors should be taken into consideration in preclinical studies and clinical investigations. First, it is helpful to identify drugs that can induce synthetic lethality when combined with glutaminase inhibitor. A recent study demonstrated that specific inhibition of the anti-apoptotic protein BCL-2 synergizes with glutaminase inhibition in a blood cancer model. Since glutamine is critical for the production of many anti-apoptosis proteins, targeting glutamine metabolism can sensitize cancer cells to apoptosis cell death in response to BCL2 inhibitor (68). Second, the tissue of origin, genetic alterations and environmental factors should also be considered. Many oncogenic signaling pathways, including mTOR and Wnt, and oncogenes, including *RAS*, *MYC,* and *PIK3CA,* have been shown to drive glutamine uptake and catabolism in cancer cells. Thus, tumors with genetic alterations in these genes are more dependent on glutamine for survival and consequently more susceptible to glutaminase inhibitor. In addition, melanoma cells that are resistant to BRAF inhibitor alter their cellular metabolism toward glutamine dependency for survival. Consequently, these drug-induced metabolic alteration render the resistant cells hypersensitive to glutaminase inhibitors treatment both *in vitro* and animal studies (33). Lastly, it is also beneficial to identify the adaptive responses employed by cancer cells to adapt and survive glutaminase inhibition treatment. Since tumor cells depend on these adaptive mechanisms to sense and adapt to nutrient limitation, targeting these survival pathways in combination with glutaminase inhibitor will yield a better therapeutic response. Indeed, a recent study demonstrated that IKKβ inhibition by a small molecule inhibitor significantly enhances the cytotoxicity of glutaminase inhibitor both *in vitro* and in animal models (53).

Organization of chapters

Metabolic reprogramming is an emerging hallmark of cancer. In addition to glucose, cancer cells often become "addicted" to glutamine to meet the high bioenergetic demands of uncontrolled proliferation. Glutamine is also a versatile nutrient that participates in different biochemical and biological processes including macromolecule biosynthesis, signaling, ROS control, and epigenetic regulations. As developing tumors grow in a poorly vascularized microenvironment, cancer cells often outstrip their local supply of nutrients leading to a period of severe glutamine deprivation. Recent studies focus intensively on how cancer cells become addicted to glutamine and the survival mechanisms that allow cancer cells to survive upon glutamine withdrawal. This dissertation investigates the potential impact of glutamine deficiency on cancer progression and therapeutic response in solid tumors.

The first chapter covers glutamine metabolism and clinical implication in cancer

The second chapter investigates how genetic alterations in the TP53 gene promote the cellular adaptation in glutamine deprivation. This study reveals that tumor-associated mutant p53 not only retains but also enhances the pro-survival function of the wildtype p53 genes in response to glutamine deprivation. Since cancer cells with mutant p53 are more resistant to glutaminase inhibitor treatment, cancer patients with wildtype p53 are more likely to benefit from glutaminase inhibitor treatment than patients carrying p53 mutation.

The third chapter explores the potential impact of environmental glutamine restriction on the DNA damage repair pathway. This study is based on an interesting observation that cancer cells under glutamine deprivation harbor extensive DNA damages. With both cellular and biochemical analysis, we show that glutamine metabolism in cancer cells through the biosynthesis of aKG

support the activity of the DNA repair enzyme Alkbh. Thus, inhibition of glutamine metabolism blocks the function of these enzymes leading to the accumulation of DNA damage as well as sensitivity to alkylating agents. These findings extend our understanding of glutamine deficiency, a form of metabolic stress, in tumor development and therapeutic response. We provide a critical molecular basis to combine glutaminase inhibitors with alkylating agents for a more effective treatment of cancer.

The fourth chapter investigates the connection between glutamine metabolism and the regulation of the oncogenic Wnt signaling pathway in colon cancer. Using intestinal organoid culture, we will examine the effect of environmental glutamine restriction on cellular differentiation and tumorigenicity. Importantly, we will test whether metabolic alterations suppresses Wnt signaling and inhibits colon cancer development.

In the last chapter, I discuss how metabolic fluctuation through epigenetics regulates tumor progression and affects therapeutic opportunity. Furthermore, I highlight some remaining questions, future research direction and clinical implications derived from these studies.

Reference

1. Altman BJ, Stine ZE, Dang CV. From Krebs to clinic: glutamine metabolism to cancer therapy. Nature reviews Cancer. 2016 Nov;16(11):749. PubMed PMID: 28704361.
2. DeBerardinis RJ, Cheng T. Q's next: the diverse functions of glutamine in metabolism, cell biology and cancer. Oncogene. 2010 Jan 21;29(3):313-24. PubMed PMID: 19881548. Pubmed Central PMCID: 2809806.
3. Smith RJ. Glutamine metabolism and its physiologic importance. JPEN Journal of parenteral and enteral nutrition. 1990 Jul-Aug;14(4 Suppl):40S-4S. PubMed PMID: 2205730.
4. Weiner ID, Verlander JW. Renal ammonia metabolism and transport. Comprehensive Physiology. 2013 Jan;3(1):201-20. PubMed PMID: 23720285. Pubmed Central PMCID: 4319187.
5. Haussinger D. Regulation of hepatic ammonia metabolism: the intercellular glutamine cycle. Advances in enzyme regulation. 1986;25:159-80. PubMed PMID: 2880476.
6. Zhou Y, Danbolt NC. Glutamate as a neurotransmitter in the healthy brain. Journal of neural transmission (Vienna, Austria : 1996). 2014;121(8):799-817. PubMed PMID: 24578174. Epub 03/01.
7. Lacey JM, Wilmore DW. Is glutamine a conditionally essential amino acid? Nutrition reviews. 1990 Aug;48(8):297-309. PubMed PMID: 2080048. Epub 1990/08/01. eng.
8. Kim H. Glutamine as an immunonutrient. Yonsei medical journal. 2011;52(6):892-7. PubMed PMID: 22028151. Epub 10/20.
9. Wilmore DW. The effect of glutamine supplementation in patients following elective surgery and accidental injury. The Journal of nutrition. 2001 Sep;131(9 Suppl):2543S-9S; discussion 50S-1S. PubMed PMID: 11533310. Epub 2001/09/05. eng.
10. Loftus RM, Finlay DK. Immunometabolism: Cellular Metabolism Turns Immune Regulator. The Journal of biological chemistry. 2016 Jan 1;291(1):1-10. PubMed PMID: 26534957. Pubmed Central PMCID: 4697146.
11. Cluntun AA, Lukey MJ, Cerione RA, Locasale JW. Glutamine Metabolism in Cancer: Understanding the Heterogeneity. Trends Cancer. 2017;3(3):169-80. PubMed PMID: 28393116.
12. Yang L, Venneti S, Nagrath D. Glutaminolysis: A Hallmark of Cancer Metabolism. Annual review of biomedical engineering. 2017 2017/06/21;19(1):163-94.
13. Zhang J, Pavlova NN, Thompson CB. Cancer cell metabolism: the essential role of the nonessential amino acid, glutamine. The EMBO journal. 2017 May 15;36(10):1302-15. PubMed PMID: 28420743. Pubmed Central PMCID: 5430235.
14. Wise DR, Thompson CB. Glutamine addiction: a new therapeutic target in cancer. Trends in biochemical sciences. 2010 Aug;35(8):427-33. PubMed PMID: 20570523. Pubmed Central PMCID: 2917518.
15. Liberti MV, Locasale JW. The Warburg Effect: How Does it Benefit Cancer Cells? Trends in biochemical sciences. 2016;41(3):211-8. PubMed PMID: 26778478. Epub 01/05.
16. Young VR, Ajami AM. Glutamine: the emperor or his clothes? The Journal of nutrition. 2001 Sep;131(9 Suppl):2449S-59S; discussion 86S-7S. PubMed PMID: 11533293.
17. Xiao D, Zeng L, Yao K, Kong X, Wu G, Yin Y. The glutamine-alpha-ketoglutarate (AKG) metabolism and its nutritional implications. Amino acids. 2016 Sep;48(9):2067-80. PubMed PMID: 27161106. Epub 2016/05/11. eng.
18. Le A, Lane AN, Hamaker M, Bose S, Gouw A, Barbi J, et al. Glucose-independent glutamine metabolism via TCA cycling for proliferation and survival in B cells. Cell

metabolism. 2012 Jan 4;15(1):110-21. PubMed PMID: 22225880. Pubmed Central PMCID: 3345194.
19. DeBerardinis RJ, Mancuso A, Daikhin E, Nissim I, Yudkoff M, Wehrli S, et al. Beyond aerobic glycolysis: transformed cells can engage in glutamine metabolism that exceeds the requirement for protein and nucleotide synthesis. Proceedings of the National Academy of Sciences of the United States of America. 2007 Dec 4;104(49):19345-50. PubMed PMID: 18032601. Pubmed Central PMCID: 2148292.
20. Mates JM, Perez-Gomez C, Nunez de Castro I, Asenjo M, Marquez J. Glutamine and its relationship with intracellular redox status, oxidative stress and cell proliferation/death. The international journal of biochemistry & cell biology. 2002 May;34(5):439-58. PubMed PMID: 11906817.
21. Michalak KP, Ma, #x107, kowska-K, #x119, dziora A, et al. Key Roles of Glutamine Pathways in Reprogramming the Cancer Metabolism. Oxidative Medicine and Cellular Longevity. 2015;2015:14.
22. Nicklin P, Bergman P, Zhang B, Triantafellow E, Wang H, Nyfeler B, et al. Bidirectional transport of amino acids regulates mTOR and autophagy. Cell. 2009 Feb 6;136(3):521-34. PubMed PMID: 19203585. Epub 2009/02/11. eng.
23. DeBerardinis RJ, Lum JJ, Hatzivassiliou G, Thompson CB. The biology of cancer: metabolic reprogramming fuels cell growth and proliferation. Cell metabolism. 2008 Jan;7(1):11-20. PubMed PMID: 18177721.
24. Tannock IF, Steele D, Roberts J. Influence of reduced concentration of L-glutamine on growth and viability of cells in monolayer, in spheroids, and in experimental tumours. British journal of cancer. 1986 Nov;54(5):733-41. PubMed PMID: 3801270. Pubmed Central PMCID: 2001537.
25. Yang L, Venneti S, Nagrath D. Glutaminolysis: A Hallmark of Cancer Metabolism. Annual review of biomedical engineering. 2017 Jun 21;19:163-94. PubMed PMID: 28301735.
26. DeBerardinis RJ, Chandel NS. Fundamentals of cancer metabolism. Science advances. 2016 May;2(5):e1600200. PubMed PMID: 27386546. Pubmed Central PMCID: 4928883.
27. Gao P, Tchernyshyov I, Chang TC, Lee YS, Kita K, Ochi T, et al. c-Myc suppression of miR-23a/b enhances mitochondrial glutaminase expression and glutamine metabolism. Nature. 2009 Apr 9;458(7239):762-5. PubMed PMID: 19219026. Pubmed Central PMCID: 2729443.
28. Wise DR, DeBerardinis RJ, Mancuso A, Sayed N, Zhang XY, Pfeiffer HK, et al. Myc regulates a transcriptional program that stimulates mitochondrial glutaminolysis and leads to glutamine addiction. Proceedings of the National Academy of Sciences of the United States of America. 2008 Dec 2;105(48):18782-7. PubMed PMID: 19033189. Pubmed Central PMCID: 2596212.
29. Yang S, Hwang S, Kim M, Seo SB, Lee JH, Jeong SM. Mitochondrial glutamine metabolism via GOT2 supports pancreatic cancer growth through senescence inhibition. Cell death & disease. 2018 Jan 19;9(2):55. PubMed PMID: 29352139. Pubmed Central PMCID: 5833441.
30. Son J, Lyssiotis CA, Ying H, Wang X, Hua S, Ligorio M, et al. Glutamine supports pancreatic cancer growth through a KRAS-regulated metabolic pathway. Nature. 2013 Apr 4;496(7443):101-5. PubMed PMID: 23535601. Pubmed Central PMCID: 3656466.
31. White MA, Lin C, Rajapakshe K, Dong J, Shi Y, Tsouko E, et al. Glutamine Transporters Are Targets of Multiple Oncogenic Signaling Pathways in Prostate Cancer. Molecular cancer

research : MCR. 2017 Aug;15(8):1017-28. PubMed PMID: 28507054. Pubmed Central PMCID: PMC5685160. Epub 2017/05/17. eng.
32. Miyo M, Konno M, Nishida N, Sueda T, Noguchi K, Matsui H, et al. Metabolic Adaptation to Nutritional Stress in Human Colorectal Cancer. Scientific reports. 2016 Dec 7;6:38415. PubMed PMID: 27924922. Pubmed Central PMCID: 5141444
(http://www.taiho.co.jp/english/), the Evidence Based Medical (EBM) Research Center (http://ebmrce.co.jp/index.html), Chugai Co., Ltd. (http://www.chugai-pharm.co.jp/english/index.html), Yakult Honsha Co., Ltd. (http://www.yakult.co.jp/english/index.html), and Merck Co., Ltd. (http://www.merck.co.jp/en/index.html). Those funders had no role in the main experimental equipment, supply expenses, study design, data collection and analysis, decision to publish, or preparation of the manuscript for this work.
33. Hernandez-Davies JE, Tran TQ, Reid MA, Rosales KR, Lowman XH, Pan M, et al. Vemurafenib resistance reprograms melanoma cells towards glutamine dependence. Journal of translational medicine. 2015 Jul 3;13:210. PubMed PMID: 26139106. Pubmed Central PMCID: PMC4490757. Epub 2015/07/04. eng.
34. Jacque N, Ronchetti AM, Larrue C, Meunier G, Birsen R, Willems L, et al. Targeting glutaminolysis has antileukemic activity in acute myeloid leukemia and synergizes with BCL-2 inhibition. Blood. 2015;126(11):1346.
35. Tanaka K, Sasayama T, Irino Y, Takata K, Nagashima H, Satoh N, et al. Compensatory glutamine metabolism promotes glioblastoma resistance to mTOR inhibitor treatment. The Journal of clinical investigation. 2015 Apr;125(4):1591-602. PubMed PMID: 25798620. Pubmed Central PMCID: 4396477.
36. Cluntun AA, Lukey MJ, Cerione RA, Locasale JW. Glutamine Metabolism in Cancer: Understanding the Heterogeneity. Trends Cancer. 2017 Mar;3(3):169-80. PubMed PMID: 28393116. Pubmed Central PMCID: 5383348.
37. Roberts E, Frankel S. Free amino acids in normal and neoplastic tissues of mice as studied by paper chromatography. Cancer research. 1949 Nov;9(11):645-8, 3 pl. PubMed PMID: 15392817.
38. Kamphorst JJ, Nofal M, Commisso C, Hackett SR, Lu W, Grabocka E, et al. Human pancreatic cancer tumors are nutrient poor and tumor cells actively scavenge extracellular protein. Cancer research. 2015 Feb 1;75(3):544-53. PubMed PMID: 25644265. Pubmed Central PMCID: 4316379.
39. Daye D, Wellen KE. Metabolic reprogramming in cancer: unraveling the role of glutamine in tumorigenesis. Seminars in cell & developmental biology. 2012 Jun;23(4):362-9. PubMed PMID: 22349059.
40. Pan M, Reid MA, Lowman XH, Kulkarni RP, Tran TQ, Liu X, et al. Regional glutamine deficiency in tumours promotes dedifferentiation through inhibition of histone demethylation. Nature cell biology. 2016 Oct;18(10):1090-101. PubMed PMID: 27617932. Pubmed Central PMCID: 5536113.
41. Reid MA, Kong M. Dealing with hunger: Metabolic stress responses in tumors. Journal of carcinogenesis. 2013;12:17-. PubMed PMID: 24227992.
42. Vousden KH, Lu X. Live or let die: the cell's response to p53. Nature reviews Cancer. 2002 Aug;2(8):594-604. PubMed PMID: 12154352.
43. Kruse JP, Gu W. Modes of p53 regulation. Cell. 2009 May 15;137(4):609-22. PubMed PMID: 19450511. Pubmed Central PMCID: 3737742.

44. Surget S, Khoury MP, Bourdon JC. Uncovering the role of p53 splice variants in human malignancy: a clinical perspective. OncoTargets and therapy. 2013 Dec 19;7:57-68. PubMed PMID: 24379683. Pubmed Central PMCID: 3872270.
45. Bieging KT, Mello SS, Attardi LD. Unravelling mechanisms of p53-mediated tumour suppression. Nature Reviews Cancer. 2014 04/17/online;14:359.
46. Jones RG, Plas DR, Kubek S, Buzzai M, Mu J, Xu Y, et al. AMP-activated protein kinase induces a p53-dependent metabolic checkpoint. Molecular cell. 2005 Apr 29;18(3):283-93. PubMed PMID: 15866171.
47. Maddocks OD, Vousden KH. Metabolic regulation by p53. Journal of molecular medicine. 2011 Mar;89(3):237-45. PubMed PMID: 21340684. Pubmed Central PMCID: 3043245.
48. Maddocks OD, Berkers CR, Mason SM, Zheng L, Blyth K, Gottlieb E, et al. Serine starvation induces stress and p53-dependent metabolic remodelling in cancer cells. Nature. 2013 Jan 24;493(7433):542-6. PubMed PMID: 23242140.
49. Bensaad K, Tsuruta A, Selak MA, Vidal MN, Nakano K, Bartrons R, et al. TIGAR, a p53-inducible regulator of glycolysis and apoptosis. Cell. 2006 Jul 14;126(1):107-20. PubMed PMID: 16839880.
50. Mauro C, Leow SC, Anso E, Rocha S, Thotakura AK, Tornatore L, et al. NF-kappaB controls energy homeostasis and metabolic adaptation by upregulating mitochondrial respiration. Nature cell biology. 2011 Aug 28;13(10):1272-9. PubMed PMID: 21968997. Pubmed Central PMCID: 3462316.
51. Reid MA, Wang WI, Rosales KR, Welliver MX, Pan M, Kong M. The B55alpha subunit of PP2A drives a p53-dependent metabolic adaptation to glutamine deprivation. Molecular cell. 2013 Apr 25;50(2):200-11. PubMed PMID: 23499005.
52. Tran TQ, Lowman XH, Reid MA, Mendez-Dorantes C, Pan M, Yang Y, et al. Tumor-associated mutant p53 promotes cancer cell survival upon glutamine deprivation through p21 induction. Oncogene. 2017 Apr 6;36(14):1991-2001. PubMed PMID: 27721412. Pubmed Central PMCID: 5383530.
53. Reid MA, Lowman XH, Pan M, Tran TQ, Warmoes MO, Ishak Gabra MB, et al. IKKbeta promotes metabolic adaptation to glutamine deprivation via phosphorylation and inhibition of PFKFB3. Genes & development. 2016 Aug 15;30(16):1837-51. PubMed PMID: 27585591. Pubmed Central PMCID: 5024682.
54. Sen N, Satija YK, Das S. PGC-1alpha, a key modulator of p53, promotes cell survival upon metabolic stress. Molecular cell. 2011 Nov 18;44(4):621-34. PubMed PMID: 22099309. Epub 2011/11/22. eng.
55. Fan J, Kamphorst JJ, Mathew R, Chung MK, White E, Shlomi T, et al. Glutamine-driven oxidative phosphorylation is a major ATP source in transformed mammalian cells in both normoxia and hypoxia. Molecular systems biology. 2013 Dec 03;9:712. PubMed PMID: 24301801. Pubmed Central PMCID: 3882799.
56. Altman BJ, Stine ZE, Dang CV. From Krebs to clinic: glutamine metabolism to cancer therapy. Nat Rev Cancer. 2016 10//print;16(10):619-34.
57. Roberts E, Caldwell AL, et al. Amino acids in epidermal carcinogenesis in mice. Cancer research. 1949 Jun;9(6):350-3. PubMed PMID: 18144236.
58. Choi YK, Park KG. Targeting Glutamine Metabolism for Cancer Treatment. Biomolecules & therapeutics. 2018 Jan 1;26(1):19-28. PubMed PMID: 29212303. Pubmed Central PMCID: 5746034.

59. Xiang Y, Stine ZE, Xia J, Lu Y, O'Connor RS, Altman BJ, et al. Targeted inhibition of tumor-specific glutaminase diminishes cell-autonomous tumorigenesis. The Journal of clinical investigation. 2015 Jun;125(6):2293-306. PubMed PMID: 25915584. Pubmed Central PMCID: 4497742.
60. Yuneva M, Zamboni N, Oefner P, Sachidanandam R, Lazebnik Y. Deficiency in glutamine but not glucose induces MYC-dependent apoptosis in human cells. The Journal of cell biology. 2007 Jul 2;178(1):93-105. PubMed PMID: 17606868. Pubmed Central PMCID: 2064426.
61. Toda K, Kawada K, Iwamoto M, Inamoto S, Sasazuki T, Shirasawa S, et al. Metabolic Alterations Caused by KRAS Mutations in Colorectal Cancer Contribute to Cell Adaptation to Glutamine Depletion by Upregulation of Asparagine Synthetase. Neoplasia. 2016 Nov;18(11):654-65. PubMed PMID: 27764698. Pubmed Central PMCID: 5071549.
62. Stalnecker CA, Ulrich SM, Li Y, Ramachandran S, McBrayer MK, DeBerardinis RJ, et al. Mechanism by which a recently discovered allosteric inhibitor blocks glutamine metabolism in transformed cells. Proceedings of the National Academy of Sciences of the United States of America. 2015 Jan 13;112(2):394-9. PubMed PMID: 25548170. Pubmed Central PMCID: 4299208.
63. Hassanein M, Qian J, Hoeksema MD, Wang J, Jacobovitz M, Ji X, et al. Targeting SLC1a5-mediated glutamine dependence in non-small cell lung cancer. International journal of cancer. 2015 Oct 1;137(7):1587-97. PubMed PMID: 25821004. Pubmed Central PMCID: 4640891.
64. Reinert RB, Oberle LM, Wek SA, Bunpo P, Wang XP, Mileva I, et al. Role of glutamine depletion in directing tissue-specific nutrient stress responses to L-asparaginase. The Journal of biological chemistry. 2006 Oct 20;281(42):31222-33. PubMed PMID: 16931516.
65. Griffiths M, Keast D, Patrick G, Crawford M, Palmer TN. The role of glutamine and glucose analogues in metabolic inhibition of human myeloid leukaemia in vitro. The International journal of biochemistry. 1993 Dec;25(12):1749-55. PubMed PMID: 8138012.
66. Robinson MM, McBryant SJ, Tsukamoto T, Rojas C, Ferraris DV, Hamilton SK, et al. Novel mechanism of inhibition of rat kidney-type glutaminase by bis-2-(5-phenylacetamido-1,2,4-thiadiazol-2-yl)ethyl sulfide (BPTES). The Biochemical journal. 2007 Sep 15;406(3):407-14. PubMed PMID: 17581113. Pubmed Central PMCID: 2049044.
67. Gross MI, Demo SD, Dennison JB, Chen L, Chernov-Rogan T, Goyal B, et al. Antitumor activity of the glutaminase inhibitor CB-839 in triple-negative breast cancer. Molecular cancer therapeutics. 2014 Apr;13(4):890-901. PubMed PMID: 24523301.
68. Jacque N, Ronchetti AM, Larrue C, Meunier G, Birsen R, Willems L, et al. Targeting glutaminolysis has antileukemic activity in acute myeloid leukemia and synergizes with BCL-2 inhibition. Blood. 2015 Sep 10;126(11):1346-56. PubMed PMID: 26186940. Pubmed Central PMCID: 4608389.

Chapter 2

Tumor-associated mutant p53 promotes cancer cell survival upon glutamine deprivation through p21 induction

This chapter is partly derived from an article published in *Oncogene*, entitled "Tumor-associated mutant p53 promotes cancer cell survival upon glutamine deprivation through p21 induction." 2017 Apr 6; 36(14): 1991–2001.

Summary

Cancer cells depend on glutamine to sustain their increased proliferation and manage oxidative stress, yet glutamine is often depleted at tumor sites due to excessive cellular consumption and poor vascularization. We have previously reported that p53 protein, while a well-known tumor suppressor, can contribute to cancer cell survival and adaptation to low glutamine conditions. However, the *TP53* gene is frequently mutated in tumors, and the role of mutant p53 (mutp53) in response to metabolic stress remains unclear. Here, we demonstrate that tumor-associated mutp53 promotes cancer cell survival upon glutamine deprivation both *in vitro* and *in vivo*. Interestingly, cancer cells expressing mutp53 proteins are more resistant to glutamine deprivation than cells with wild type p53 (wtp53). Depletion of endogenous mutp53 protein in human lymphoma cells leads to cell sensitivity to glutamine withdrawal, while expression of mutp53 in p53 null cells results in resistance to glutamine deprivation. Furthermore, we found that mutp53 proteins hyper-transactivate p53 target gene *CDKN1A* upon glutamine deprivation, thus triggering cell cycle arrest and promoting cell survival. Together, our results reveal an unidentified mechanism by which mutp53 confers oncogenic functions by promoting cancer cell adaptation to metabolic stresses.

Introduction

Glutamine is essential for survival and proliferation of most malignant cells (23). The amino acid sustains highly proliferative cells by contributing to the biosynthesis of amino acids and nucleotides(14, 16). Additionally, glutamine protects cells from oxidative stress by maintaining healthy glutathione levels(20). To ensure sufficient energy production, some cancer cells also rely on glutamine to synthesize alpha-ketoglutarate (α-KG) to replenish TCA cycle intermediates (18). Therefore, inhibition of glutaminolysis alone is sufficient to inhibit tumor growth in some cancers(66). Even though glutamine directly supports tumorigenesis, developing tumors are often subject to severe glutamine restriction due to increased uptake and poor vascularization at tumor sites(38, 67). For example, glutamine falls to almost undetectable levels relative to normal tissues *in vivo* in hepatomas and sarcomas(67). Consistently, a recent study using metabolomics analysis comparing paired pancreatic tumor patient samples with benign adjacent tissue specimens revealed that glutamine is one of the most strongly depleted metabolites in tumors(38). Thus, tumors need to develop multiple strategies to survive and grow in the low glutamine conditions.

Tumor suppressor p53 has been commonly described as a transcription factor that contributes to cell death and cell cycle arrest in response to various stresses(43). Interestingly, recent reports have established that p53 also contributes to cell survival upon metabolic stress(48). For example, p53 induces *CDKN1A* expression to trigger reversible cell-cycle arrest upon serine depletion, which allows cancer cells to pause and manage oxidative stress thus leading to enhanced survival, whereas p53 deficient cells lacking the adaptive response display drastic cell death(49). In addition, it was demonstrated that activation of p53 in response to low glucose levels promotes cell adaptation through a cell cycle arrest check point(47). Similarly, we have

reported that p53 is activated upon glutamine deprivation and is required for cell survival under low glutamine conditions both *in vitro* and *in vivo*(41). Therefore, unlike numerous DNA-damage induced p53 signaling cascades that result in apoptosis, it appears that p53 is important for cell survival under broad nutrient restrictions. Besides promoting cell survival upon metabolic stress through induction of cell cycle arrest, p53 also activates other metabolic regulators in response to nutritional stress. For example, under glucose starvation, p53 promotes expression of Sco2 or Lpin1 to decrease the rate of glycolysis by upregulating mitochondrial oxidative phosphorylation or promoting fatty acid oxidation(51, 68). Moreover, by driving the expression of the metabolic enzyme GLS2, and the metabolic reprogramming protein TIGAR, p53 contributes to cell survival by enhancing antioxidant capacity in nutrient depleted cells(50, 69, 70). Thus, depending on cellular context, p53 may promote multiple survival mechanisms in response to metabolic stress.

The p53 protein is mutated in over 50% of all human cancers, and is often associated with a *poor prognosis*(71-73). The majority of these cancers carry a missense mutation in the DNA binding domain of the p53 protein, with arginine residue 248 or 273 among the most frequently mutated. These are commonly referred to as 'hot spot' mutations, and often result in a more stable full-length protein with gain-of-function activity(74). Intriguingly, several phenotypes of tumor-associated mutp53 suggest that tumors acquire the ability to promote cancer aggression and invasion(75). Despite evidence supporting the role of wild type p53 in cell survival upon metabolic stress, it remains unclear whether mutp53 proteins could confer a survival advantage in response to metabolic stress.

In this study, we investigate the cellular response of mutp53 proteins upon glutamine withdrawal. We found that mutp53 promotes cell survival upon glutamine deprivation and glutaminase inhibitor treatment both *in vitro* and *in vivo*. Our study demonstrates that mutp53 amplifies the pro-survival effects of wtp53 protein to protect cancer cells from low glutamine conditions.

Results

Cancer cells with mutp53 are more resistant to glutamine deprivation than cells with wtp53

To determine whether p53 status can impact the survival of cancer cells upon glutamine starvation, we analyzed a panel of lymphoma cell lines with known p53 status by withdrawing glutamine over time. Strikingly, we found cells expressing mutp53 (CA46, DB and SupT1) were significantly more resistant to glutamine deprivation than cells expressing wtp53 (EB3, LY3 and DOHH2) (Figure 2-1a). Consistent with this, we found increased apoptosis, as measured by cleaved-PARP and cleaved-caspase 3 in EB3 cells expressing wtp53 compared to CA46 cells expressing mutp53 upon glutamine starvation (Figure 2-1b). Moreover, using annexin-V and PI staining, we confirmed substantial induction of early and late apoptosis in wtp53 cells, but not in mutp53 cells (Figure 2-1c-d). To further confirm resistance to cell death in glutamine restricted conditions, we measured cell viability of EB3 and CA46 cells after treatment with the glutaminase inhibitor 6-Diazo-5-oxo-L-norleucine (L-DON). While L-DON, a glutamine analogue, has been shown to directly bind and inhibit human glutaminase, the compound also affects the activity of other glutamine utilizing enzymes(76). Therefore, we also treated cells with other identified glutaminase inhibitors such as Bis-2-(5-phenylacetamido-1,3,4-thiadiazol-2-yl)ethyl sulfide (BPTES)(63) and Compound 968(66). Consistently, we found that L-DON, BPTES and Compound 968 treatments induced cell death in a dose-dependent manner in wtp53

expressing EB3 cells, while having no effect on cell viability of CA46 cells harboring mutp53 (Figure 2-1e). Together, these results demonstrated that mutp53 status correlates with better survival in glutamine deprived conditions and upon glutaminase inhibitor treatment.

Loss of mutp53 sensitizes cancer cells to glutamine deprivation and glutaminase inhibitor treatment.

To determine whether loss of mutp53 could sensitize cancer cells to glutamine starvation, we used shRNA to knock down mutp53 in CA46 cells. We generated stable cell lines with p53 knocked down (Figure 2-2a and 2b) and found that mutp53 deficiency significantly sensitized CA46 cells to glutamine deprivation compared to control (Figure 2-2c). Based on the annexin V/PI staining, glutamine deprivation resulted in more dramatic apoptotic cell death in mutp53 knockdown cells compared to vector control cells (Figure 2-2d and 2e). In addition, we found that knockdown of mutp53 promoted cell sensitivity to different glutaminase inhibitor treatment, such as L-DON, BPTES and Compound 968 (Figure 2-2f). These results demonstrated that mutp53 is required for cell survival under glutamine deprivation and glutaminase inhibitor treatment.

Expression of mutp53 promotes cell survival upon glutamine deprivation and glutaminase inhibitor treatment

To directly test whether mutp53 promotes cell survival upon glutamine deprivation, we stably transduced p53 deleted colorectal carcinoma HCT116 cells with retroviral vectors expressing tumor-associated p53 hotspot mutants R248Q or R273H (Figure 2-3a). Expression of either p53 mutant in HCT116 p53-/- cells largely protected cells upon glutamine deprivation compared to

control (Figure 2-3b). In agreement, cells expressing mutp53 displayed less apoptosis as measured by cleaved-PARP and cleaved-caspase 3 upon glutamine deprivation compared to vector control cells (Figure 2-3c). In addition, we compared survival upon glutamine deprivation in HCT116 cells with p53 deletion (Vec), and cells expressing either endogenous wtp53 or exogenous mutant p53 (R248Q, R273H). Consistent with previous reports, cells with wtp53 are more resistant to glutamine deprivation than p53 null cells (Figure 2-3d)(41). More interestingly, we found that cells expressing mutp53 displayed better survival than cells expressing wtp53, indicating mutp53 may acquire additional function to promote cell survival in response to glutamine deprivation. Consistent with the cellular response to glutamine deprivation, cells expressing mutp53 are significantly more resistant to both L-DON treatment and Compound 968 treatment than vector control cells (Figure 2-3e). Interestingly, expression of mutp53 had no significant protection upon treatment of different genotoxic agents including camptothecin (CPT), doxorubicin (DOX) and docetaxel (DTX) (Figure 2-3f), suggesting that mutp53 might specifically promote cell survival upon metabolic stress. Altogether, these results strongly support a robust survival role of mutp53 proteins in protecting cancer cells from glutamine starvation.

Mutp53 induces expression of p53 target genes upon glutamine deprivation

It has been reported that cell survival promoted by wtp53 upon metabolic stress is often mediated by the induction of cell cycle arrest and metabolic reprogramming genes including *CDKN1A, GADD45A, GLS2* and *TIGAR*(49, 50, 69). Therefore, we asked whether mutp53 contributes to the induction of these genes upon glutamine deprivation. Consistent with previous investigations, we found p53 was phosphorylated on Serine 15, a critical site for p53 activation,

upon glutamine deprivation in EB3 cells with wild type p53 (Figure 2-4a)(41). Moreover, mutp53 in CA46 cells was also phosphorylated upon glutamine deprivation (Figure 2-4a). Consistent with the phosphorylation, we found that p53-targeted pro-survival genes were significantly induced in CA46 cells upon glutamine deprivation (Figure 4b). Interestingly, the induction of these genes was more robust in CA46 cells harboring mutp53 than EB3 cells with wtp53 (Figure 2-4b). Importantly, we found that knockdown of p53 in both wtp53 and mutp53 cells dramatically inhibited the induction of the survival genes upon glutamine deprivation, demonstrating that, similar to wtp53, mutp53 contributes to the upregulation of the p53 target genes (Figure 2-4c and 4d). To further confirm that mutp53 promotes the induction of these p53-target genes, we evaluated the effect of ectopically expressed mutp53 on gene expression upon glutamine deprivation. Consistent with previous investigations, expression of *CDKN1A*, *GLS2*, *GADD45A* and *TIGAR* are significantly higher in wtp53 expressing cells compared with p53 deleted cells (Figure 2-4e and 4f). Strikingly, we found that expression of R248Q or R273H mutp53 in HCT116 cells robustly induced *CDKN1A*, *GLS2*, *GADD45A* and *TIGAR* expression upon glutamine starvation compared with p53 deleted cells or wtp53 expressing cells (Figure 2-4f). Conversely, no significant changes were found in the expression of pro-apoptotic gene, *BAX* (Figure 2-4f). Together, these results suggest that mutp53 not only retains, but also exaggerates the transactivation activity of the wtp53 protein toward pro-survival genes to promote cell survival in response to glutamine deprivation.

Mutp53 directly binds to the promoter of p53 target genes upon glutamine deprivation

To investigate whether mutp53 can regulate the expression of the pro-survival genes via direct binding to DNA, we performed chromatin immunoprecipitation assays (ChIP) to assess p53

occupancy on promoter regions of target genes upon glutamine deprivation. We found that binding of endogenous mutp53 R248Q to the promoters of *CDKN1A, GLS2* and *BAX* in CA46 cells was very weak in complete medium (Figure 2-5a). However, the binding of mutp53 to the promoter of *CDKN1A* and *GLS2* dramatically increased upon glutamine deprivation (Figure 5a), consistent with the increased gene expression as shown in Figure 4f. Interestingly, no noticeable binding of mutp53 to the promoter of the pro-apoptotic gene *BAX* was found, even upon glutamine deprivation, supporting that mutp53 gains transactivation activity toward "survival" genes, but not "death" genes in response to metabolic stress, consistent with BAX expression (Figure 2-4f) and previously published reports (77-79). To further confirm this, HCT116 p53-/- cells expressing either mutp53 or vector control were subjected to glutamine deprivation overnight before the chromatin complexes were harvested for ChIP analysis (Figure 2-5b). Consistently, we found that binding of mutp53 to promoters of *CDKN1A*, *GADD45A*, *TIGAR* and *GLS2* increased strikingly upon glutamine withdrawal. No binding of mutp53 to the promoter region of pro-apoptotic gene *BAX* was found in cells cultured in either complete or glutamine free medium, while binding of wtp53 with *BAX* promoter was detected and increased upon glutamine deprivation (Figure 2-5b). Together, these results suggest that mutp53 can directly bind to p53 response elements in the promoter region of the "survival" genes in response to glutamine withdrawal with possible selectivity towards pro-survival but not pro-death gene activation.

Mutp53 promotes cell survival upon glutamine deprivation through p21 induction

It has been reported that wtp53-dependent p21 activation and cell cycle arrest promoted cell survival upon serine starvation(49). To determine if mutp53 promotes cell survival upon

glutamine deprivation via a similar mechanism, we first examined the cell cycle profile of HCT116 p53-/- cells with ectopic mutp53 or control vector in response to glutamine deprivation. We found that glutamine deprivation led to significant cell cycle arrest at G1/S phase in cells expressing mutp53 (Figure 2-6a and 6b). On the other hand, glutamine deprivation did not result in G1/S arrest of p53 deleted cells, indicating that cell cycle arrest may contribute to cell survival upon glutamine deprivation in mutp53 cells. The cell cycle arrest upon glutamine deprivation seen in mutp53 expressing cells is likely to be mediated by p21 induction, due to the role of p21 in inhibiting G1/S cell cycle progression(80, 81). To further test this, we examined p21 levels in HCT116 p53-/- cells expressing mutp53 or an empty vector cultured in either complete or glutamine free medium using Western blot analysis. Consistent with Figure 4f and 5b, p21 protein was significantly induced upon glutamine deprivation in cells expressing mutp53 R248Q, but not in vector control cells (Figure 2-6c). To further determine if the induction of p21 in mutp53 cells contributes to cell survival in low glutamine conditions, we used siRNA to transiently knock down p21 in HCT116 p53-/- cells expressing either mutp53 or vector control. Importantly, we found that p21 depletion increased cell sensitivity in response to glutamine deprivation in cells expressing mutp53, suggesting that the protective effects of mutp53 are mediated through p21 expression (Figure 2-6d). In addition, this increased sensitivity correlated with an increase in apoptosis, as indicated by Western blot analysis of cleaved-PARP (Figure 2-6e). Conversely, p21 depletion had no effect on cell viability upon glutamine deprivation in p53 deleted cells expressing vector control (Figure 2-6d and 6e). Taken together, these results demonstrate that mutp53 induces p21-dependent cell cycle arrest, which promotes cell survival in low glutamine conditions.

Tumors expressing mutp53 are more resistant to glutaminase inhibitor treatment *in vivo*

To further investigate whether mutp53 can protect cancer cells from glutamine starvation *in vivo*, we established xenograft tumors using HCT116 p53-/- cells expressing either an empty vector or mutp53 R248Q. Once tumors were established, mice were treated with the glutaminase inhibitor L-DON, and tumor volume was measured over time (Figure 2-7a and 7b). As expected, inhibition of glutamine metabolism by L-DON dramatically suppressed tumor growth in mice with p53 null tumors. In contrast, L-DON treatment had no significant effect on tumor growth in mice harboring tumors with mutp53 R248Q (Figure 2-7a and 7b). Consistent with our previous results, L-DON treatment induced apoptosis as indicated by cleaved-PARP in p53 null tumors, but not in tumors expressing mutp53 (Figure 2-7c). Together, these results show that mutp53 may play a role in tumor resistance to glutamine deprivation *in vivo*.

Discussion

More than half of human cancers carry mutations in the TP53 gene. These tumor-associated mutp53 proteins have been previously shown to drive aggressive cancer growth, metastasis and chemotherapeutic drug resistance(82). However, whether mutp53 proteins can protect cancer cells from metabolic stress that commonly occurs in the tumor microenvironment is not well established. Our results demonstrate that tumor-associated mutp53 proteins promote cancer cell survival in response to glutamine starvation both *in vitro* and *in vivo*. Altogether, the data reveals a previously unidentified mechanism by which mutp53 promotes tumorigenesis through resistance to metabolic stresses.

In this paper, we found that mutp53 can directly bind to the promoters of p53-target genes that regulate either cell cycle or metabolism and induce their expression upon glutamine deprivation (Figure 4 and Figure 5). While mutp53 proteins acquire non-canonical transactivation activity to promote cancer growth and invasion, recent studies demonstrate that mutp53 can bind to the response elements of wtp53 (83). Studies in both yeast and mammalian systems reveal that mutp53 proteins have differential transactivation activity towards canonical p53 target genes including loss of function, reduced transactivation activity, and super-transactivation activity(84). Moreover, mutp53 proteins can differentially regulate canonical p53 target genes to modulate cellular response to stress. For example, mutp53 may confer a survival advantage through its ability to transactivate the cell cycle arrest gene *CDKN1A,* but not the pro-apoptotic gene *BAX* (77-79). These evidences support our findings that mutp53 can transactivate the expression of p53 target genes to support cell survival and adaptation during metabolic stress. However, it still remains unclear how these mutp53 proteins are recruited to promoters of the target genes in response to metabolic stress. Based on our ChIP analysis, the binding of mutp53 to the target promoters remained minimal in normal conditions, but dramatically increased in response to glutamine withdrawal. These results suggest that other factors or pathways induced by glutamine deprivation might be required for the transactivation activity of mutp53. For example, upon glucose deprivation, PGC-1 protein can bind and preferentially promote p53 transactivation activity toward genes associated with cell cycle arrest and metabolic regulation (54). Therefore, it will be of interest to determine the molecular mechanisms that modulate the transactivation of mutp53 towards pro-survival genes in response to metabolic stress.

Our data also demonstrate that induction of CDKN1A (p21) is required for mutp53-mediated cell survival under low glutamine conditions. It has been well established that activation of wtp53 upon metabolic stress can contribute to survival through induction of cell cycle arrest genes. For example, AMPK-dependent p53 activation upon glucose starvation promotes cell cycle arrest at the G1/S phase transition leading to improved cellular survival (47). In addition, p53 in serine depleted cells can promote CDKN1A-dependent cell cycle arrest and antioxidant biosynthesis, which together support adaptation and cellular survival (49). Here, we found that mutp53 proteins not only retain, but also amplify the survival effect of wtp53 to protect cancer cells from glutamine deprivation via induction of p21. Specifically, mutp53 hyper-induces p21 expression to promote G1/S cell cycle arrest to protect cells from glutamine deprivation. Moreover, we observed that p21 knockdown is sufficient to restore cell sensitivity of mutp53 cells to glutamine deprivation. Cell cycle arrest upon metabolic stress can serve as a critical initial response that stops the energy-demanding process of cell proliferation to allow other cellular repair and adaptive processes to occur. Therefore, elimination of cell cycle arrest in glutamine deprived cells leads to unchecked proliferation and failure to adapt to metabolic stress, causing decreased cell viability. Besides p21, other p53 target genes involved in cell cycle arrest or metabolism are also highly induced in cells expressing mutp53 upon glutamine deprivation. Although our data support that p21 is critical for mutp53-mediated survival, we cannot exclude that other mutp53-regulated pathways also contribute to cell survival under glutamine deprivation. For example, it was recently reported that mutp53 proteins can directly bind to the metabolic protein sensor, AMPK, and inhibit its function to promote cancer cell growth (85). In addition, tumor-associated mutp53 has been shown to stimulate the Warburg effect (86).

The resistance to glutamine restriction in mutp53-expressing cells can impact tumor physiology and therapeutic response. First, glutamine levels at tumor sites can drop to nearly undetectable levels, partially because tumors heavily use exogenous glutamine to sustain their growth and survival. As glutamine is depleted in poorly vascularized tumor microenvironment, cancer cells expressing mutp53 protein are able to adapt and survive the metabolic stress, whereas p53 deficient cells and wtp53 expressing cells will experience impaired proliferation and increased cell death. Therefore, the glutamine depleted environment within the tumors is more favorable for the development of cancer cells expressing mutp53 proteins. Second, targeting glutamine metabolism underscores a therapeutic benefit against cancers (87-89). Recently, there is an increasing effort to inhibit anabolic glutamine metabolism using small molecule inhibitors targeting glutaminase. For examples, BPTES has been shown to inhibit growth of lymphoma xenografts with minimal toxicity, and a more potent glutaminase inhibitor CB-839 is currently in clinical trial for triple negative breast cancer (56, 64). However, we found that mutp53 expressing cells are strongly resistant to glutamine depletion and glutaminase inhibitor treatment compared to p53 deficient cells. These findings suggest a potential benefit in using glutaminase inhibitors to treat patients with p53-deficient tumors, but not those with tumors harboring mutp53.

Materials and methods

Cell culture and reagents

HCT116 p53+/+ and HCT116 p53-/- cells were cultured in Dulbecco's modified Eagle medium (DMEM, Corning) supplemented with 10% fetal bovine serum (FBS, Gemini Bio-Products), 100 units/mL of penicillin, and 100 □g/mL of streptomycin (Gemini Bio-Products). These cells have

been generated previously(90). EB3, SUPT1, DB (purchased from ATTC) and DOHH2 (purchased from DSMZ) lymphoma cell lines were cultured in RPMI 1640 medium (Corning) with 10% FBS, 100 units/mL of penicillin, and 100 □g/mL of streptomycin (Gemini Bio-Products). CA46 (purchased from ATTC) and LY3 (purchased from DSMZ) cells were cultured in RPMI medium with 20% FBS. All cells were cultured at 37˚C with 5% CO2. All cells were routinely tested for mycoplasma contamination using MycoAlert™ Mycoplasma Detection Kit (Lonza). L-DON, BPTES and camptothecin were purchased from Sigma. Docetaxel was purchased from Selleckchem, and Compound 968 was purchased from Calbiochem.

Glutamine starvation

For glutamine deprivation experiments, cells were washed once with 1x PBS and cultured in glutamine free medium or complete medium. To make glutamine free medium, DMEM and RPMI without glutamine (Corning) were supplemented with 10% dialyzed FBS (Gemini). To make the complete medium, 2 mM L-Glutamine (Corning) was added back to the glutamine free medium.

Flow Cytometry

To assess cell viability, cells were washed once with PBS and stained with 1 μg/mL propidium iodide (PI, Molecular Probes) for 10 minutes at room temperature. To assess apoptotic cell death, cells were washed once with PBS and stained with PI and Annexin-V (eBioscience) and processed according to the manufacturer's protocol. Flow analysis was carried out using the 9-color CyAn™ ADP from Beckman Coulter (Miami, FL). To assess cell viability by Trypan Blue

exclusion, cells were washed once with PBS and stained with Trypan Blue solution (Sigma). Cell viability was determined using TC20 automated cell counter (BioRad).

Cell cycle staining

To assess cell cycle profiles, cells were washed once with PBS and fixed with ice-cold 70% ethanol overnight. Fixed cells were washed twice with PBS and then treated with RNase A (Sigma) for 10 minutes at 37˚C. The cells were then stained with PI (Molecular Probes) and analyzed by flow cytometry on the CyAn™ ADP.

RT-PCR

RNA extractions were performed using Trizol (Invitrogen) according to the manufacturer's guidelines. 1 □g of RNA was used for each cDNA synthesis reaction (Quanta Biosciences). Real time reverse transcription PCR (qRT-PCR) reactions were performed with SYBR Green PCR reagents (Quanta Biosciences) using an iQ5 thermal cycler (Bio-Rad). The Ct values of the target genes were normalized to Ct values of Actin or 18S. Forward and reverse primers were generated to check gene expression. 18S F: 5'-CGCTTCCTTACCTGGTTGAT-3' R: 5'-GAGCGACCAA AGGAACCATA-3' ACTIN- F: 5'-CACCAACTGGGAGGACAT-3' R: 5'GCACAGCCT GGATAGCAAC-3' CDKN1A- F: 5'-AGGTGGACCTGGAGACTCTCAG-3' R: 5'TCCTCTTGGAGAAGATCA GCCG-3' GADD45A- F: 5'-CTGGAGGAAGTGC TCAGCAAAG-3'R: 5'-AGAGCCACA TCTCTGTCGTCGT-3' GLS2- F: 5'-CAGAAGG CACAGACATGGTTGG-3' R: 5'-GGCA GAAACCACCATTAGCCAG-3' TIGAR- F: 5'-TTCGGGAAAGGAAATACGGGG-3' R: 5'-CCACGCATTTTCACCTGGTC-3' SESN2- F:

5’-GCGCTTTCATTCCAGTGGAAGAG-3’ R: 5’-CAGAAGCTGCTAAGGTAGTCCG-3’

BAX- F: 5’-CCCGAGAGGTCTTTTTCCGAG-3’ R: 5’-CCAGCCCATGATGGTTCTGAT -3’

Western Blotting

Immunoblotting was carried out as described previously(91). Briefly, cells were washed 3 times with PBS and lysed in ice-cold RIPA lysis buffer supplemented with protease inhibitor (Roche) for 5 minutes. Immunoblotting was performed with the following antibodies: p53 (Santa Cruz, DO-1, SC126), p-p53 Ser-15 (Cell Signaling,9284), total PARP and cleaved PARP (Cell Signaling, 9542 and 5625), caspase 3 and cleaved caspase 3 (Cell Signaling, 9664 and 9665), Beta Actin (Sigma), p21 (Cell Signaling,2947).

shRNA knockdown

p53 shRNA constructs (TRCN0000003753) were purchased from GE Dharmacon. shRNA lentiviral particles were generated in 293T cells as described previously (91). Briefly, 293T cells were co-transfected with pLKO.1 empty vector or p53 shRNA vector, pMDL, pCMV-VSV-G and pRSV-Rev at a ratio of 4:2:1:1. After the transfection, lentiviral particles were collected at day 2 and day 3. Lymphoma cells were spin-infected twice with the lentiviral particles for 50 minutes at 2000 rpm at 30˚C. Cells were selected with 0.25 □g/ml puromycin.

siRNA knockdown

On-target plus human CDKN1A siRNA from Dharmacon (SMARTpool L-003471) was used to transiently knock down p21 protein in HCT116 cells. Cells were transfected with CDKN1A

siRNA or control siRNA (Dharmacon) using RNAi max lipofectamine reagent (Invitrogen). Glutamine deprivation experiments were performed 48 hours post siRNA transfection.

Generation of stable cell lines expressing mutp53 proteins

pLPCX retroviral vectors expressing mutp53 R248Q or R273H were generous gifts from Dr. Zhaohui Feng's Laboratory (Rutgers University, New Jersey). 293T cells were transfected with the mutp53 expressing vectors and the pLPCX empty vectors as previously described to generate retroviral particles(91). HCT116 p53-/- cells were cultured with the virus containing medium with 10 □g/ml polybrene overnight followed by puromycin selection (1 □g/ml).

Chromatin immunoprecipitation assay

The chromatin immunoprecipitation assay was performed using a ChIP assay kit (Millipore) according to the manufacturer's guideline. In brief, cells were cultured in complete medium or glutamine free medium overnight. Cells were cross-linked with 1% formaldehyde for 10 minutes at room temperature. Cells were washed 3 times with PBS and lysed in ice cold lysis buffer with protease inhibitors on ice for 5 minutes. Samples were sonicated to yield 200-1000bp DNA fragments. After centrifugation, cell supernatant was diluted in immunoprecipitation buffer with protease inhibitors and pre-cleared with Salmon Sperm DNA/ Protein A Agarose for 1 hour at 4˚C with rotation. 1 □g of p53 (DO-1, Santa Cruz) or IgG antibody was used for each overnight immunoprecipitation with rotation at 4˚C. Binding sites of p53 were amplified by 30-35 cycles of PCR using Hotstart Taq DNA polymerase (Bioneer). The PCR products were detected using agarose gel electrophoresis. PCR primers for the ChIP assays:

CDKN1A- F: 5’-GCTGTGGCTCTGATTGGCTTT-3’ R: 5’-ACAGGCAGCCCAAGGACAA A-3’ GADD45A- F: 5’-AGCGGAAGAGATCCCTGTGA-3’ R: 5’-CGGGAGGCAGGCAGA TG-3’ GLS2- F: 5’-GGCCTCCCAAGTCACCAGTTCA-3’ R:5’TGTTTTTGCTTGTTTTCG CCTTCT-3’ TIGAR- F: 5’-GCTTCAGACGTATATATAGA-3’ R: 5’GGGGCTATTCT TGGTAGTAA-3’ BAX F 5’-GGGTTATCTCTTGGGCTCACAA-3’ R 5’-GAGCTCTCCCCAGCGCA-3’ Negative primer: - F: 5’-TAAATGGGACAGGTAGGACC-3’ - R: 5’- TCCACCGCTTCTTGTCCTGC-3’

Mouse Xenografts

All animal procedures were approved by the Institutional Animal Care and Use Committee at City of Hope Cancer Center in compliance with ethical regulations. Animal were randomized before treatments. Sample size was generally chosen based on preliminary data indicating the variance within each group and the differences between groups. 7 week old Athymic Nude male mice (Taconic Laboratories) were injected subcutaneously with 1x106 cells. HCT116 p53-/- cells expressing vector control were injected in the left flank and HCT116 p53-/- cells expressing mutp53 R248Q were injected in the right flank. When the tumor size reached an average of 60 mm3, mice were treated with 15 mg/kg of L-DON or PBS 3 times per week. The tumor size was measured every other day as described previously(33). Eleven days after drug treatment, the mice were sacrificed and the tumors were harvested for Western Blot analysis.

Statistical analysis

Results are shown as averages; error bars represent either the standard error of the mean (S.E.M.) or standard deviation (S.D.) as indicated. The unpaired Student's t test was used to determine the

statistical significance of differences between means (*P<.05, **P<.01, ***$P\leq$.001). All western blot experiments were repeated at least three times with a representative gel being shown. For all other experiments, each was repeated independently at least two times with similar results.

References

1. DeBerardinis RJ, Lum JJ, Hatzivassiliou G, Thompson CB. The biology of cancer: metabolic reprogramming fuels cell growth and proliferation. Cell metabolism. 2008 Jan;7(1):11-20. PubMed PMID: 18177721.
2. Young VR, Ajami AM. Glutamine: the emperor or his clothes? The Journal of nutrition. 2001 Sep;131(9 Suppl):2449S-59S; discussion 86S-7S. PubMed PMID: 11533293.
3. Wise DR, Thompson CB. Glutamine addiction: a new therapeutic target in cancer. Trends in biochemical sciences. 2010 Aug;35(8):427-33. PubMed PMID: 20570523. Pubmed Central PMCID: 2917518.
4. Mates JM, Perez-Gomez C, Nunez de Castro I, Asenjo M, Marquez J. Glutamine and its relationship with intracellular redox status, oxidative stress and cell proliferation/death. The international journal of biochemistry & cell biology. 2002 May;34(5):439-58. PubMed PMID: 11906817.
5. Le A, Lane AN, Hamaker M, Bose S, Gouw A, Barbi J, et al. Glucose-independent glutamine metabolism via TCA cycling for proliferation and survival in B cells. Cell metabolism. 2012 Jan 4;15(1):110-21. PubMed PMID: 22225880. Pubmed Central PMCID: 3345194.
6. Wang JB, Erickson JW, Fuji R, Ramachandran S, Gao P, Dinavahi R, et al. Targeting mitochondrial glutaminase activity inhibits oncogenic transformation. Cancer cell. 2010 Sep 14;18(3):207-19. PubMed PMID: 20832749. Pubmed Central PMCID: 3078749.
7. Roberts E, Caldwell AL, et al. Amino acids in epidermal carcinogenesis in mice. Cancer research. 1949 Jun;9(6):350-3. PubMed PMID: 18144236.
8. Kamphorst JJ, Nofal M, Commisso C, Hackett SR, Lu W, Grabocka E, et al. Human pancreatic cancer tumors are nutrient poor and tumor cells actively scavenge extracellular protein. Cancer research. 2015 Feb 1;75(3):544-53. PubMed PMID: 25644265. Pubmed Central PMCID: 4316379.
9. Vousden KH, Lu X. Live or let die: the cell's response to p53. Nature reviews Cancer. 2002 Aug;2(8):594-604. PubMed PMID: 12154352.
10. Maddocks OD, Vousden KH. Metabolic regulation by p53. Journal of molecular medicine. 2011 Mar;89(3):237-45. PubMed PMID: 21340684. Pubmed Central PMCID: 3043245.
11. Maddocks OD, Berkers CR, Mason SM, Zheng L, Blyth K, Gottlieb E, et al. Serine starvation induces stress and p53-dependent metabolic remodelling in cancer cells. Nature. 2013 Jan 24;493(7433):542-6. PubMed PMID: 23242140.

12. Jones RG, Plas DR, Kubek S, Buzzai M, Mu J, Xu Y, et al. AMP-activated protein kinase induces a p53-dependent metabolic checkpoint. Molecular cell. 2005 Apr 29;18(3):283-93. PubMed PMID: 15866171.
13. Reid MA, Wang WI, Rosales KR, Welliver MX, Pan M, Kong M. The B55alpha subunit of PP2A drives a p53-dependent metabolic adaptation to glutamine deprivation. Molecular cell. 2013 Apr 25;50(2):200-11. PubMed PMID: 23499005.
14. Mauro C, Leow SC, Anso E, Rocha S, Thotakura AK, Tornatore L, et al. NF-kappaB controls energy homeostasis and metabolic adaptation by upregulating mitochondrial respiration. Nature cell biology. 2011 Oct;13(10):1272-9. PubMed PMID: 21968997. Pubmed Central PMCID: 3462316.
15. Assaily W, Rubinger DA, Wheaton K, Lin Y, Ma W, Xuan W, et al. ROS-mediated p53 induction of Lpin1 regulates fatty acid oxidation in response to nutritional stress. Molecular cell. 2011 Nov 4;44(3):491-501. PubMed PMID: 22055193.
16. Hu W, Zhang C, Wu R, Sun Y, Levine A, Feng Z. Glutaminase 2, a novel p53 target gene regulating energy metabolism and antioxidant function. Proceedings of the National Academy of Sciences of the United States of America. 2010 Apr 20;107(16):7455-60. PubMed PMID: 20378837. Pubmed Central PMCID: 2867677.
17. Bensaad K, Tsuruta A, Selak MA, Vidal MN, Nakano K, Bartrons R, et al. TIGAR, a p53-inducible regulator of glycolysis and apoptosis. Cell. 2006 Jul 14;126(1):107-20. PubMed PMID: 16839880.
18. Budanov AV. The role of tumor suppressor p53 in the antioxidant defense and metabolism. Sub-cellular biochemistry. 2014;85:337-58. PubMed PMID: 25201203. Pubmed Central PMCID: 4206257.
19. Muller PA, Vousden KH. p53 mutations in cancer. Nature cell biology. 2013 Jan;15(1):2-8. PubMed PMID: 23263379.
20. Gaidano G, Ballerini P, Gong JZ, Inghirami G, Neri A, Newcomb EW, et al. p53 mutations in human lymphoid malignancies: association with Burkitt lymphoma and chronic lymphocytic leukemia. Proceedings of the National Academy of Sciences of the United States of America. 1991 Jun 15;88(12):5413-7. PubMed PMID: 2052620. Pubmed Central PMCID: 51883.
21. Kandoth C, McLellan MD, Vandin F, Ye K, Niu B, Lu C, et al. Mutational landscape and significance across 12 major cancer types. Nature. 2013 Oct 17;502(7471):333-9. PubMed PMID: 24132290. Pubmed Central PMCID: 3927368.
22. Zheng T, Wang J, Zhao Y, Zhang C, Lin M, Wang X, et al. Spliced MDM2 isoforms promote mutant p53 accumulation and gain-of-function in tumorigenesis. Nature communications. 2013;4:2996. PubMed PMID: 24356649. Pubmed Central PMCID: 3960723.
23. Muller PA, Caswell PT, Doyle B, Iwanicki MP, Tan EH, Karim S, et al. Mutant p53 drives invasion by promoting integrin recycling. Cell. 2009 Dec 24;139(7):1327-41. PubMed PMID: 20064378.
24. Thangavelu K, Chong QY, Low BC, Sivaraman J. Structural basis for the active site inhibition mechanism of human kidney-type glutaminase (KGA). Scientific reports. 2014;4:3827. PubMed PMID: 24451979. Pubmed Central PMCID: 4929687.
25. Robinson MM, McBryant SJ, Tsukamoto T, Rojas C, Ferraris DV, Hamilton SK, et al. Novel mechanism of inhibition of rat kidney-type glutaminase by bis-2-(5-phenylacetamido-1,2,4-thiadiazol-2-yl)ethyl sulfide (BPTES). The Biochemical journal. 2007 Sep 15;406(3):407-14. PubMed PMID: 17581113. Pubmed Central PMCID: 2049044.

26. Campomenosi P, Monti P, Aprile A, Abbondandolo A, Frebourg T, Gold B, et al. p53 mutants can often transactivate promoters containing a p21 but not Bax or PIG3 responsive elements. Oncogene. 2001 Jun 14;20(27):3573-9. PubMed PMID: 11429705.
27. Friedlander P, Haupt Y, Prives C, Oren M. A mutant p53 that discriminates between p53-responsive genes cannot induce apoptosis. Molecular and cellular biology. 1996 Sep;16(9):4961-71. PubMed PMID: 8756655. Pubmed Central PMCID: 231498.
28. Ryan KM, Vousden KH. Characterization of structural p53 mutants which show selective defects in apoptosis but not cell cycle arrest. Molecular and cellular biology. 1998 Jul;18(7):3692-8. PubMed PMID: 9632751. Pubmed Central PMCID: 108951.
29. Harper JW, Adami GR, Wei N, Keyomarsi K, Elledge SJ. The p21 Cdk-interacting protein Cip1 is a potent inhibitor of G1 cyclin-dependent kinases. Cell. 1993 Nov 19;75(4):805-16. PubMed PMID: 8242751.
30. Waldman T, Kinzler KW, Vogelstein B. p21 is necessary for the p53-mediated G1 arrest in human cancer cells. Cancer research. 1995 Nov 15;55(22):5187-90. PubMed PMID: 7585571.
31. Muller PA, Vousden KH. Mutant p53 in cancer: new functions and therapeutic opportunities. Cancer cell. 2014 Mar 17;25(3):304-17. PubMed PMID: 24651012. Pubmed Central PMCID: 3970583.
32. Strano S, Dell'Orso S, Di Agostino S, Fontemaggi G, Sacchi A, Blandino G. Mutant p53: an oncogenic transcription factor. Oncogene. 2007 Apr 2;26(15):2212-9. PubMed PMID: 17401430.
33. Resnick MA, Inga A. Functional mutants of the sequence-specific transcription factor p53 and implications for master genes of diversity. Proceedings of the National Academy of Sciences of the United States of America. 2003 Aug 19;100(17):9934-9. PubMed PMID: 12909720. Pubmed Central PMCID: 187891.
34. Sen N, Satija YK, Das S. PGC-1alpha, a key modulator of p53, promotes cell survival upon metabolic stress. Molecular cell. 2011 Nov 18;44(4):621-34. PubMed PMID: 22099309.
35. Zhou G, Wang J, Zhao M, Xie TX, Tanaka N, Sano D, et al. Gain-of-function mutant p53 promotes cell growth and cancer cell metabolism via inhibition of AMPK activation. Molecular cell. 2014 Jun 19;54(6):960-74. PubMed PMID: 24857548. Pubmed Central PMCID: 4067806.
36. Zhang C, Liu J, Liang Y, Wu R, Zhao Y, Hong X, et al. Tumour-associated mutant p53 drives the Warburg effect. Nature communications. 2013;4:2935. PubMed PMID: 24343302. Pubmed Central PMCID: 3969270.
37. Korangath P, Teo WW, Sadik H, Han L, Mori N, Huijts CM, et al. Targeting Glutamine Metabolism in Breast Cancer with Aminooxyacetate. Clinical cancer research : an official journal of the American Association for Cancer Research. 2015 Jul 15;21(14):3263-73. PubMed PMID: 25813021. Pubmed Central PMCID: 4696069.
38. Chakrabarti G, Moore ZR, Luo X, Ilcheva M, Ali A, Padanad M, et al. Targeting glutamine metabolism sensitizes pancreatic cancer to PARP-driven metabolic catastrophe induced by ss-lapachone. Cancer & metabolism. 2015;3:12. PubMed PMID: 26462257. Pubmed Central PMCID: 4601138.
39. Lukey MJ, Wilson KF, Cerione RA. Therapeutic strategies impacting cancer cell glutamine metabolism. Future medicinal chemistry. 2013 Sep;5(14):1685-700. PubMed PMID: 24047273. Pubmed Central PMCID: 4154374.
40. Xiang Y, Stine ZE, Xia J, Lu Y, O'Connor RS, Altman BJ, et al. Targeted inhibition of tumor-specific glutaminase diminishes cell-autonomous tumorigenesis. The Journal of clinical

investigation. 2015 Jun;125(6):2293-306. PubMed PMID: 25915584. Pubmed Central PMCID: 4497742.
41. Gross MI, Demo SD, Dennison JB, Chen L, Chernov-Rogan T, Goyal B, et al. Antitumor activity of the glutaminase inhibitor CB-839 in triple-negative breast cancer. Molecular cancer therapeutics. 2014 Apr;13(4):890-901. PubMed PMID: 24523301.
42. Bunz F, Dutriaux A, Lengauer C, Waldman T, Zhou S, Brown JP, et al. Requirement for p53 and p21 to sustain G2 arrest after DNA damage. Science. 1998 Nov 20;282(5393):1497-501. PubMed PMID: 9822382.
43. Rosales KR, Reid MA, Yang Y, Tran TQ, Wang WI, Lowman X, et al. TIPRL Inhibits Protein Phosphatase 4 Activity and Promotes H2AX Phosphorylation in the DNA Damage Response. PloS one. 2015;10(12):e0145938. PubMed PMID: 26717153. Pubmed Central PMCID: 4696667.
44. Hernandez-Davies JE, Tran TQ, Reid MA, Rosales KR, Lowman XH, Pan M, et al. Vemurafenib resistance reprograms melanoma cells towards glutamine dependence. Journal of translational medicine. 2015;13:210. PubMed PMID: 26139106. Pubmed Central PMCID: 4490757.

Figures

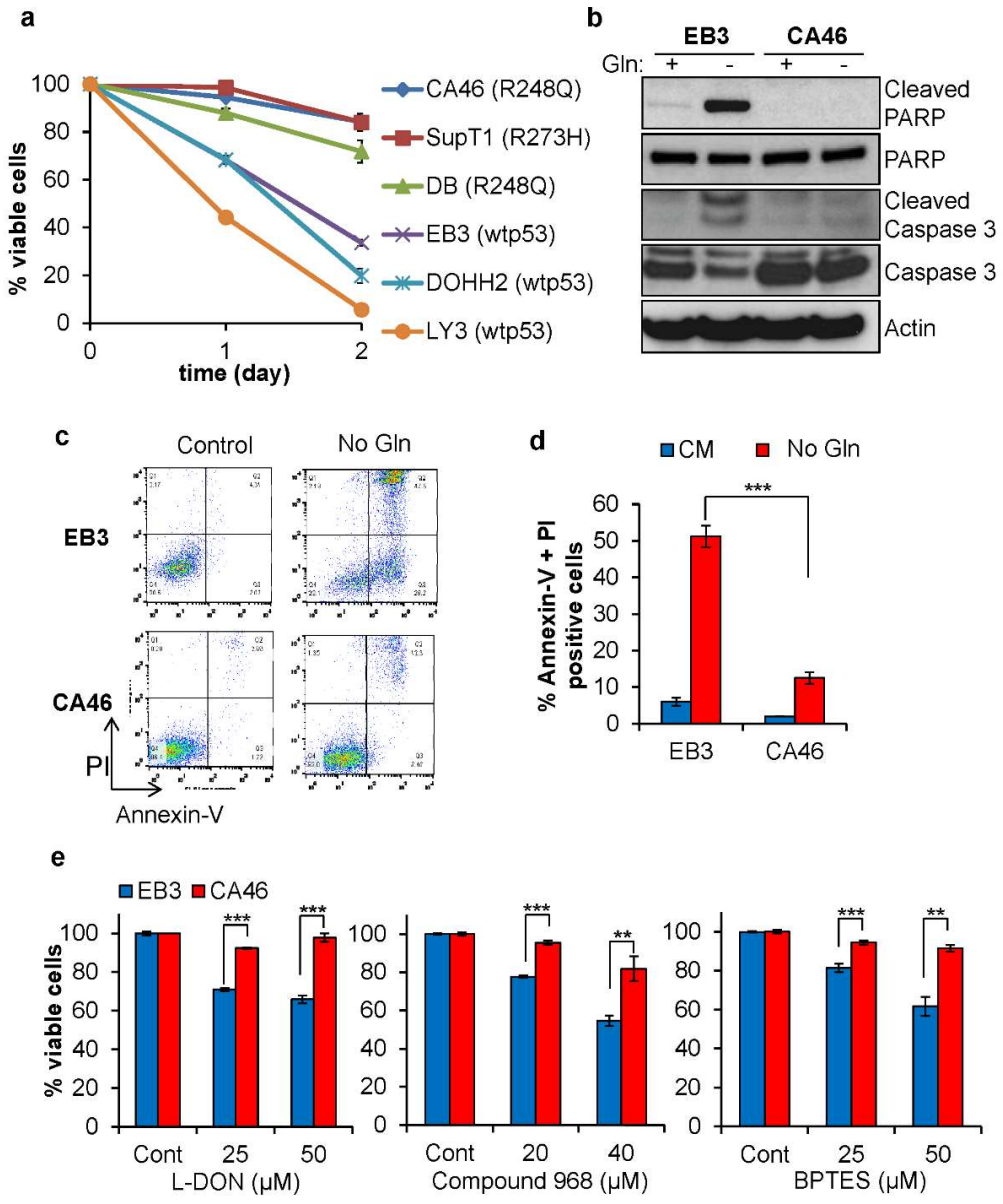

Figure 2-1. Cancer cells with mutp53 are more resistant to glutamine deprivation than cells with wtp53. (a) Lymphoma cell lines with known p53 status were cultured in complete or glutamine (Gln) free medium for 2 days. Viability was determined by propidium iodide (PI) exclusion and normalized to cells cultured in complete medium. Mutp53 cells: CA46, SupT1, DB. Wtp53 cells: EB3, DOHH2, LY3. **(b)** EB3 and CA46 cells were cultured in Gln free

medium for 24 hrs. Western blot was performed using antibodies as indicated. **(c,d)** EB3 and CA46 cells were cultured in complete or Gln free medium for 48 hrs. Apoptosis was assessed by staining cells with annexin-V and PI. Positive staining was measured by flow cytometry and analyzed with FlowJo. Representative graphs and percentage of late apoptotic cells (PI and annexin-V positive cells) are shown. Data represent mean ± S.D. of three independent experiments (***$P \leq .001$, Student's t test). **(e)** EB3 and CA46 cells were treated with L-DON for 3 days, Compound 968 and BPTES for 4 days. Cell viability was assessed by PI exclusion, and normalized to control treated cells. Data represents mean ± S.D. of three independent experiments (**$P < .01$, ***$P \leq .001$, Student's t test).

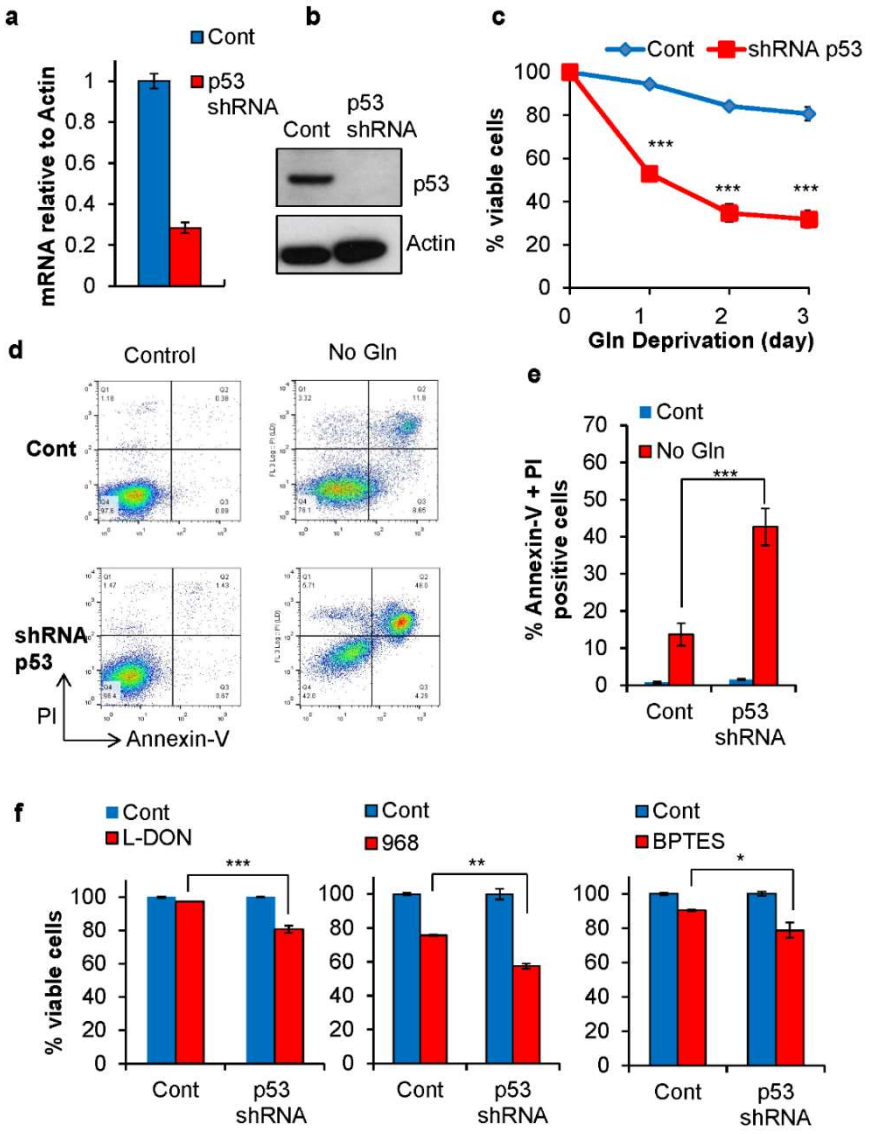

Figure 2-2. Loss of mutp53 sensitizes cancer cells to glutamine deprivation and glutaminase inhibitor treatment. (a-b) p53 mRNA levels **(a)** relative to actin and protein levels **(b)** in control vector and p53 shRNA transduced CA46 cells was assessed using qRT-PCR and Western blot. **(c)** The indicated control vector or shRNA p53 transduced cells were cultured in complete or Gln free medium for the indicated time points. Viability was assessed by PI exclusion and normalized to cells cultured in complete medium. Data represent mean ± S.D. of three independent experiments (***$P \leq .001$, Student's t test). **(d-e)** Annexin-V and PI staining of

stably transfected CA46 cells cultured in Gln free medium or complete medium for 24 hrs. Representative graphs of cells in late apoptosis (annexin-V and PI positive) are shown. Data represent mean ± S.D. of three independent experiments (***$P \leq .001$, Student's t test). **(f)** The control vector transduced cells and p53 shRNA transduced cells were treated with 12.5 μM L-DON for two days, 40 μM Compound 968 and 50 μM BPTES for four days. Cell viability was assessed by PI exclusion and normalized to control treated cells. Data represent mean ± S.D. of three independent experiments (*$P < .05$, **$P < .01$, ***$P \leq .001$, Student's t test).

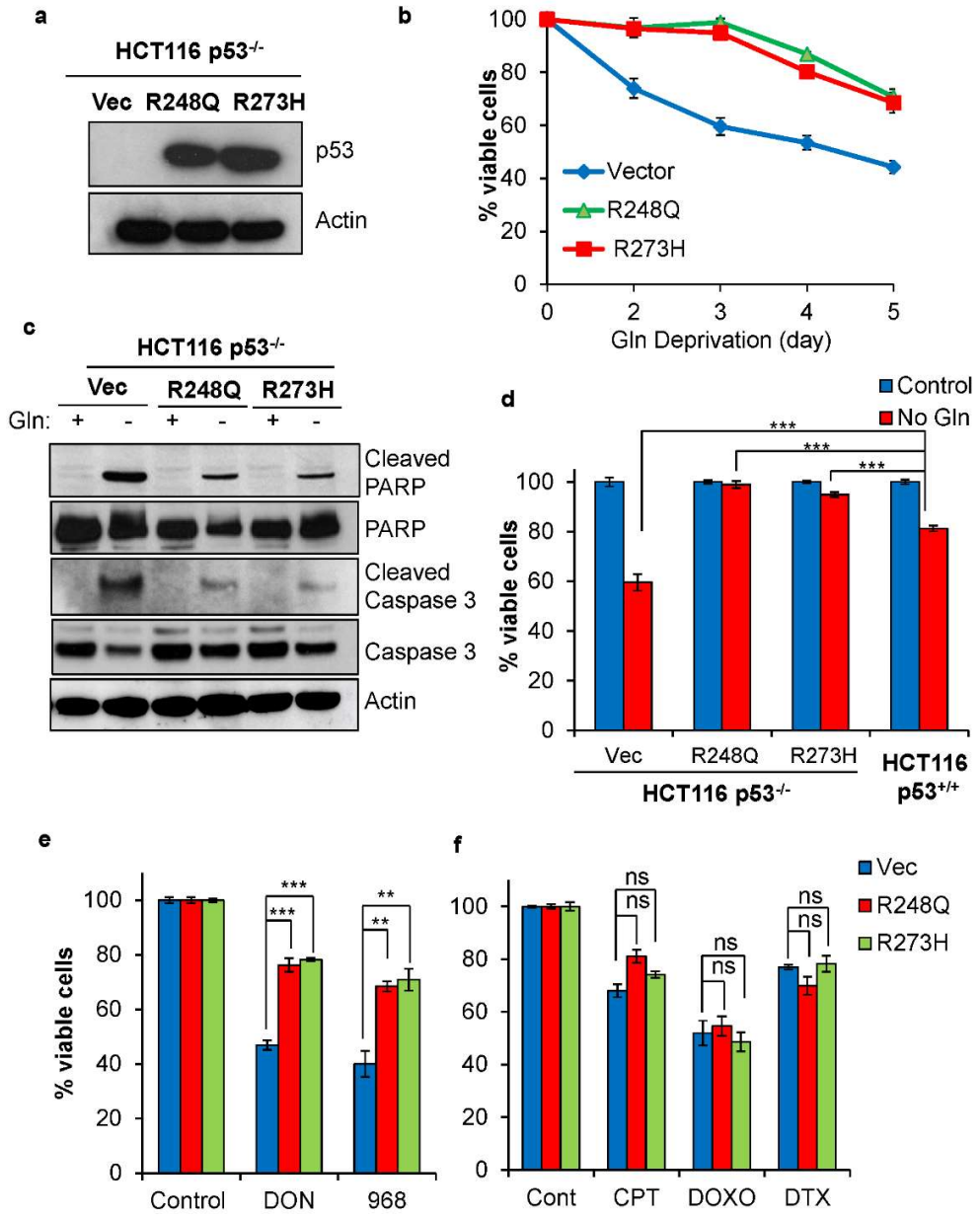

Figure 2-3. Expression of mutp53 promotes cell survival upon glutamine deprivation and glutaminase inhibitor treatment. (a) Mutp53 R248Q or R273H were stably expressed in p53 $^{-/-}$ HCT116 cells. Protein levels were assessed by Western blot using antibodies against p53 (DO-1) and actin. **(b)** HCT116 p53 $^{-/-}$ cells expressing an empty vector or mutp53 protein were cultured in either Gln free or complete medium for the indicated time points. Cell viability was determined by Trypan blue exclusion and normalized to cells cultured in complete medium. Data

represent mean ± S.E.M. of three independent experiments. **(c)** HCT116 $p53^{-/-}$ cells expressing an empty vector or mutp53 protein were cultured in Gln free medium or complete medium for 4 days. Lysate was extracted to perform Western blot analysis using antibodies as indicated. **(d)** HCT116 $p53^{-/-}$ cells expressing R248Q, R273H, or empty vector and HCT116 $p53^{+/+}$ cells were cultured in Gln free medium or complete medium for three days. **(e)** HCT116 $p53^{-/-}$ cells expressing R248Q, R273H, or empty vector were treated with 50μM L-DON for four days, or 40μM Compound 968 for five days. **(f)** HCT116 $p53^{-/-}$ cells expressing R248Q, R273H, or empty vector were treated with 5μM camptothecin (CPT) for three days, 10μM doxorubicin (DOXO) for four days, or 10 nM docetaxel (DTX) for two days. **(d-f)** Cell viability was determined by Trypan blue exclusion and normalized to cells cultured in complete medium. Data represent mean ± S.E.M. of three independent experiments (∗∗P<.01, ∗∗∗P≤.001, Student's t test).

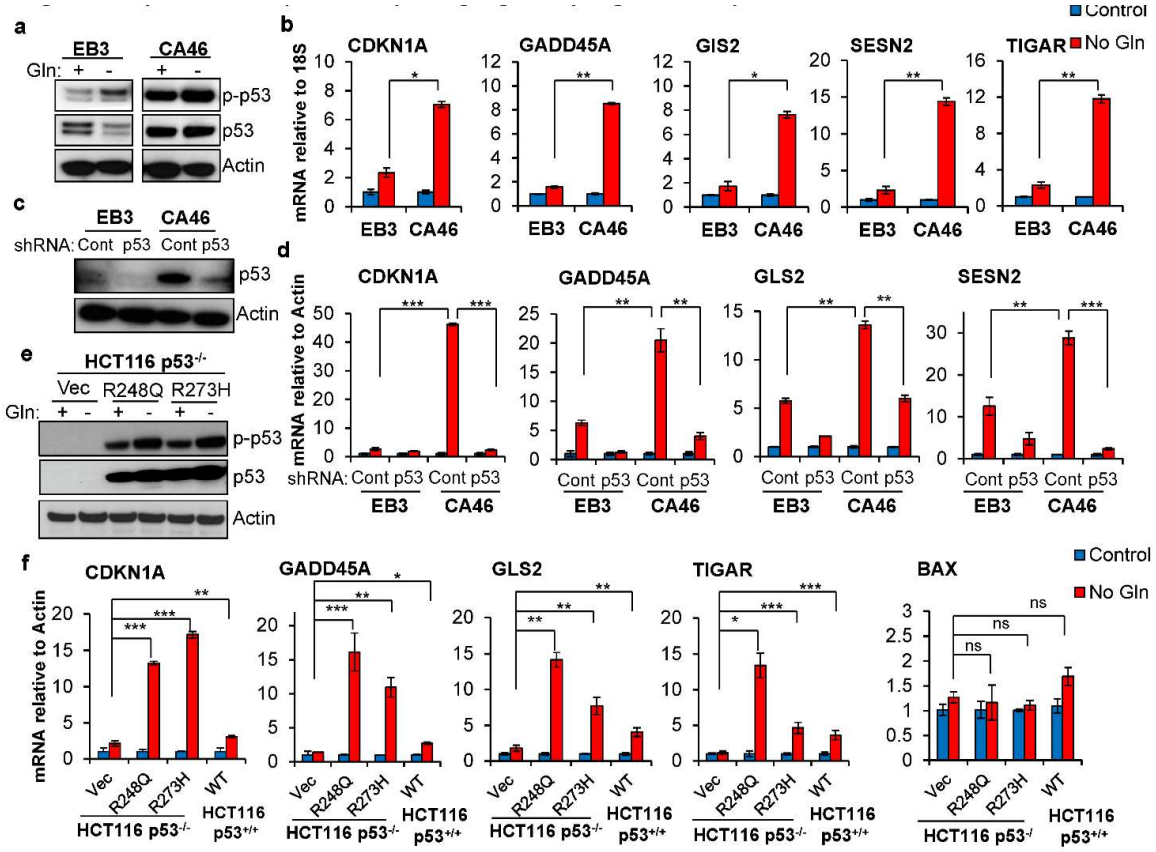

Figure 2-4. Mutp53 induces expression of p53 target genes upon glutamine deprivation. (a) EB3 and CA46 cells were cultured in complete or Gln free medium for 24 hrs. Cells were lysed for Western blot using antibodies as indicated. **(b)** EB3 and CA46 cells were cultured in complete or Gln free medium overnight. mRNA expression of p53 target genes relative to 18S was determined using qRT- PCR and normalized to the complete medium. **(c)** Cells were transduced with lenti-viral particles followed by puromycin selection to generate stable knockdown of wtp53 in EB3 cells and mutp53 in CA46. p53 protein levels were determined by Western blot. **(d)** EB3 and CA46 cells infected with virus containing control vector or shRNA against p53 were cultured in Gln free medium overnight. mRNA expression of p53 target genes relative to actin was determined using qRT- PCR and normalized to the complete control medium. **(e)** HCT116 $p53^{-/-}$ cells expressing R248Q, R273H, or empty vector were cultured in

Gln free medium for three days. p53 activation and total p53 expression was determined by Western blot analysis using anti-phospho-p53 (Ser15) and anti-p53 antibody. **(f)** HCT116 $p53^{+/+}$ cells and HCT116 $p53^{-/-}$ cells expressing R248Q, R273H, or empty vector were cultured in complete or Gln free medium overnight. mRNA expression of p53 target genes relative to actin was determined using qRT-PCR and normalized to the complete medium. Data represent mean ± S.D. of duplicates from two independent experiments (*P<.05, **P<.01, ***P≤.001, Student's t test).

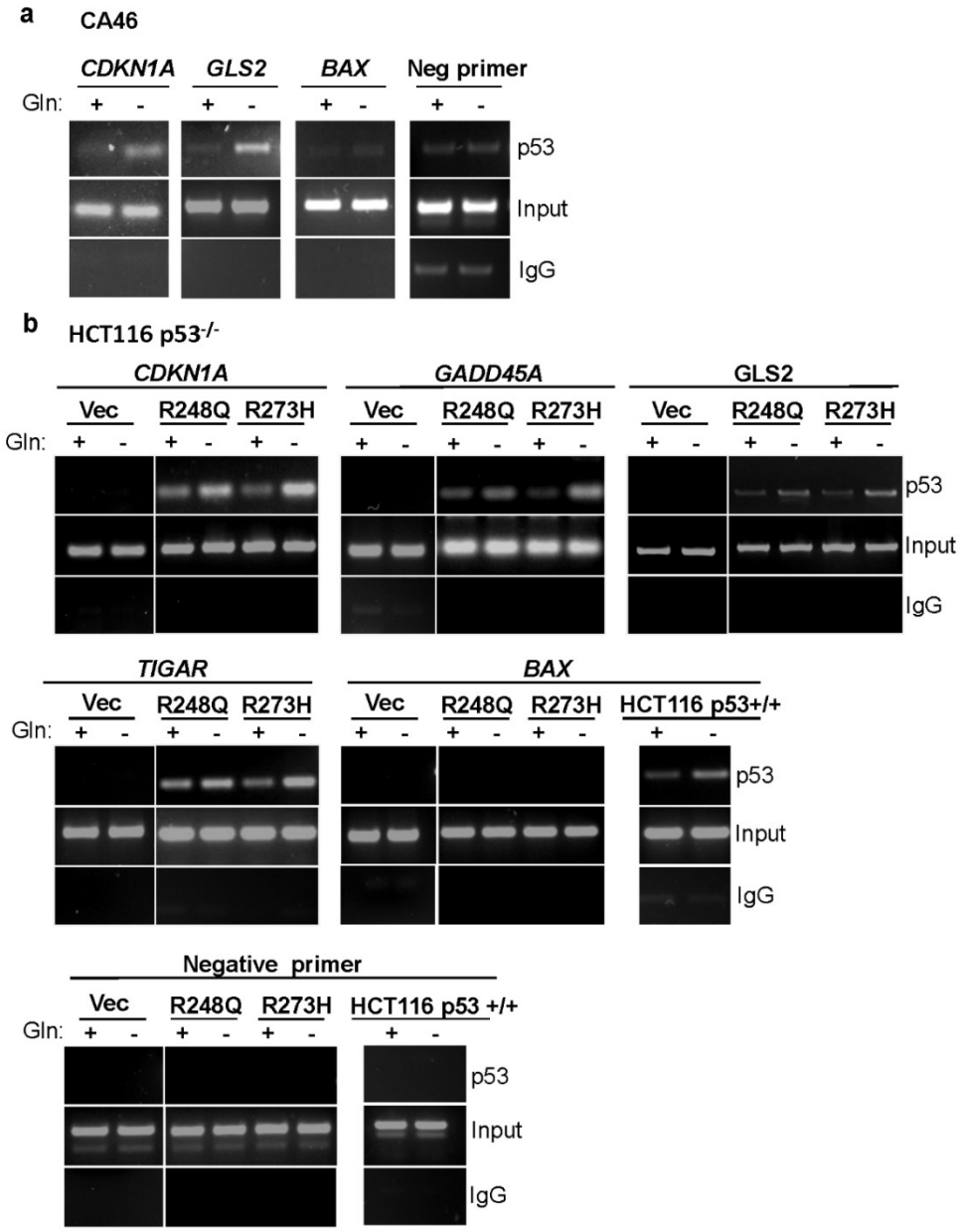

Figure 2-5. Mutp53 directly binds to the promoter of p53 target genes upon glutamine deprivation. (a) CA46 cells (R248Q) were cultured in complete or Gln free medium for 16 hrs. ChIP analysis was performed to determine p53 binding to the promoter of p53 target genes in response to Gln deprivation. **(b)** HCT116 $p53^{+/+}$ cells or HCT116 $p53^{-/-}$ cells expressing R248Q, R273H, or vector control were cultured in complete or Gln free medium for 16 hrs. ChIP analysis was performed to determine p53 binding to the promoter of p53 target genes. DNA-

protein complexes were pulled down using total p53 antibody (DO-1) or isotype matched IgG. All p53 binding sites were assessed by PCR. PCR products were separated using agarose electrophoresis.

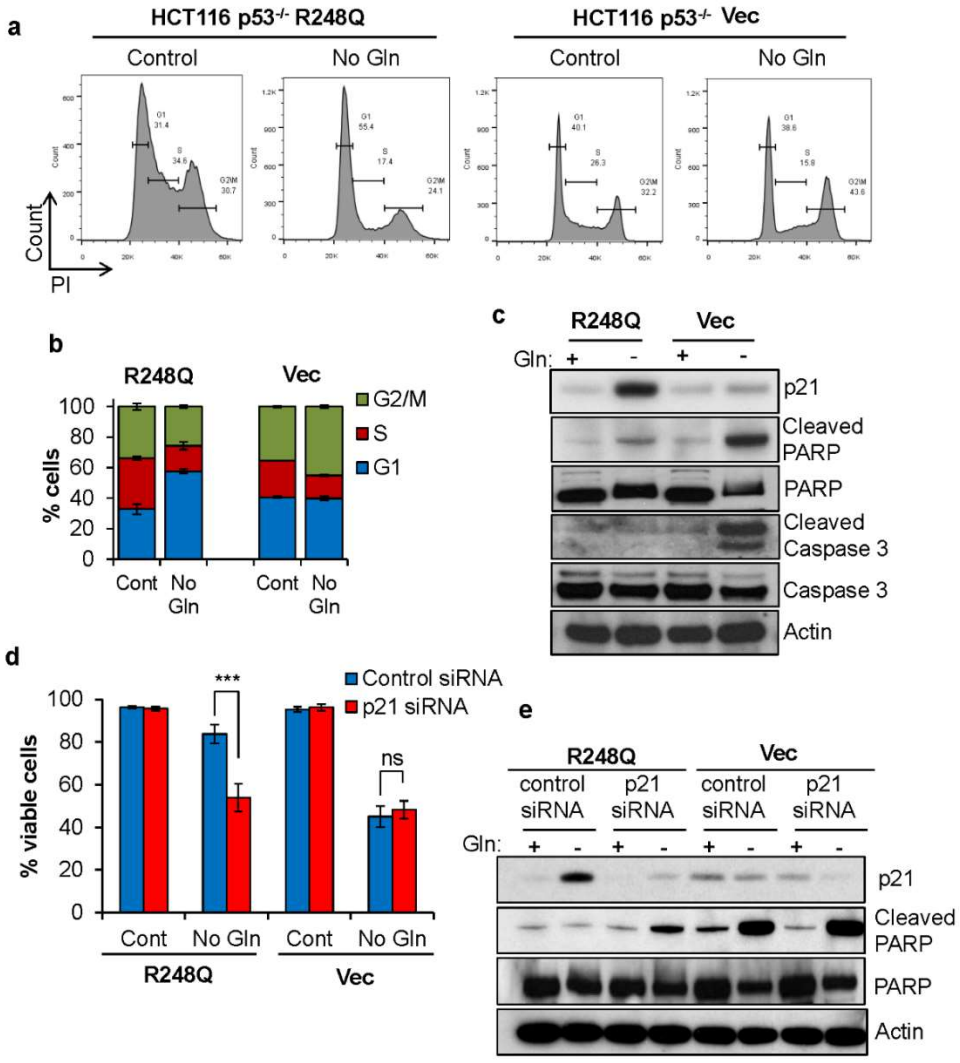

Figure 2-6. Mutp53 promotes cell survival upon glutamine deprivation through p21 induction. (a,b) HCT116 p53$^{-/-}$ cells expressing mutp53 (R248Q) or empty vector were cultured in complete or Gln free medium for 24 hrs. PI staining followed by Flow Cytometry was performed to assess cell cycle profile. Representative graphs of three independent experiments are shown. Data represent the mean ± S.D. **(c)** HCT116 p53$^{-/-}$ cells expressing mutp53 R248Q or empty vector were cultured in complete or Gln free medium for 24 hours. Western blots were performed using antibodies as indicated. **(d)** p21 was transiently knocked down in HCT116 p53$^{-/-}$ cells expressing mutp53 R248Q or empty vector using siRNA (20nM). 48 hrs after the siRNA

transfection, cells were cultured in complete or Gln free medium for four days. Cell viability was determined by Trypan blue exclusion. Data represent the mean ± S.D. of four independent experiments, (***$P \leq .001$, Student's t-test). **(e)** Western blot was performed using antibodies as indicated.

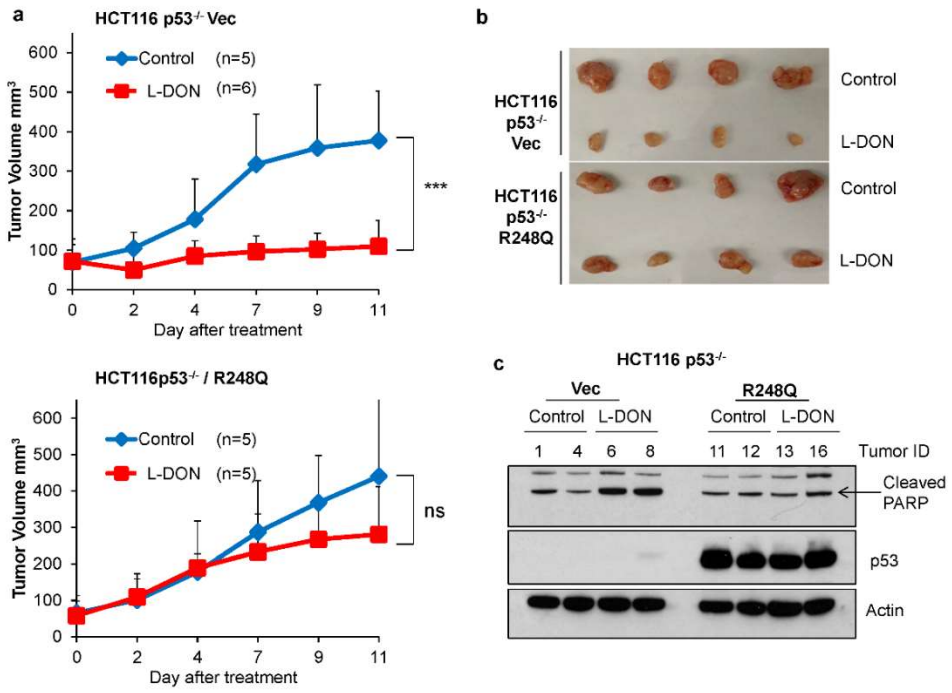

Figure 2-7. Tumors expressing mutant p53 are more resistant to glutaminase inhibitor treatment *in vivo.* (**a,b**) Athymic Nude mice at 7 weeks old were injected with HCT116 p53 $^{-/-}$ cells on the left flank. HCT116 p53 $^{-/-}$ cells expressing mutp53 R248Q were injected on the right flank. Once the tumor size reached an average of 60 mm^3, the mice were treated with 15 mg/kg of L-DON every other day by i.p. injection. Tumor size was measured over time. Data represent the mean ± S.D. (n=5 or 6 tumors as indicated), ***$P \leq .001$, Student's t-test. **(c)** Tumors with L-DON or vehicle treatment were harvested at day 11. Western blot was performed using the indicated antibodies.

Chapter 3

Glutamine deficiency induces DNA alkylation damage and sensitizes cancer cells to alkylating agents through inhibition of ALKBH enzymes

This chapter is partly derived from an article published in PLOS Biology, entitled "Glutamine deficiency induces DNA alkylation damage and sensitizes cancer cells to alkylating agents through inhibition of ALKBH enzymes." 10.1371. Journal.pbio.2002810

Summary

Driven by oncogenic signaling, glutamine addiction exhibited by cancer cells often leads to severe glutamine depletion in solid tumors. Despite this nutritional environment that tumor cells often experience, the effect of glutamine deficiency on cellular responses to DNA damage and chemotherapeutic treatment remains unclear. Here, we show that glutamine deficiency, through the reduction of alpha-ketoglutarate, inhibits the ALKBH enzymes activity and induces DNA alkylation damage. As a result, glutamine deprivation or glutaminase inhibitor treatment, triggers DNA damage accumulation independent of cell death. In addition, low glutamine-induced DNA damage is abolished in ALKBH deficient cells. Importantly, we show that glutaminase inhibitors, DON or CB-839, hypersensitize cancer cells to alkylating agents both *in vitro* and *in vivo*. Together, the crosstalk between glutamine metabolism and the DNA repair pathway identified in this study highlights a potential role of metabolic stress in genomic instability and therapeutic response in cancer.

Introduction

Metabolic alterations exhibited by cancer cells can potentiate tumorigenesis and promote cell survival (1, 2). Unlike normal cells, cancer cells favor aerobic glycolysis, also known as the Warburg effect, to support rapid proliferation (3). As most glucose is converted into lactate, cancer cells become heavily dependent on glutamine as a major carbon and nitrogen source (4). Glutamine metabolism supports rapidly proliferating cells by facilitating the biosynthesis of different amino acids and nucleotides (3, 5). Moreover, glutamine supports the increased energetic demand and suppresses accumulated reactive oxygen species (ROS) exhibited in cancer cells (6). Specifically, glutamine is diverted to synthesize the tricarboxylic acid cycle (TCA cycle) intermediate, alpha-ketoglutarate (αKG), to replenish the truncated TCA cycle and maintain healthy NADH and NADPH levels (6-8). Moreover, the amino acid drives the production of glutathione, a major antioxidant, to protect cancer cells from ROS accumulation (9). Inhibition of glutamine metabolism with small molecule inhibitors results in an energetic crisis leading to cellular death in some cancers (10, 11).

On the other hand, the increased glutamine uptake in cancer cells coupled with poor vascularization in tumors often leads to severe glutamine shortage in the tumor microenvironment (12, 13). For example, metabolomics studies on human pancreatic cancers patient samples have clearly demonstrated that glutamine, besides glucose, is one of the most depleted metabolites in tumors compared to adjacent healthy tissues (13). In addition, core regions of solid tumors display extreme glutamine deficiency compared to peripheral regions in melanoma xenografts and transgenic mouse tumors (14). Interestingly, many cancer cells appear to adapt to this strong metabolic stress through multiple mechanisms, including p53 and IKKβ

activation (15-17). However, it remains unclear how glutamine deficiency observed in tumors impacts tumor development and therapeutic response.

Genomic instability plays a significant role in tumorigenesis and aging (18). While cellular DNA is constantly exposed to both endogenous and exogenous DNA damaging agents, the damages are regularly repaired by the robust DNA damage repair pathways (19). The ALKBH enzymes are dioxygenases that directly reverse DNA alkylation damage caused by both endogenous and exogenous sources, and help maintain genomic integrity (20, 21). Interestingly, ALKBH overexpression in cancer promotes drug resistance leading to poor prognosis in multiple cancers (22, 23). For example, ALKBH2 overexpression induces cellular resistance to alkylating agent treatment in glioblastoma and promotes cancer progression in bladder cancer (23, 24). Moreover, ALKBH3 overexpression promotes alkylation damage resistance in prostate cancer and apoptotic resistance in pancreatic cancer (25-27). In response to DNA alkylation damage, the Fe(II) dependent ALKBH enzymes use αKG as a key substrate to directly remove alkyl groups from DNA adducts (21). The requirement of αKG by the ALKBH enzymes to repair DNA alkylation damage underlines the potential crosstalk between cellular metabolism and the DNA damage repair pathway. Because glutamine catabolism directly contributes to cellular αKG pools in many cancers (14), it will be of interest to examine whether glutamine deficiency affects the DNA repair function of the αKG-dependent ALKBH enzymes.

In this study, we found that glutamine deficiency inhibits the ALKBH enzymes from repairing DNA alkylation damage, leading to DNA damage in the absence of the genotoxic agent. Importantly, our results demonstrate that targeting glutamine metabolism significantly sensitizes cancer cells to alkylating agent treatments both *in vitro* and *in vivo*. Together, our study reveals a previously unidentified role of glutamine deficiency in modulating the DNA damage response

and provides a molecular basis for combinational therapy using glutaminase inhibitors and alkylating agents.

Results

Glutamine deficiency specifically triggers DNA damage accumulation independent of cell death

To determine the impact of glutamine deficiency on genomic integrity, we first asked whether glutamine depletion leads to accumulation of DNA damage. Mouse embryonic fibroblast (MEF) cells and prostate cancer PC3 cells were cultured in complete or glutamine free medium for 24 hours followed by immunofluorescence for γH2AX, an established biomarker for DNA damage (28). We found that glutamine withdrawal led to a significant induction of γH2AX in both MEF and PC3 cells (Fig 3-1A). Using immunoblotting, we found that low glutamine-induced γH2AX signal was both dose-dependent and time-dependent (S1A, B Fig). Consistently, glutamine withdrawal resulted in striking accumulation of DNA damage as marked by γH2AX in multiple cancer cell lines (Fig 3-1B). Compared to glutamine deprivation, starvation of any other amino acid failed to induce γH2AX (Fig 3-1C). Unlike glutamine deprivation, deprivation of glucose for the same amount of time, failed to induce γH2AX in both MEF and EB3 cells, supporting that glutamine deficiency specifically induces DNA damage (Fig 3-1D).

While prolonged glutamine starvation triggers cell death (29), γH2AX induction was detected when the majority of cells were still viable (Fig 3-1D). To further confirm that glutamine deficiency induces γH2AX independent of cell cycle arrest and cell death, we assessed γH2AX levels in MEF cells cultured in low glutamine conditions or low glucose conditions over time. Glutamine deficiency dramatically induced γH2AX on day 1 and peaked on day 2 when

apoptotic cell death was not detected. In contrast, the γH2AX induction in low glucose conditions was marginal compared to low glutamine conditions, and possibly caused by the activation of apoptotic cell death as marked by the induced cleaved PARP (Fig 3-1E). Interestingly, we found that low glutamine and low glucose inhibited cell proliferation to a similar extent, suggesting that cell cycle arrest may not significantly contribute to the DNA damage (Fig 3-1E). In addition, immunofluorescence for γH2AX and the apoptotic marker, cleaved caspase-3, further revealed that the majority of γH2AX positive cells were not apoptotic cells (Fig 3-S1C). To further confirm that glutamine deprivation induced γH2AX is independent of apoptosis, we used *Bax*$^{-/-}$/*Bak*$^{-/-}$ MEF cells, which lack apoptotic machinery (Fig 3-S1D) (30). We found that glutamine deprivation still promotes γH2AX in apoptosis-deficient cells (Fig 1F). Lastly, while γH2AX is a reliable marker for DNA damage, γH2AX is also induced during DNA replication stress (31) and cellular death (32). To examine whether glutamine depletion triggers physical breaks in DNA, we performed immunofluorescence to detect γH2AX and 53BP1 colocalizations, which occur at DNA double strand breaks (DSB) (33, 34). Similar to doxorubicin treatment that induced DSB, glutamine depletion triggered γH2AX and 53BP1 foci colocalization in both MEF and PC3 cells, demonstrating that glutamine depletion can result in DSBs (Fig 3-1G). Consistently, DNA damage-induced signaling pathways are increased upon glutamine deprivation (Fig 3-1H). Taken together, these results demonstrate that glutamine deficiency specifically triggers DNA damage accumulation independent of cell death.

Inhibition of glutamine metabolism with a glutaminase inhibitor triggers DNA damage accumulation both *in vitro* and *in vivo*

Glutamine withdrawal not only hinders glutaminolysis but also affects other functions of intracellular glutamine including, but not limited to, protein synthesis and mTOR regulation (35,

36). To determine whether inhibition of glutaminolysis alone can trigger DNA damage, we assayed for the induction of γH2AX by immunofluorescence in PC3 cells after treatment with the glutaminase inhibitor, 6-Diazo-5-oxo-L-norleucine (DON). The drug treatment significantly induces γH2AX in PC3 cells (Fig 3-2A, B). In addition, the glutaminase inhibition in PC3 cells induced robust DSBs as indicated by the γH2AX and 53BP1 co-localization (Fig 3-2C). Moreover, different glutaminase inhibitors, such as DON and BPTES, induced γH2AX in multiple cell lines (Fig 3-2D). Importantly, DON and BPTES also induced DNA damage in apoptosis-deficient cells (Fig 3-2E). To determine whether inhibition of glutamine metabolism also triggers DNA damage *in vivo*, we treated HT1080 xenograft tumors with DON. Immunohistochemistry (IHC) staining revealed that DON treatment dramatically induced γH2AX levels, but not cleaved caspase-3 levels (Fig 3-2F). Using immunoblotting, we also confirmed dramatic γH2AX induction in the DON treated tumors compared to control treated tumors in HT1080, PC3 and HCT116 xenograft tumors (Fig 3-2G-I). Therefore, similar to glutamine starvation, inhibition of glutamine metabolism also triggered DNA damage both *in vitro* and *in vivo*.

Glutamine deficiency-induced DNA damage is αKG dependent

Cancer cells convert glutamine into glutamate that can be subsequently used to synthesize the antioxidant glutathione (GSH) and αKG (Fig 3-3A) (7, 9). To test whether glutamine deficiency induces ROS that contributes to DNA damage, we measured ROS levels after glutamine withdrawal and found that glutamine starvation rapidly promoted ROS accumulation, which was fully abolished with an antioxidant supplement of either N-Acetyl Cysteine (NAC) or glutathione (GSH) (Fig 3-3B). Next, we confirmed that glutamine depletion and glutaminase inhibitor treatment diminished intracellular αKG levels in cells, consistent with previous studies (Fig 3-3C

and S2) (7, 37). However, despite the ability of both NAC and GSH to block ROS induction, they failed to inhibit the DNA damage caused by glutamine deficiency (Fig 3-3D). Interestingly, supplementing with dimethyl-αKG (DM-αKG) completely abolished low-glutamine induced DNA damage, suggesting that αKG plays a critical role in maintaining genomic integrity in glutamine depleted cells (Fig 3-3D,E). Consistently, DM-αKG reversed the γH2AX induction upon glutaminase inhibitor treatment (Fig 3F). Thus, the induction of DNA damage upon glutamine deprivation or glutaminase inhibitor treatment is mediated by the depletion of intracellular αKG.

Glutamine deficiency inhibits ALKBH activity and induces endogenous DNA alkylation damage

ALKBH enzymes require αKG as an essential cofactor to repair DNA alkylation damage and maintain genomic integrity (38). Because glutamine deficiency leads to dramatic reduction of intracellular αKG levels, we next investigated if such metabolic stress inhibits the DNA damage repair by ALKBH enzymes. We first performed enzymatic activity assays for ALKBH3 using extracted intracellular metabolites from cells cultured in complete medium or low glutamine medium. Both αKG and the extracted metabolites from control cells robustly promoted the ALKBH3 enzyme to remove methyl groups from 3-methyl cytosine (3meC) adducts (Fig 3-4A, B). In contrast, extracted metabolites from glutamine deprived cells failed to support ALKBH3 enzymatic activity in both MEF and EB3 cell lines, suggesting that glutamine deprivation inhibits the activity of ALKBH enzymes through the alteration of intracellular metabolites, but not other signaling pathways. To further determine whether glutamine deficiency inhibits ALKBH enzymes to repair alkylated DNA adducts in the cells, we performed dot blot analysis with a 3meC specific antibody to measure global genomic 3meC in cells cultured in complete

medium or glutamine free medium. As shown in Fig 4C, glutamine deficiency significantly induced 3meC in cells to a similar extent as methyl methanesulfonate (MMS) treatment, consistent with the ALKBH activity and γH2AX levels. Importantly, glutamine deficiency induced 3meC accumulation was largely rescued by DM-αKG supplementation (Fig 3-4D). Furthermore, glutamine deprivation failed to induce further alkylation damage as marked by 3meC levels in the ALKBH3 depleted cells (Fig 3-S3A).

To test the hypothesis that low glutamine-induced DNA damage is caused by ALKBH inhibition, we cultured *Alkbh2*$^{-/-}$ MEF, *Alkbh3*$^{-/-}$ MEF, and paired *wild-type* MEF cells in glutamine free medium or complete medium overnight. We found that *Alkbh2*$^{-/-}$ and *Alkbh3*$^{-/-}$ MEF cells exhibited higher γH2AX levels in complete medium compared to the *wild-type* MEF cells (Fig 3-4E, F and S3B), suggesting that ALKBH actively protects cells from endogenous alkylating agents. Importantly, glutamine depletion failed to further promote γH2AX induction in ALKBH3 knockout or ALKBH2 knockout MEF cells compared to the wild-type cells (Fig 3-4E, F and S3B). Similarly, we found no further increase in γH2AX upon glutamine starvation in ALKBH3 knockdown PC3 cancer cells (Fig 3-4G, H). In contrast, treatment of the topoisomerase inhibitor camptothecin (CPT) further promoted DNA damage in the ALKBH3 knockdown cells (Fig 3-S3C). In addition, we found that DM-αKG, which rescued low-glutamine induced DNA damage in control cells, failed to rescue the DNA damage in ALKBH deficient cells (Fig 3-S4A, B). Together, these data indicate that glutamine depletion, by reducing the key cofactor αKG, inhibits the ALKBH enzyme from repairing endogenous DNA alkylation damage.

Glutamine deficiency sensitizes cells to alkylating-agent induced DNA damage

We next sought to determine whether glutamine deficiency can sensitize cells to alkylating-agent induced DNA damage. We cultured cells that were initially exposed to the alkylating agent, MMS, for 1 hour in complete medium or low glutamine medium. Induction of γH2AX was absent in the non-treated cells, but was present after MMS treatment (Fig 3-5A). For cells cultured in complete medium, the γH2AX signal peaked 3 hours after MMS treatment but diminished after 6 hours upon removal of the drug. In contrast, γH2AX signals in low glutamine conditions remained high after the drug removal even after 9 hours later while low glutamine alone at 9 hours had no effect on γH2AX (Fig 3-5A). These results indicate that low glutamine conditions inhibit the ability of ALKBH enzymes to repair DNA damage caused by the alkylating agent. Consistently, immunofluorescence of γH2AX revealed that glutamine deficiency potentiated DNA damage caused by the alkylating agent (Fig 3-5B). Interestingly, glutamine starvation did not affect the DNA damage caused by other classes of chemotherapy, including the topoisomerase inhibitor doxorubicin (Doxo) and CPT, suggesting that glutamine deficiency only affects alkylation damage repair, but not other DNA damage repair pathways (Fig 3-5C). To further determine whether glutamine deficiency attenuates ALKBH activities to repair methylated DNA adducts upon alkylating agent treatment, we cultured alkylating agent-treated cells in either complete or glutamine free medium, and measured global genomic 3meC levels. The 3meC levels increased after MMS treatment for 1 hour. The drug was then washed out and cells were cultured in complete medium or glutamine free medium for 8 hours. Intriguingly, MMS treatment in combination with glutamine starvation at 8 hours resulted in the highest induction of 3meC compared to the single treatments, highlighting that glutamine deficiency potentiates alkylating agent-induced DNA damage by directly interfering with the ALKBH enzymes to repair alkylation damage (Fig 3-5D). Furthermore, the addition of cell

permeable DM-αKG largely blocked MMS-induced γH2AX, suggesting that glutamine deficiency potentiates the MMS effect via αKG reduction (Fig 3-5E).

Inhibition of glutamine metabolism hypersensitizes cells to alkylating agents

Alkylating agents, one of the earliest classes of chemotherapy, remain as frontline therapies for multiple aggressive types of cancer (39). To investigate the effect of glutamine deficiency on cellular response to alkylating agents, we treated Ras-transformed MEF cells with different glutaminase inhibitors in combination with alkylating agents. Inhibition of glutamine metabolism with either DON or BPTES hyper-sensitized cancer cells to MMS treatment at multiple doses (Fig 3-6A). Importantly, low glutamine conditions and glutaminase inhibitor treatment had similar effects on cellular response to alkylating agents, suggesting that these glutaminase inhibitors function via inhibition of glutamine catabolism (Fig 3-6A). Consistently, impairing glutamine metabolism in combination with the alkylating agent resulted in robust apoptotic cell death compared to the single treatment as measured by cleaved caspase-3, cleaved PARP (Fig 6B), and Annexin/PI staining (Fig 3-6C, D). Interestingly, the glutaminase inhibitor treatment failed to sensitize cancer cells to other DNA damaging agents, such as DOXO or CPT, indicating that inhibition of glutamine metabolism only affects methylation damage repairs, but not DSB repairs (Fig 3-S5). Additionally, we confirmed the striking synergistic killing seen in human fibrosarcoma cells HT1080. The glutaminase inhibitor BPTES significantly sensitized cancer cells to both MMS and the clinical alkylating agent Lomustine (CCNU), confirming that the combination works on a broad range of alkylating agents and across a broad range of cancers (Fig 3-6E, F). Overexpression of ALKBH enzyme in prostate cancer and glioblastoma results in cell resistance to alkylating agents leading to poor prognosis as shown in multiple studies (22, 24, 27). Therefore, we further tested whether inhibition of glutamine metabolism can indirectly

inhibit ALKBH and restore cancer cell sensitivity to alkylating agents. Significantly, the combination treatment of MMS and BPTES resulted in a striking synergistic killing of PC3 cells which have high expression levels of ALKBH3 compared to other prostate cancer cell lines (Fig 3- 6G) (27). Moreover, we confirmed that the ALKBH enzymes primarily mediated the combinational effect because the knockdown of ALKBH3 was sufficient to sensitize the PC3 cells to alkylating agents and abolish the effect of glutaminase inhibitor (Fig 3-6H). In addition, we also found that αKG plays a critical role in cell survival upon alkylating agent treatment as the addition of DM-αKG prevented MMS-induced cell death (Fig 3-6I). Importantly, exogenous DM-αKG abolished the ability of low-glutamine to sensitize cells to MMS treatment, suggesting that glutamine deprivation sensitizes cancer cells to alkylating agent via the depletion of αKG (Fig 3- S6A, B).

Combination treatment of glutaminase inhibitor and alkylating agent suppresses tumor growth *in vivo*

We tested whether the combinational treatment can be used to inhibit cancer growth *in vivo*. Athymic nude mice were used to establish xenograft tumors with alkylating agent resistant PC3 cells. Once the tumors reached an average tumor size of 60 mm^3, the mice were treated with PBS control, DON, MMS or combination of DON and MMS, and the tumor volumes were measured over time. MMS treatment alone and a low dose of DON treatment did not dramatically affect tumor growth. However, the combination treatment significantly impaired tumor growth compared to the single drug treatment (Fig 3-7A). We also found that DON treatment significantly depleted αKG levels in tumors (Fig 3-S7A). Additionally, IHC analysis with the proliferation marker Ki-67 revealed that combination drug treatment effectively inhibited cancer cell growth, while single drug treatment only had a marginal effect on cell proliferation,

consistent with tumor growth over time (Fig 3-7B). While MMS or DON single treatments marginally induced γH2AX, the combination of DON and MMS treatment significantly induced γH2AX levels, suggesting that glutaminase inhibitor enhanced the DNA damage induced by the alkylating agent *in vivo* (Fig 3-7C). To further confirm the potential clinical applicability of the drug combination, we performed an additional *in vivo* experiment with MMS and CB-839, a specific and effective glutaminase inhibition which is currently in clinical trials. To determine the combinational effect on tumor growth, mice harboring tumors were treated with 200mg/kg of CB-839 once a day which is half the dose used in the previous publication (40). We found that the CB-839 treatment significantly depleted αKG levels in tumors (Fig 3- S7B). Importantly, combination treatment suppressed tumor growth and reduced tumor weight more effectively than the single drug treatment alone (Fig 3-7D). Together, these results suggest that inhibition of glutamine metabolism offers a substantial therapeutic benefit when combined with alkylating agents.

Discussion

Poorly organized vasculature regions of tumors are often subjected to glutamine limitation, yet the impact of the metabolic stress on tumor development and drug response remains largely unknown. In this study, we found that glutamine deficiency inhibits ALKBH enzymes from repairing DNA alkylation damage. As a result, glutamine deficiency triggers robust DNA damage accumulation both *in vitro* and *in vivo* (Fig 1, 2). Importantly, inhibition of glutamine metabolism with small molecule inhibitors hyper-sensitizes cancer cells to alkylating agents both in cell culture and animal models (Fig 3-6, 7). Together, the study reveals previously unidentified roles of glutamine deficiency in potentiating genomic instability and modulating drug response in cancer.

We identified a novel crosstalk between glutamine metabolism and the DNA damage response. Our data reveals that glutamine deficiency, through diminishing αKG levels, inhibits the DNA repair ALKBH enzymes (Fig 3- 3, 4). It is well established that glutamine can be diverted to synthesize the TCA intermediate αKG in many cancer cell types to fuel the truncated TCA cycle and maintain redox homeostasis (7, 41). However, recent studies indicated that glutamine's contribution to the TCA is both environment and tumor specific. For example, while it has been shown that glutamine is not a major source of αKG in gliomas and lung tumors (42, 43), other studies support that glutamine metabolism is the main source of TCA intermediates *in vivo* in liver tumors, kidney tumors, and melanoma (14, 44, 45). Indeed, metabolomics analysis using ^{13}C-glutamine tracing have demonstrated that αKG is directly derived from glutamine in MYC-driven tumors and KRAS-driven tumors (7, 37). Here, we measured αKG levels upon glutaminase inhibitor treatment *in vivo* and found that both DON treatment and CB-839 treatment significantly reduced intracellular αKG levels in prostate cancer xenograft tumors (S7 Fig). In addition, our results indicate that low-glutamine mediated αKG depletion blocks the DNA repair activity of ALKBH (Fig 3-3,4). To repair DNA methylation damage, the ALKBH enzymes transfer a methyl group from the DNA adduct onto αKG and release succinate and formaldehyde as by-products (20). We demonstrated that the reduced αKG availability is sufficient to inhibit ALKBH activity leading to both endogenous DNA alkylation damage and sensitivity to alkylating agents. Importantly, this effect is only specific to glutamine limitation, but not genotoxic stress or glucose starvation. Consistently, the oncometabolite 2-hydroxyglutarate, produced by mutated IDH enzymes, is an αKG structural analog that competitively binds and inhibits many αKG dependent enzymes including ALKBH (46, 47).

Our results provide insights into the mechanism by which metabolic stress, such as glutamine deficiency, contributes to tumorigenesis. It is well established that glutamine metabolism via glutathione production contributes to the suppression of ROS and ROS-induced DNA damage (48, 49). Surprisingly, we now show that glutamine metabolism plays an important role in maintaining genomic integrity by maintaining the ALKBH activity instead of suppressing ROS accumulation (Fig 3-3). A variety of alkylating agents from the environment as well as by-products of intracellular metabolism, such as S-adenosylmethionine (SAM) (39, 50) often lead to intracellular alkylation damage, which is estimated to be equivalent to the exposure of 20 nM MMS (39, 51). The ALKBH enzymes contribute significantly to the repair of these sites of alkylation damage, as ALKBH3 knockdown alone is sufficient to induce alkylated DNA adducts in some cancers as demonstrated in previous reports and Figure 4 (27). Our data indicate that glutamine deficiency in tumors inhibits the repair of endogenous DNA damage mediated by the ALKBH enzymes leading to the accumulation of alkylated DNA adducts and DSBs. Thus, metabolic stress, such as glutamine deficiency, may contribute to genomic instability and promote tumorigenesis.

Lastly, our study provides an important molecular basis for combinational therapy to sensitize cells to alkylating agent treatment using glutaminase inhibitors. Alkylating agents remain important frontline antineoplastic drugs for many highly aggressive and metastatic cancers despite high toxicity and carcinogenic potential (39). However, malignant cells often become resistant to such treatments due to robust DNA repair machineries (52, 53). For example, ALKBH enzymes have been shown to be overexpressed in some human cancers to promote drug resistance and tumor progression (24). Our study demonstrates that targeting glutamine metabolism inhibits the DNA repair activity of the ALKBH enzymes and sensitizes cancer cells

to alkylating agent treatment. Therefore, this novel combination drug treatment can improve efficacy and minimize the side effects of alkylating agents. In addition, glutaminase inhibitor treatment, by indirectly inhibiting the ALKBH enzymes, may serve as an effective strategy to block the oncogenic function of ALKBH enzymes and restore cancer cell sensitivity to alkylating agents. Moreover, a new glutaminase inhibitor, CB-839, is well tolerated in patients and has passed phase 1 clinical trials for multiple cancers (54, 55). Our data here provides a new direction to use CB-839 clinically to sensitize cancer cells, particularly cancers with ALKBH overexpression, to alkylating agents.

Materials and methods

Ethics Statement

All animal work have been conducted according to the approved Institutional Animal Care and Use Committee (IACUC) protocols at the City of Hope Cancer Center (11011).

Cell culture and reagents

3T3-MEF and HT1080 cells were purchased from American Type Culture Collection (ATCC). HCT116 $p53^{-/-}$, Ras transformed 3T3-MEF cells, and M229 have been generated previously (14, 56). *Bak*$^{-/-}$ /*Bax*$^{-/-}$ MEF and paired wild-type MEF were gifts from Dr. Craig Thompson laboratory at Sloan-Kettering Cancer Center (30). *Alkbh3*$^{-/-}$ MEF and paired *wild-type* MEF were obtained from Dr. Timothy O'Connor laboratory at City of Hope (57). These cells were cultured in Dulbecco's Modified Eagle Medium (DMEM, Corning) supplemented with 10% fetal bovine serum (FBS, Gemini Bio-Products), 100 units/mL of penicillin, and 100 µg/mL of streptomycin

(Gemini Bio-Products). PC3, EB3, Namalwa, DB and CA46 were purchased from ATCC and cultured in RPMI 1640 medium supplemented with 10% FBS and penicillin/streptomycin. All cells were cultured at 37˚C with 5% CO_2. Cells were routinely tested for mycoplasma contamination using MycoAlert Mycoplasma Detection Kit.

Reagents: L-DON, BPTES, camptothecin (CPT), doxorubicin (Doxo), N-Acetyl-L-cysteine (NAC), methyl methanesulfonate (MMS), dimethyl 2-oxoglutarate (dimethyl-αKG) were purchased from Sigma. Glutathione monoethyl ester (353905) was purchased from Calbiochem. Lomustine (CCNU) and CB-839 was purchased from Selleckchem.

Glutamine and amino acid starvation

Glutamine starvation was described previously (16). Briefly, cells were washed once with PBS and cultured in complete medium or glutamine free medium. For the glucose starvation experiment, DMEM without glucose (Invitrogen 11966) was supplemented with 10% dialyzed FBS (Gemini) to make glucose free medium. Glucose (Sigma) was added back to the glucose free medium to make the complete medium (25mM) or low-glucose medium (1mM). For the amino acid starvation experiments, DMEM Ham's F-12 medium without amino acids (US Biological D9811-01) was supplemented with 10% dialyzed FBS. Different amino acids (purchased from Sigma) were added back to amino-acid free medium to make a medium without glutamine, serine, asparagine, aspartate, arginine, leucine or glycine. To make medium without essential amino acid,

the amino acid free medium was supplemented with non-essential amino acid solution (Sigma M7145) and 4 mM L-glutamine.

Flow Cytometry

To assess cell death, cells after treatment were washed twice with PBS and stained with AnnexinV and/or PI (eBioscience) for 10 minutes at room temperature and processed according to the manufacturer's protocol. For ROS measurement, cells after treatment were washed once with PBS and incubated with 2.5 μM Dihydroethidium (Thermo) and DAPI for 20 min at 37ºC. Flow analysis was carried out using the 9-color CyAn ADP from Beckman Coulter (Miami, FL)

Cell proliferation and viability assay

Cell viability was determined by MTS assay using CellTiter 96 AQueous MTS Reagent Powder (Promega). 2mg/ml 3-(4,5-dimethylthiazol-2-yl)-5-(3-carboxymethoxyphenyl)-2-(4-sulfophenyl)-2H-tetrazolium (MTS) and 0.92mg/ml phenazine methosulfate (PMS) were mixed in the ratio 20:1 to make the 10x stock solution. The mixture was added directly to the cells in a 96-well plate followed by incubation at 37ºC for 1-4 hours. The absorbance was measured at 490nm. Cell proliferation was determined by CellTiter Glo assay (Promega) according to the manufacturer's protocol.

Western Blotting

Western blotting was carried out as previously described (15). Briefly, cells after treatment were washed three times with PBS and lysed in pre-cooled RIPA buffer supplemented with protease inhibitor (Roche) and phosphatase inhibitor (Thermo). The cells lysates were then sonicated briefly, and protein concentration was determined by BCA protein assay kit (Thermo). The

protein lysates were loaded on precast NuPAGE Bis-Tris Gels (Life Technologies) followed by transfer onto nitrocellulose. Immunoblotting was performed with the following antibodies: γH2AX (Cell Signaling (CS), 9718 and 2577), Actin (Sigma), Cleaved Caspase 3 (CS, 9665), Cleaved PARP (CS, 5625), ALKBH3 (Santa Cruz Biotechnology), Bak (CS, 5023), p-ATM (CS, 5883), p-BRCA (CS, 9009), p-Chk1 (CS, 2348), and GAPDH (SC, 5174).

siRNA knockdown

Smartpool On-target plus human ALKBH3 siRNA from Dharmacon (L-004289-00-0005) was used to transiently knock down ALKBH3 protein in PC3 cells. Cells were transfected with ALKBH3 siRNA or control siRNA (Dharmacon) using RNAi Max lipofectamine reagent (Invitrogen) according to the manufacturer's protocol. Two days after the first transfection, the cells were transfected again with the siRNA to increase transfection efficiency. Glutamine deprivation or drug treatment was performed 2 days post the second transfection.

Dot Blot assay

Dot blot assay was performed as described previously (27). Briefly, genomic DNA was isolated after treatment using DNeasy Blood & Tissue Kit (Qiagen). DNA concentrations were measured by Nanodrop and equal amounts of DNA were loaded onto positively charged nylon membrane (Amersham Hybond-N+, GE Healthcare). After UV cross-linking and blocking with 5% milk, the membranes were incubated with anti-3meC antibody (1:2000 dilution, Active Motif, 61179) at 4˚C with shaking overnight. The membrane was then probed with horseradish-peroxidase-conjugated anti-rabbit secondary antibodies. The dot blot signal was visualized using Western

Lightning Plus-ECL (PerkinElmer). For the methylene blue staining, the membrane was incubated with 0.02% methylene blue in 0.3M sodium acetate (pH 5.2) with shaking for 10 minutes at room temperature.

Immunofluorescence and immunohistochemistry

Immunofluorescence was performed as described previously (58). Briefly, cells were fixed with 4% formaldehyde, blocked with 1% BSA followed by staining with antibodies against γH2AX (Novus NB100-78356), 53BP1 (Abcam ab36823), cleaved caspase-3 (CS, 9661) and DAPI. Secondary antibodies, goat anti-rabbit Alexa Fluor 488 and goat anti-mouse Alexa Fluor 594, were purchased from Millipore. Images were captured 20x or 40x magnification using a Zeiss LSM 700 Confocal Microscope using the ZEN Blue image acquisition software. Immunohistochemistry assays were performed as previously described (14). The staining was performed with the following antibodies: γH2AX (Cell Signaling, 9718), Ki67 (Dako). Images were acquired using Olympus BX50 Upright Microscope at 20x magnification.

Metabolite extraction and mass spectrometry

Mass spectrometry was performed as previously described (14). After amino acid starvation, medium was aspirated quickly and pre-cooled 80% methanol was added directly to the cells. The cells were then incubated at -80ºC for 15min followed by centrifugation at 4ºC. The supernatant was then dried with a speed vacuum and the extracted metabolite pellet was stored at -80ºC. Liquid chromatography–mass spectrometry (LC-MS) and data analysis was processed at Duke University (Durham NC, USA) and described previously (59). Intracellular αKG levels were also

measured using Alpha Ketoglutarate Assay Kit (Abcam) according to the manufacturer's protocol for colorimetric assay without the deproteinization step.

ALKBH enzymatic activity assay

DNA repair reactions were performed with the recombinant ALKBH3 proteins and oligonucleotide substrates in the reaction buffer (50 mM Hepes-KOH, 40mM αketoglutarate, 2mM Ascorbate, 40mM FeSO4) for 1 hour at 37ºC. The 3meC containing oligonucleotide substrate is 5'AAAGCAAGCAGATYATTCGAAAAAGCGAAA-3', Y=3-meC. The complementary oligonucleotide with fluorescent tag is 5'TTTCGCTTTTTCGAATGATCTGCTTGCTTT-Cy5.5-3'. The oligonucleotide substrate and the complementary oligonucleotide were mixed and heated to 90ºC for 1 minute and cooled at 1ºC /minute to 4ºC to anneal. The reactions were then digested with DpnII restriction enzyme and the products were separated by 20% non-denaturing TBE-PAGE gel.

Mouse Xenografts

For glutaminase inhibitor treatment, 7 weeks-old athymic nude male mice (Taconic Laboratories) were injected subcutaneously on the flank with $1x10^6$ cells of PC3, HT1080 or HCT116 $p53^{-/-}$. Once the tumors were established, the mice were treated with PBS control or 5-15mg/kg DON as indicated three times per week. For combination drug treatment of MMS and DON, 7 weeks-old athymic nude male mice were injected subcutaneously on the flank with $1x10^6$ PC3 cells. After the tumors were established, mice were randomly placed into four groups and treated with PBS control, 5mg/kg DON, 30 mg/kg MMS or combination of 5mg/kg DON and 30 mg/kg MMS three times per week. For combination drug treatment of MMS and CB-839, 6 weeks-old nude male

mice were injected subcutaneously on the flank with $3x10^6$ PC3 cells. After the tumors were established, mice were randomly placed into four groups and treated with vehicle control, 200mg/kg CB-839 prepared in vehicle by oral gavage once a day, 30 mg/kg MMS by intraperitoneal injection three times per week or combination of CB-839 and MMS. The vehicle consisted of 5% DMSO in corn oil (Sigma). The tumor size was measured every other day and tumor volume was calculated using the formula $0.5 \times r_1^2 \times r_2$. All studies involving animals were performed according to approved IACUC protocols at the City of Hope Cancer Center.

Statistical analysis

Results are shown as averages; error bars represent either the standard error of the mean (S.E.M.) or standard deviation (S.D.) as indicated. The unpaired Student's *t*-test was used to determine the statistical significance of differences between means (∗P<.05, ∗∗P<.01, ∗∗∗P<.001).

Figures

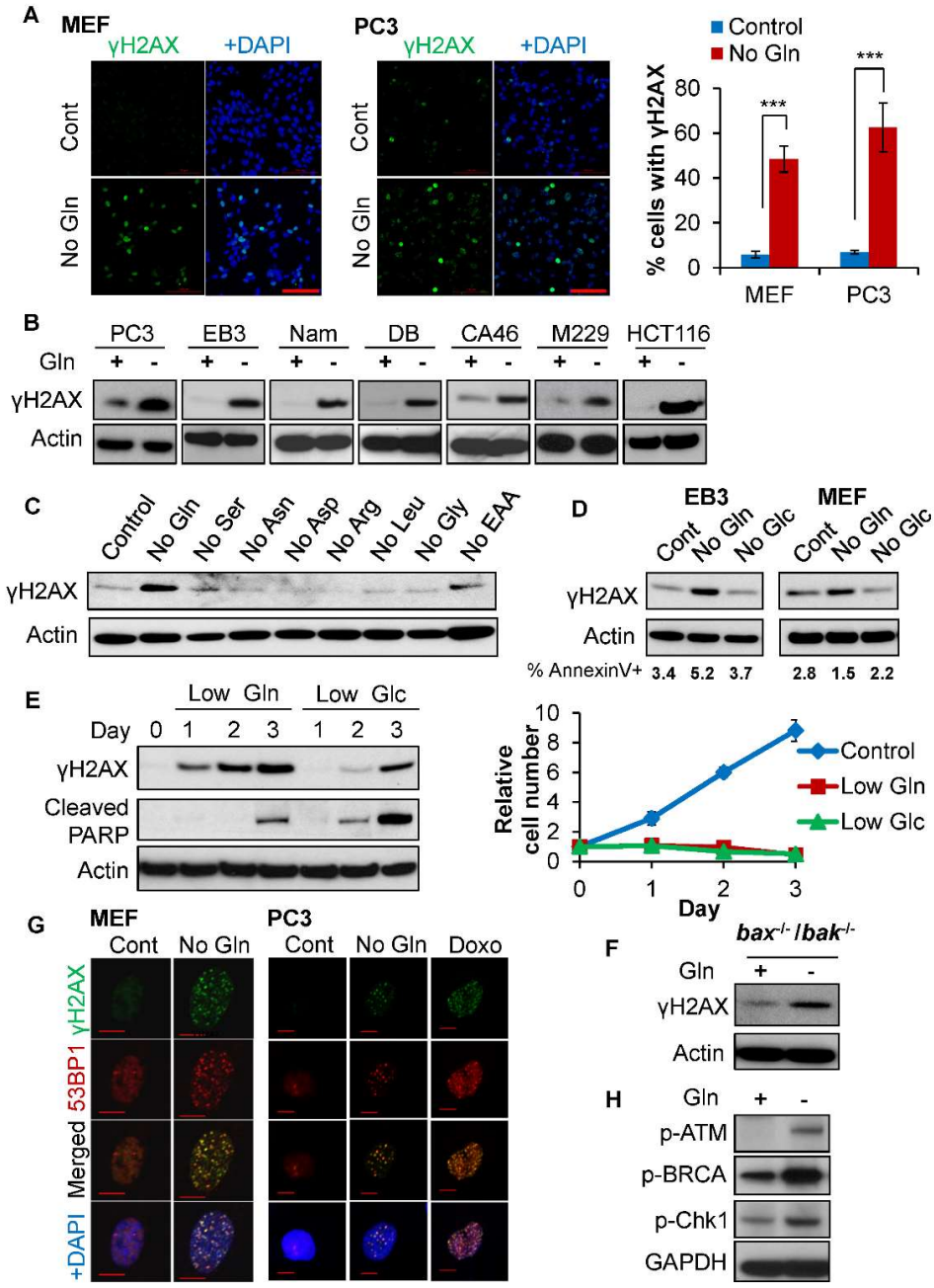

Figure 3-1. Glutamine deficiency specifically triggers DNA damage accumulation independent of cell death. (A) MEF and PC3 cells were cultured in complete (Cont) or glutamine free medium (No Gln) for 24 hours. Cells were fixed for immunofluorescence with

γH2AX antibody and DAPI. Scale bar 100μm. Data represent mean ± S.D. of 4 independent cell cultures, ***P<.001, shown is the percentage of cells showing >10 foci. (B) The indicated cancer cell lines were cultured in complete or glutamine free medium. (C) MEF cells were cultured in medium deprived of the indicated amino acid for 48 hours. (D) EB3 and MEF cells were cultured in complete medium, glutamine free or glucose free medium for 6 hours. Early apoptotic cell death was determined by AnnexinV staining with flow cytometry. (E) MEF cells were cultured in either low glutamine (0.1mM) or low glucose (1mM) for the indicated time points; relative cell growth was determined by CellTiter-Glo assay. (*B*-*E*) The treated cells were lysed for immunoblotting using indicated antibodies. (F) $Bak^{-/-}$/$Bax^{-/-}$ MEF cells were starved of glutamine for 48 hours, and cells were lysed for immunoblotting. (G) MEF and PC3 cells were cultured in complete or glutamine free medium overnight. PC3 cells were also treated with 3.4μM doxorubicin for 4 hours to induce DNA double strand breaks. The cells were fixed for immunofluorescence using the indicated antibodies. Scale bar 10μm. (H) EB3 cells were cultured in complete or glutamine free medium overnight; cells were lysed for western blot analysis using the indicated antibodies.

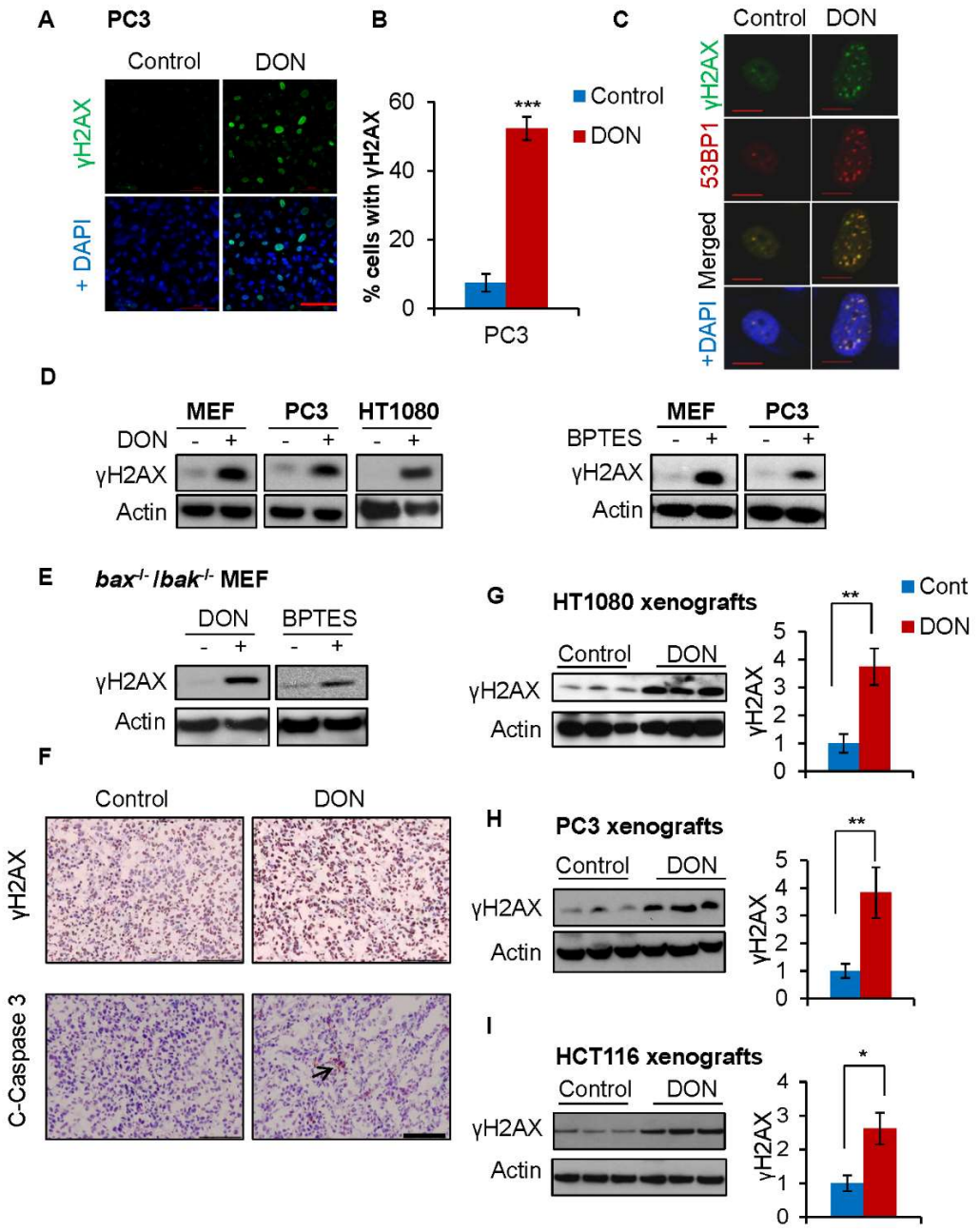

Figure 3-2. Inhibition of glutamine metabolism with a glutaminase inhibitor triggers DNA damage accumulation both *in vitro* and *in vivo*. (A-B) PC3 cells were treated with 50μM DON for 48 hours. The cells were fixed for immunofluorescence using γH2AX antibody. Data represent mean ± S.D. of 4 independent cell cultures, $***P < 0.001$, shown is the percentage of cells showing >10 foci. Scale bar 100μm. (C) PC3 cells were treated with 50μM DON for 48

hours and the cells were fixed for immunofluorescence using the indicated antibodies. Scale bar 10μm. (D) MEF, PC3 or HT1080 cells were treated with 50μM DON or 50μM BPTES for 48 hours. (E) *Bak*$^{-/-}$/*Bax* $^{-/-}$ MEF cells were treated with 50μM DON or 50μM BPTES for 48 hours, and the cells were lysed for immunoblotting using the indicated antibodies. (F-G) Mice bearing HT1080 xenograft tumors were treated with 10 mg/kg DON every other day for 2 weeks. The tumors were harvested and fixed for immunohistochemistry and immunoblotting using the indicated antibodies. (H-I) Mice bearing PC3 xenograft tumors were treated with 5 mg/kg DON and mice bearing HCT116 p53-/- xenograft tumors were treated with 15 mg/kg DON every other day for 2 weeks. The control and DON treated tumors were harvested and lysed for immunoblotting using the indicated antibodies. Each lane represents an individual tumor, and immunoblots were quantified by ImageJ and normalized to the control group. Data represent mean ± S.D. of 3 individual tumors, $**P<.01$.

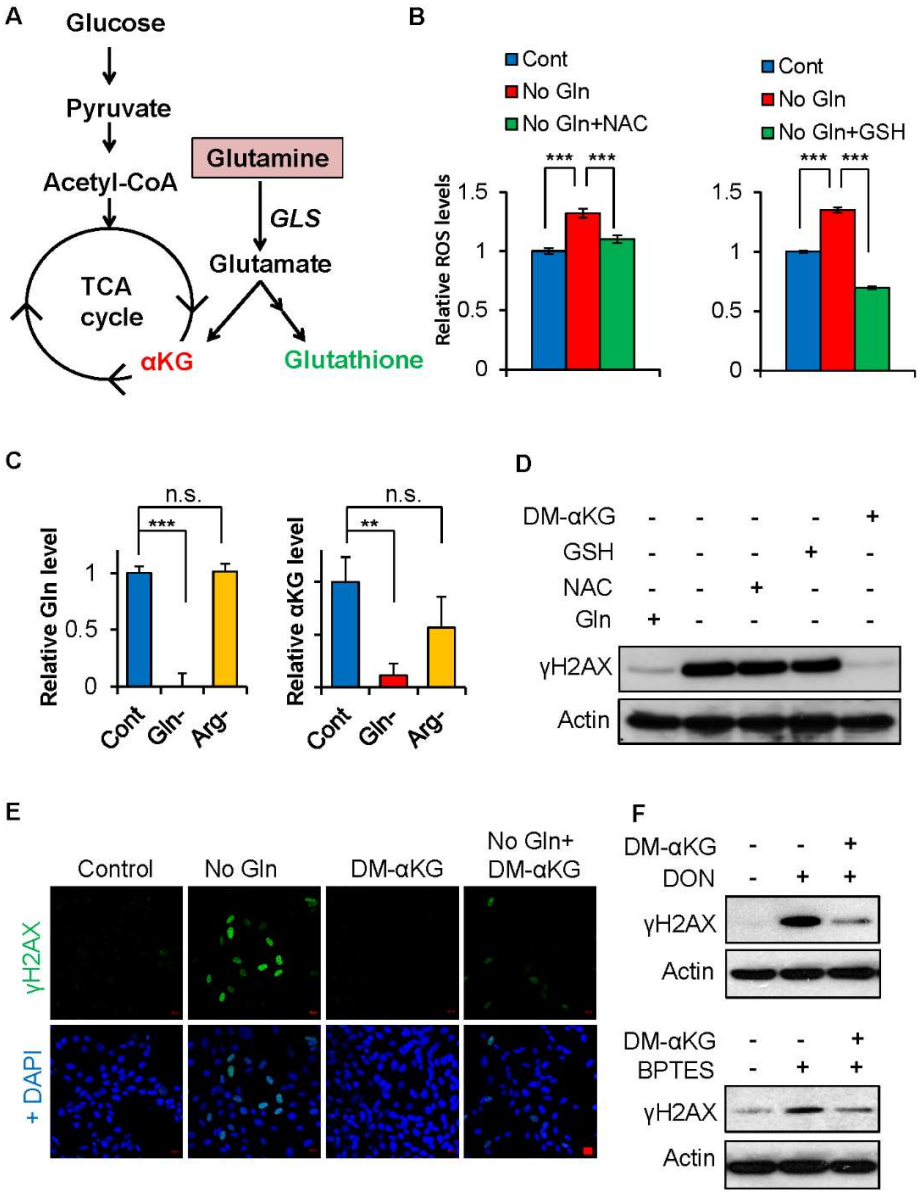

Figure 3-3. Glutamine deficiency-induced DNA damage is αKG dependent. (A) Diagram of glutamine metabolism in cancer. (B) EB3 cells were cultured in complete, glutamine free medium or glutamine free medium supplemented with 10mM N-Acetyl Cysteine (NAC) or 15mM glutathione (GSH) for 6 hours. The cells were harvested for flow cytometry analysis with dihydroethidium dye to determine relative ROS levels normalized to the control, data represent mean ± S.D. of minimum 3 independent cell cultures, ***P<.001. (C) MEF cells were cultured in glutamine free medium or arginine free medium (negative control) overnight. Metabolites

were extracted for mass spectrometry analysis to measure the indicated total intracellular metabolites, normalized to the control. Data represent mean ± S.D. of 3 independent cell cultures, ***P<.001 , n.s. not significant. (D) EB3 cells were cultured in complete or glutamine free medium supplemented with 10mM NAC, 15mM GSH or 7mM DM-αKG for 6 hours. Cells were lysed for immunoblotting with the indicated antibodies. (E) MEF cells were cultured in complete or glutamine free medium supplemented with 3.5mM DM-αKG overnight, the cells were fixed for immunofluorescence with the indicated antibodies. Scale bar 20μm. (F) EB3 cells were treated with 50μM DON or 50μM BPTES in control medium or medium supplemented with 3.5mM DM-αKG for 48 hours, cells were lysed for immunoblotting with the indicated antibodies.

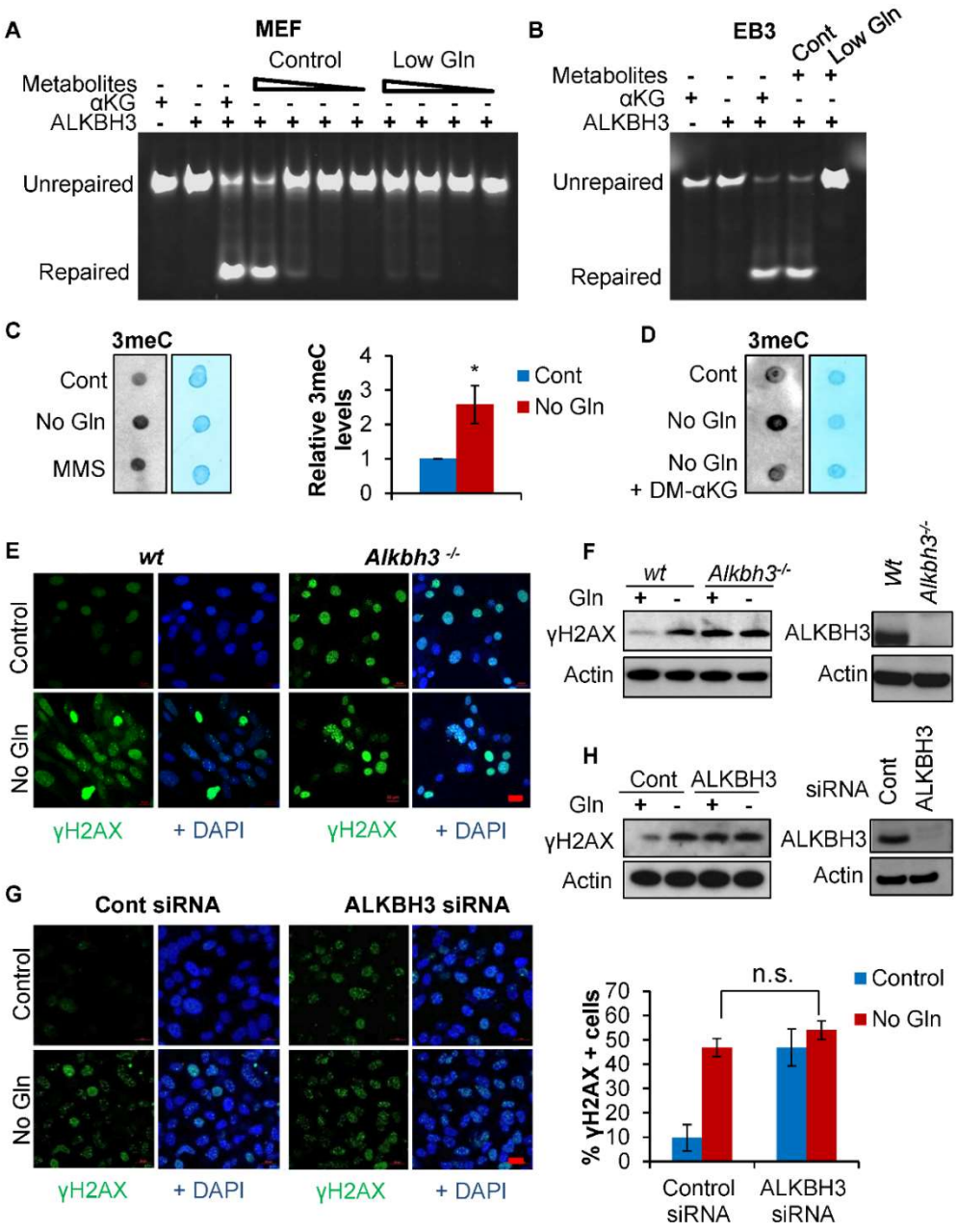

Figure 3-4. Glutamine deficiency inhibits ALKBH activity and induces endogenous DNA alkylation damage. (A) MEF cells were cultured in complete or 0.1mM glutamine medium for 48 hours, and methanol was used to extract intracellular metabolites from an equal number of viable cells. To perform the ALKBH3 enzymatic activity assay, the extracted metabolites or αKG (positive control) were incubated with the 3meC-containing DNA probe and recombinant ALKBH3. (B) EB3 cells were cultured in complete or low glutamine medium for 24 hours, and

the cells were then processed as in Fig 4A. (C) MEF cells were cultured in complete, glutamine free medium for 48 hours or treated with 2mM MMS for 1 hour. Genomic DNA was extracted to perform dot blot analysis using the 3meC antibody. DNA loading was assessed by methylene blue dye. Data represent mean ± S.D. of 4 independent cell cultures, $*P<.05$. (D) Cells were cultured in complete, glutamine free medium or glutamine free medium supplemented with 3.5mM DM-αKG for 48 hours followed by dot blot analysis. (E-F) *Wild type* (*wt*) MEF or *Alkbh3*$^{-/-}$ MEF cells were cultured in complete or glutamine free medium overnight, cells were fixed for immunofluorescence and immunoblotting using the indicated antibodies. (G-H) PC3 cells were transfected with ALKBH3 siRNA twice. Four days after transfection, control PC3 cells and ALKBH3 knockdown cells were cultured in complete or glutamine free medium for 2 days, cells were fixed for immunofluorescence and immunoblotting using the indicated antibodies. Scale bar 20μm. Data represent mean ± S.D from 2 independent cell cultures, n.s. not significant, shown is the percentage of cells showing >10 foci.

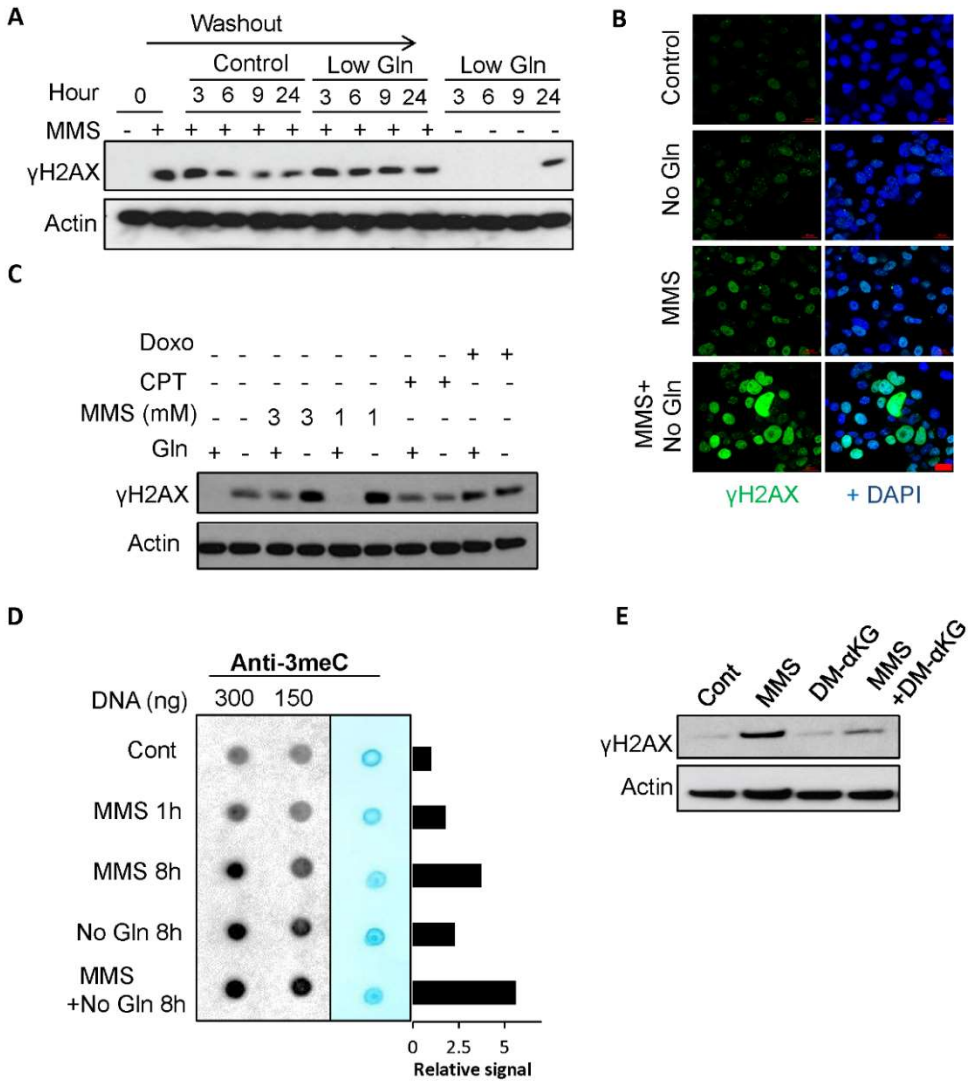

Figure 3- 5. Glutamine deficiency sensitizes cells to alkylating-agent induced DNA damage. (A) MEF cells were treated with 1mM MMS for 1 hour, washed and subsequently cultured in complete medium with 2mM Gln or low glutamine medium with 0.1mM Gln for the indicated time points. Cells were lysed for immunoblotting with the indicated antibodies. (B) PC3 cells were treated with 1mM MMS for 1 hour, washed and subsequently cultured in complete medium or glutamine free medium for 48 hours. Cells were fixed for immunofluorescence with the γH2AX antibody and DAPI. Scale bar 20μm (C) MEF cells were treated with 1 or 3 mM MMS, 5μM camptothecin (CPT) or 3.4 μM doxorubicin (Doxo) in complete or low glutamine medium

for 24 hours, cells were lysed for immunoblotting. (D) MEF cells were treated with 1mM MMS for 1 hour, washed and subsequently cultured in complete or glutamine free medium for 8 hours. Genomic DNA was extracted to perform dot blot analysis using the 3meC specific antibody. DNA loading was assessed by methylene blue dye. 3meC signals relative to the control were quantified by ImageJ and normalized to methylene blue. (E) MEF cells were treated with 1mM MMS for 1 hour, washed and subsequently cultured in complete medium or medium supplemented with 1mM DM-αKG for 24 hours. Cells were lysed for immunoblotting using the indicated antibodies.

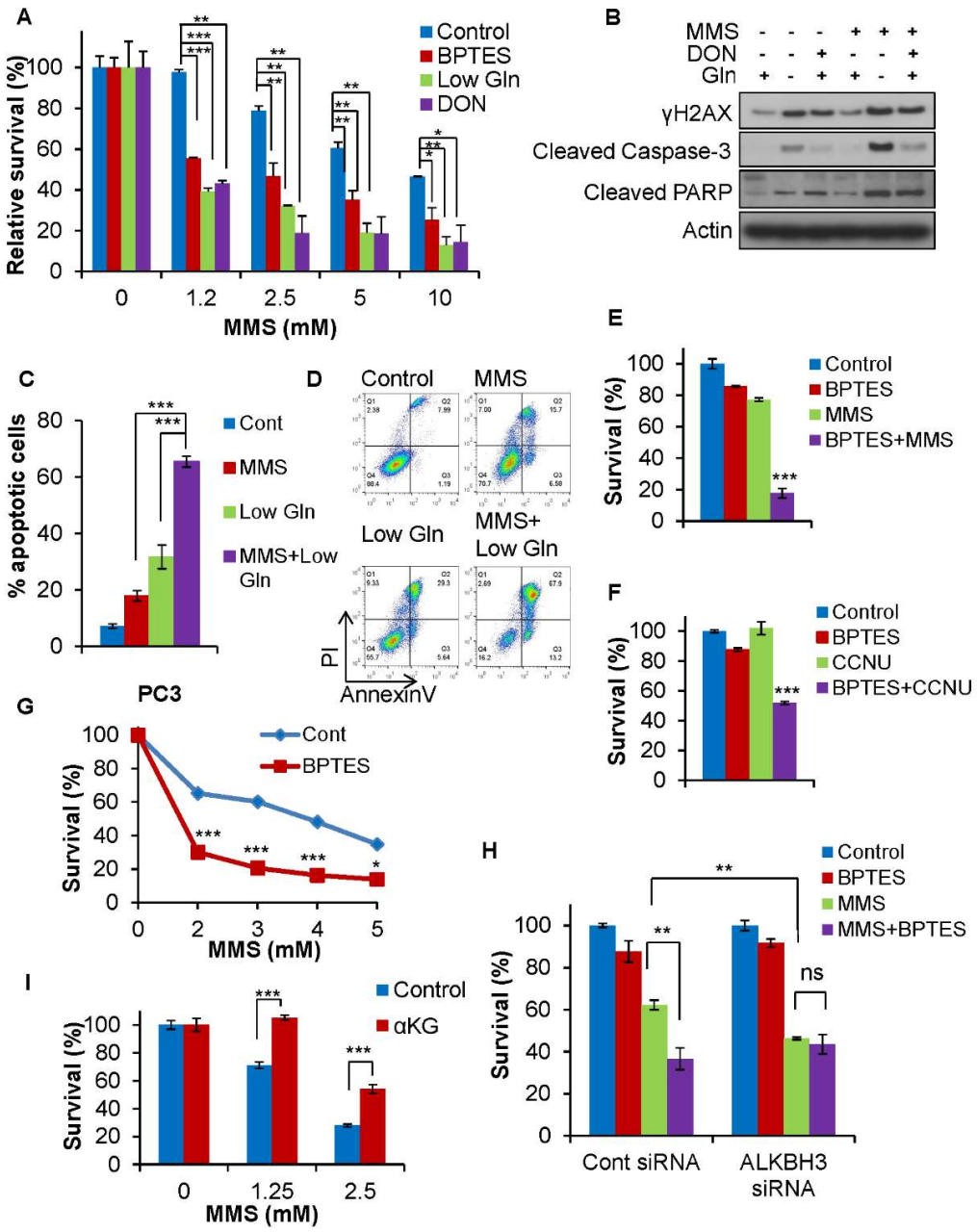

<u>Figure 3-6</u>. Inhibition of glutamine metabolism hypersensitizes cells to alkylating agents.

(A) Ras-transformed MEF cells were treated with the indicated concentration of MMS for 1 hour, washed and subsequently cultured in 0.1 mM glutamine medium, complete medium supplemented with 20μM BPTES or 25μM DON for 48 hours. Relative cell survival was assessed by MTS assay, and normalized to the control of each group. Data represent mean ± S.D.

of minimum 2 independent cell cultures, $*P<.05$, $**P<.01$, $***P<.001$. (B) Cells were treated as in (A) and lysed for immunoblotting with the indicated antibodies. (C-D) Ras-transformed MEF cells were treated with 1mM MMS for 1 hour, subsequently cultured in complete medium or 0.1mM glutamine medium for 48 hours. Apoptotic cell death was assessed by flow cytometry with AnnexinV/PI staining, data represent mean ± S.D. of 4 independent cell cultures, $***P<.001$. (E) HT1080 cells were treated with 2.5mM MMS for 1 hour, subsequently cultured in control medium or medium supplemented with 20μM BPTES for 48 hour. (F) HT1080 cells were treated with 10μM BPTES, 35μM CCNU or combination of BPTES and CCNU. (G) PC3 cells were treated with indicated concentration of MMS for 1 hour, washed and subsequently cultured in medium supplemented with 25μM BPTES for 48 hours. (H) Control cells and siRNA-mediated ALKBH3 knockdown cells were treated as in (G) with 2mM MMS and 25μM BPTES. (E-H) Relative cell survival was assessed by MTS assay, normalized to the control. Data represent mean ± S.D. of 3 independent cell cultures, $**P<.01$, $***P<.001$. (I) MEF cells were treated with the indicated concentration of MMS, washed and subsequently cultured in complete medium or medium supplemented with 1mM DM-αKG for 24 hours, relative cell survival was assessed by MTS assay, normalized to the control. Data represent mean ± S.D. of 4 independent cell cultures, $***P<.001$.

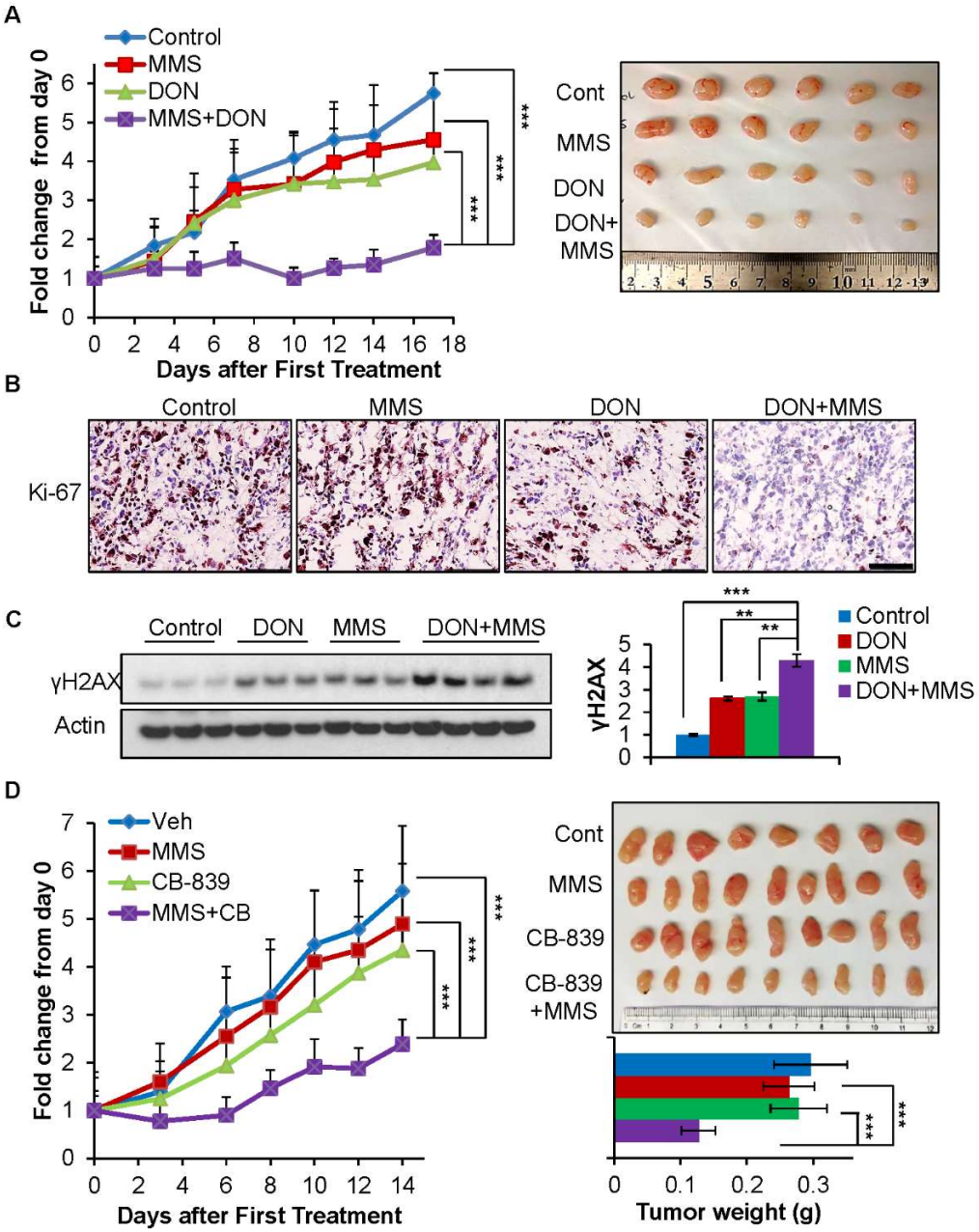

Figure 3-7. Combination treatment of glutaminase inhibitor and alkylating agent suppresses tumor growth in vivo. (A) Athymic nude mice at 7 weeks old were injected subcutaneously on the flank with $1x10^6$ PC3 cells. Once the tumor size reached an average of 60 mm^3, mice were randomly placed into four groups and treated with PBS control (n=9 tumors), 5mg/kg DON (n=8 tumors), 30 mg/kg MMS (n=8 tumors) or a combination of 5mg/kg DON and 30 mg/kg MMS (n=9 tumors) three times per week by i.p. injection. Tumor size was measured

overtime, and data represent mean ± S.D., ***P<.001by unpaired two-tailed Student's t-test. (B) The tumors were harvested at day 18, processed for immunohistochemistry with the Ki-67 antibody. Scale bar, 100 μm. (C) The harvested tumors were lysed for immunoblotting with the indicated antibodies. Immunoblots were quantified using ImageJ and normalized to the control group, data represent mean ± S.E.M., **P<.01, ***P<.001. (D) Nude mice at 6 weeks old were injected subcutaneously on the flank with $3x10^6$ PC3 cells. Once the tumor size reached an average of 80 mm^3, mice were randomly placed into four groups and treated with vehicle control (n=10 tumors), 200mg/kg CB-839 once a day (n=12 tumors), 30 mg/kg MMS three times per week by i.p. injection (n=13 tumors) or a combination of CB-839 and MMS (n=12 tumors). Tumor size was measured overtime, and data represent mean ± S.D., ***P<.001.

Supplemental figures

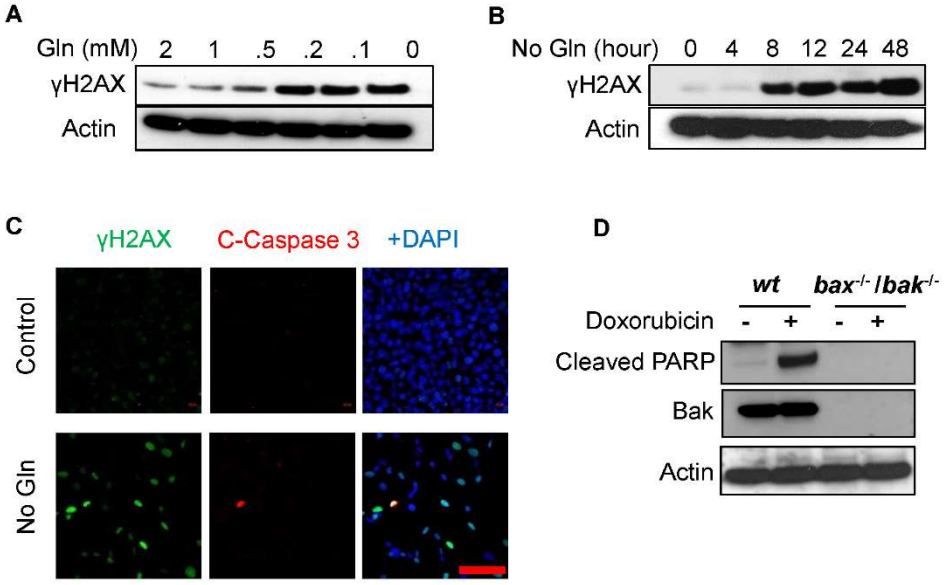

<u>Figure 3-S1</u>. Glutamine deficiency induces DNA damage independent of cell death. (A) EB3 cells were cultured in cell medium with the indicated glutamine concentration for 48 hours. (B) EB3 cells were cultured in glutamine free medium or complete medium for the indicated time up to 48 hours; cells were lysed for immunoblotting (C) MEF cells were cultured in complete or glutamine free medium for 48 hours. Cells were fixed for immunofluorescence using the indicated antibodies. Scale bar 100μm. (D) Bak-/- /Bax -/- MEF and littermate wild type MEF cells were treated with 3.4μM doxorubicin overnight, cells were lysed for western blot analysis using the indicated antibodies.

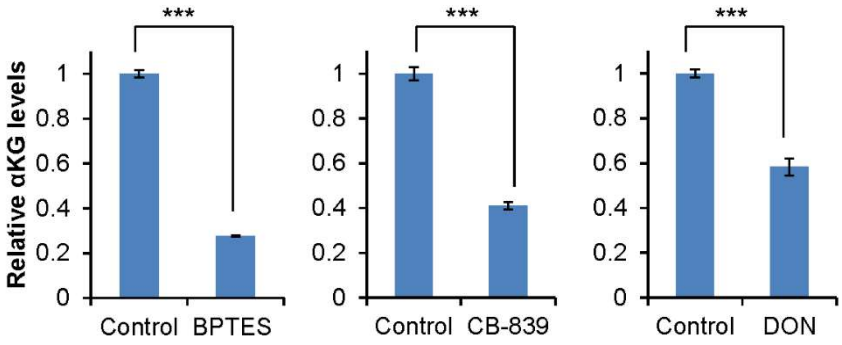

<u>Figure 3-S2</u>. Glutaminase inhibitor treatment depletes intracellular αKG levels in vitro.

MEF cells were treated with 50μM BPTES, 25μM CB-839 or 50μM DON for 48 hours. Relative intracellular αKG levels were determined using an αKG assay kit, and normalized to the protein level. Data represent mean ± S.D. of 3 independent cell cultures. (***P<.001)

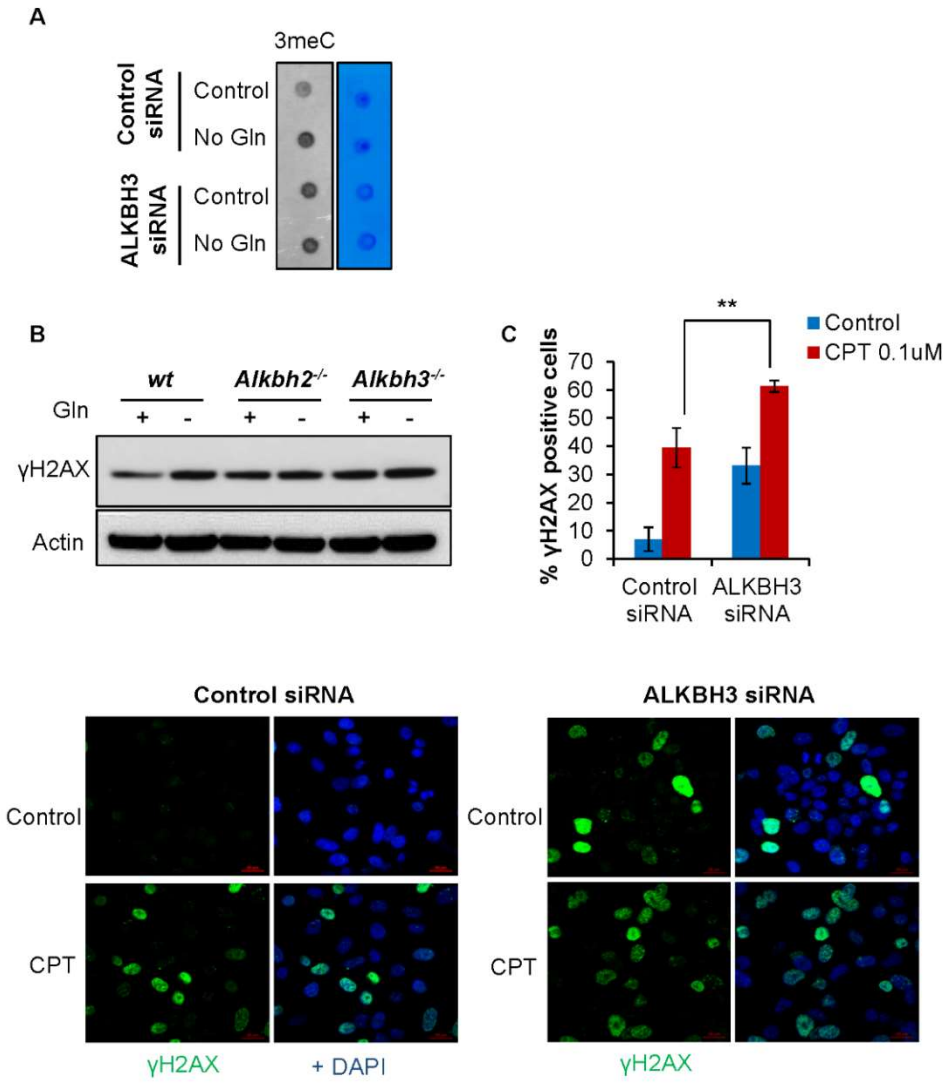

Figure 3-S3. Glutamine deficiency inhibits the ALKBH enzymes leading to DNA damage accumulation. (A) PC3 cells were transfected with ALKBH3 siRNA or control siRNA. Two days after transfection, control PC3 cells and ALKBH3 knockdown cells were cultured in complete or glutamine free medium for 3 days, genomic DNA was extracted to perform dot blot analysis using the 3meC specific antibody. (B) Wild type MEF, Alkbh2-/- MEF or Alkbh3-/- MEF cells were cultured in complete or glutamine free medium overnight. Cells were lysed for immunoblotting using the indicated antibodies. (C) PC3 cells were transfected with ALKBH siRNA or control siRNA twice. 4 days after siRNA transfection, control cells and ALKBH3

knockdown cells were treated with 0.1μM CPT overnight, cells were fixed for immunofluorescence using the indicated antibodies. Scale bar 20 μm. Data represent mean ± S.D from 2 independent cell cultures, **P < 0.01, shown is the percentage of cells showing >10 foci.

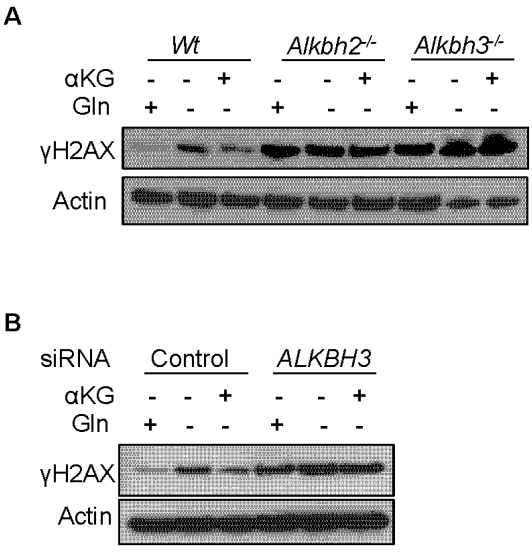

Figure 3-S4. Exogenous αKG fails to rescue low glutamine induced DNA damage in Alkbh deficient cells. (A) Wild type MEF, Alkbh2-/- MEF or Alkbh3-/- MEF cells were cultured in completed, glutamine free medium or glutamine free medium supplemented with 3.5mM αKG for 12 hours. Cells were lysed for immunoblotting using the indicated antibodies. (B) PC3 cells were transfected with ALKBH3 siRNA twice. Four days after transfection, control PC3 cells and ALKBH3 knockdown cells were cultured in complete, glutamine free medium or glutamine free medium supplemented with 3.5mM DM-αKG for 2 days, clls were lysed for immunoblotting using the indicated antibodies.

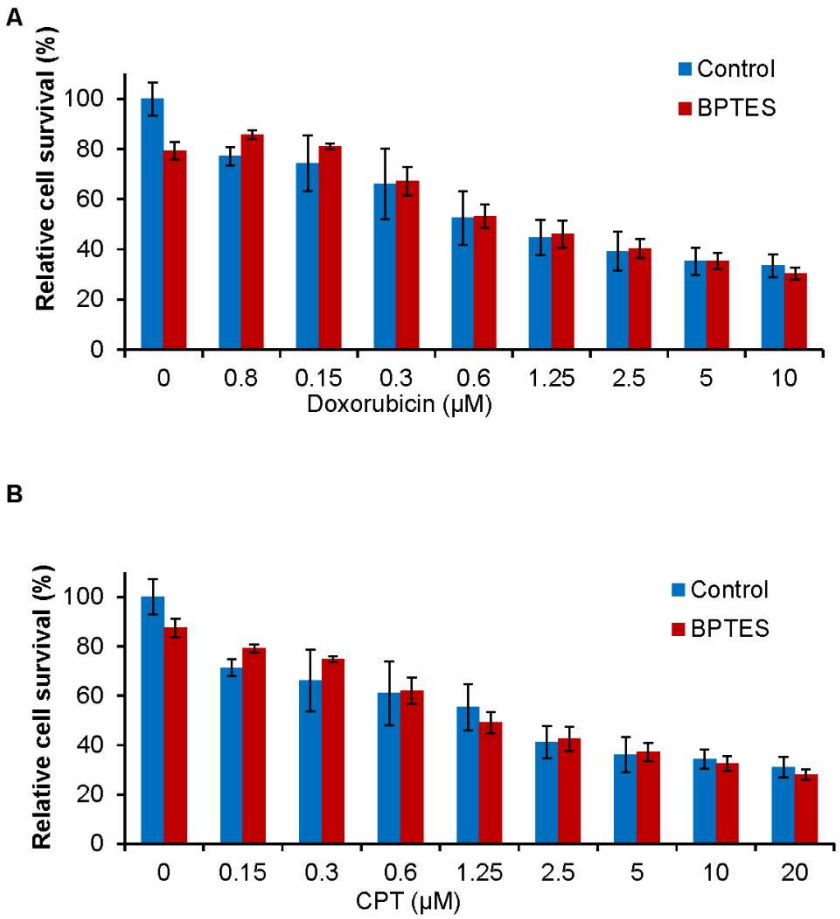

<u>Figure 3-S5.</u> Inhibition of glutamine metabolism does not sensitize cell to other classes of chemotherapy drug. (A) Ras-transformed MEF cells were treated with the indicated concentration of Doxorubicin alone or in combination with 20μM BPTES for 48 hr. (B) Ras-transformed MEF cells were treated with the indicated concentration of CPT alone or in combination with 20μM BPTES for 48 hr. Relative cell survival was assessed by MTS assay, normalized to the control. Data represent mean ± S.D of 3 independent cell cultures.

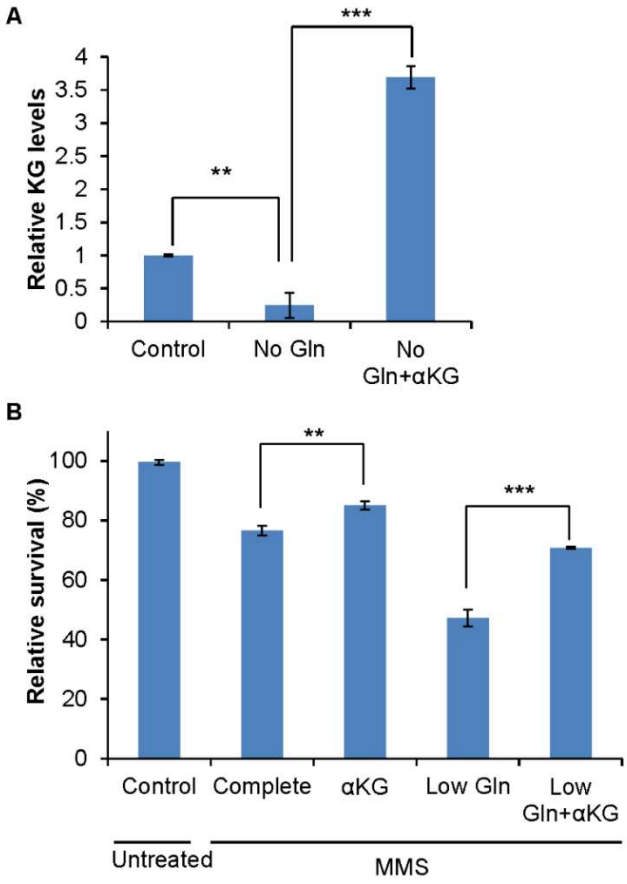

<u>Figure 3-S6</u>. Glutamine deprivation sensitizes cells to alkylating agent through the depletion of αKG. (A) MEF cells were cultured in complete (control) media, glutamine free medium or glutamine free medium supplemented with 3.5mM DM-αKG overnight. Intracellular αKG levels were measured by an αKG assay kit, normalized to total protein levels. Data represent mean ± S.D of 3 independent cell cultures. (**P<.01,***P<.001). (B) MEF cells were treated with 2mM MMS for 1 hour, washed and subsequently cultured in complete medium, complete medium supplemented with 3.5mM DM-αKG, low (0.1mM) glutamine medium or low glutamine medium supplemented with 3.5mM DM-αKG for 12 hours. Relative survival was determined by MTS assay normalized to the control of each group. Data represent mean ± S.D of 3 independent cell cultures. (** P<.01)

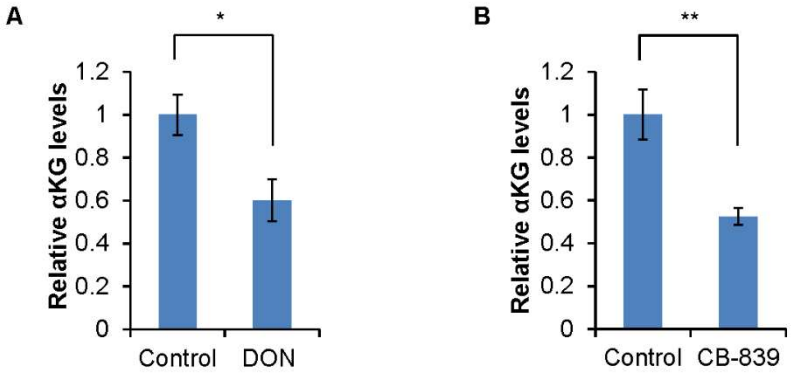

Figure 3-S7. Glutaminase inhibitor treatment depletes intracellular αKG levels in vivo.

Control tumors, DON treated tumors (A) or CB839 treated tumors (B) from Figure 7A, D were lysed, and αKG levels relative to the control were determined using an αKG assay kit, normalized to the tumor weight. Data represent mean ± S.E.M of 4 different tumors. (*P<.05, **P<.01, ***P<.001)

References

1. DeBerardinis RJ, Lum JJ, Hatzivassiliou G, Thompson CB. The biology of cancer: metabolic reprogramming fuels cell growth and proliferation. Cell metabolism. 2008 Jan;7(1):11-20. PubMed PMID: 18177721.
2. Dang CV. Links between metabolism and cancer. Genes & development. 2012 May 1;26(9):877-90. PubMed PMID: 22549953. Pubmed Central PMCID: 3347786.
3. Liberti MV, Locasale JW. The Warburg Effect: How Does it Benefit Cancer Cells? Trends in biochemical sciences. 2016 Mar;41(3):211-8. PubMed PMID: 26778478. Pubmed Central PMCID: 4783224.
4. Wise DR, Thompson CB. Glutamine addiction: a new therapeutic target in cancer. Trends in biochemical sciences. 2010 Aug;35(8):427-33. PubMed PMID: 20570523. Pubmed Central PMCID: 2917518.
5. Cory JG, Cory AH. Critical roles of glutamine as nitrogen donors in purine and pyrimidine nucleotide synthesis: asparaginase treatment in childhood acute lymphoblastic leukemia. In vivo. 2006 Sep-Oct;20(5):587-9. PubMed PMID: 17091764.
6. Altman BJ, Stine ZE, Dang CV. From Krebs to clinic: glutamine metabolism to cancer therapy. Nature reviews Cancer. 2016 Oct;16(10):619-34. PubMed PMID: 27492215.
7. Le A, Lane AN, Hamaker M, Bose S, Gouw A, Barbi J, et al. Glucose-independent glutamine metabolism via TCA cycling for proliferation and survival in B cells. Cell metabolism. 2012 Jan 4;15(1):110-21. PubMed PMID: 22225880. Pubmed Central PMCID: 3345194.
8. Lukey MJ, Wilson KF, Cerione RA. Therapeutic strategies impacting cancer cell glutamine metabolism. Future medicinal chemistry. 2013 Sep;5(14):1685-700. PubMed PMID: 24047273. Pubmed Central PMCID: 4154374.
9. Sappington DR, Siegel ER, Hiatt G, Desai A, Penney RB, Jamshidi-Parsian A, et al. Glutamine drives glutathione synthesis and contributes to radiation sensitivity of A549 and H460 lung cancer cell lines. Biochimica et biophysica acta. 2016 Apr;1860(4):836-43. PubMed PMID: 26825773. Pubmed Central PMCID: 4768472.
10. Xiang Y, Stine ZE, Xia J, Lu Y, O'Connor RS, Altman BJ, et al. Targeted inhibition of tumor-specific glutaminase diminishes cell-autonomous tumorigenesis. The Journal of clinical investigation. 2015 Jun;125(6):2293-306. PubMed PMID: 25915584. Pubmed Central PMCID: 4497742.
11. Korangath P, Teo WW, Sadik H, Han L, Mori N, Huijts CM, et al. Targeting Glutamine Metabolism in Breast Cancer with Aminooxyacetate. Clin Cancer Res. 2015 Jul 15;21(14):3263-73. PubMed PMID: 25813021. Pubmed Central PMCID: 4696069.
12. Roberts E, Caldwell AL, et al. Amino acids in epidermal carcinogenesis in mice. Cancer research. 1949 Jun;9(6):350-3. PubMed PMID: 18144236.
13. Kamphorst JJ, Nofal M, Commisso C, Hackett SR, Lu W, Grabocka E, et al. Human pancreatic cancer tumors are nutrient poor and tumor cells actively scavenge extracellular protein. Cancer research. 2015 Feb 1;75(3):544-53. PubMed PMID: 25644265. Pubmed Central PMCID: 4316379.
14. Pan M, Reid MA, Lowman XH, Kulkarni RP, Tran TQ, Liu X, et al. Regional glutamine deficiency in tumours promotes dedifferentiation through inhibition of histone demethylation. Nature cell biology. 2016 Oct;18(10):1090-101. PubMed PMID: 27617932. Pubmed Central PMCID: 5536113.

15. Reid MA, Wang WI, Rosales KR, Welliver MX, Pan M, Kong M. The B55alpha subunit of PP2A drives a p53-dependent metabolic adaptation to glutamine deprivation. Molecular cell. 2013 Apr 25;50(2):200-11. PubMed PMID: 23499005.
16. Tran TQ, Lowman XH, Reid MA, Mendez-Dorantes C, Pan M, Yang Y, et al. Tumor-associated mutant p53 promotes cancer cell survival upon glutamine deprivation through p21 induction. Oncogene. 2016 Oct 10. PubMed PMID: 27721412.
17. Reid MA, Lowman XH, Pan M, Tran TQ, Warmoes MO, Ishak Gabra MB, et al. IKKbeta promotes metabolic adaptation to glutamine deprivation via phosphorylation and inhibition of PFKFB3. Genes & development. 2016 Aug 15;30(16):1837-51. PubMed PMID: 27585591. Pubmed Central PMCID: 5024682.
18. Hanahan D, Weinberg RA. Hallmarks of cancer: the next generation. Cell. 2011 Mar 4;144(5):646-74. PubMed PMID: 21376230.
19. Ciccia A, Elledge SJ. The DNA damage response: making it safe to play with knives. Molecular cell. 2010 Oct 22;40(2):179-204. PubMed PMID: 20965415. Pubmed Central PMCID: 2988877.
20. Fedeles BI, Singh V, Delaney JC, Li D, Essigmann JM. The AlkB Family of Fe(II)/alpha-Ketoglutarate-dependent Dioxygenases: Repairing Nucleic Acid Alkylation Damage and Beyond. The Journal of biological chemistry. 2015 Aug 21;290(34):20734-42. PubMed PMID: 26152727. Pubmed Central PMCID: 4543635.
21. Falnes PO, Johansen RF, Seeberg E. AlkB-mediated oxidative demethylation reverses DNA damage in Escherichia coli. Nature. 2002 Sep 12;419(6903):178-82. PubMed PMID: 12226668.
22. Tasaki M, Shimada K, Kimura H, Tsujikawa K, Konishi N. ALKBH3, a human AlkB homologue, contributes to cell survival in human non-small-cell lung cancer. British journal of cancer. 2011 Feb 15;104(4):700-6. PubMed PMID: 21285982. Pubmed Central PMCID: 3049579.
23. Fujii T, Shimada K, Anai S, Fujimoto K, Konishi N. ALKBH2, a novel AlkB homologue, contributes to human bladder cancer progression by regulating MUC1 expression. Cancer science. 2013 Mar;104(3):321-7. PubMed PMID: 23279696.
24. Johannessen TC, Prestegarden L, Grudic A, Hegi ME, Tysnes BB, Bjerkvig R. The DNA repair protein ALKBH2 mediates temozolomide resistance in human glioblastoma cells. Neuro-oncology. 2013 Mar;15(3):269-78. PubMed PMID: 23258843. Pubmed Central PMCID: 3578482.
25. Yamato I, Sho M, Shimada K, Hotta K, Ueda Y, Yasuda S, et al. PCA-1/ALKBH3 contributes to pancreatic cancer by supporting apoptotic resistance and angiogenesis. Cancer research. 2012 Sep 15;72(18):4829-39. PubMed PMID: 22826605.
26. Konishi N, Nakamura M, Ishida E, Shimada K, Mitsui E, Yoshikawa R, et al. High expression of a new marker PCA-1 in human prostate carcinoma. Clinical cancer research : an official journal of the American Association for Cancer Research. 2005 Jul 15;11(14):5090-7. PubMed PMID: 16033822. Epub 2005/07/22. eng.
27. Dango S, Mosammaparast N, Sowa ME, Xiong LJ, Wu F, Park K, et al. DNA unwinding by ASCC3 helicase is coupled to ALKBH3-dependent DNA alkylation repair and cancer cell proliferation. Molecular cell. 2011 Nov 04;44(3):373-84. PubMed PMID: 22055184. Pubmed Central PMCID: PMC3258846. Epub 2011/11/08. eng.
28. Mah LJ, El-Osta A, Karagiannis TC. gammaH2AX: a sensitive molecular marker of DNA damage and repair. Leukemia. 2010 Apr;24(4):679-86. PubMed PMID: 20130602.

29. Qing G, Li B, Vu A, Skuli N, Walton ZE, Liu X, et al. ATF4 regulates MYC-mediated neuroblastoma cell death upon glutamine deprivation. Cancer cell. 2012 Nov 13;22(5):631-44. PubMed PMID: 23153536. Pubmed Central PMCID: 3510660.
30. Wei MC, Zong WX, Cheng EH, Lindsten T, Panoutsakopoulou V, Ross AJ, et al. Proapoptotic BAX and BAK: a requisite gateway to mitochondrial dysfunction and death. Science. 2001 Apr 27;292(5517):727-30. PubMed PMID: 11326099. Pubmed Central PMCID: PMC3049805. Epub 2001/04/28. eng.
31. Tu WZ, Li B, Huang B, Wang Y, Liu XD, Guan H, et al. gammaH2AX foci formation in the absence of DNA damage: mitotic H2AX phosphorylation is mediated by the DNA-PKcs/CHK2 pathway. FEBS letters. 2013 Nov 1;587(21):3437-43. PubMed PMID: 24021642.
32. Gagou ME, Zuazua-Villar P, Meuth M. Enhanced H2AX phosphorylation, DNA replication fork arrest, and cell death in the absence of Chk1. Molecular biology of the cell. 2010 Mar 1;21(5):739-52. PubMed PMID: 20053681. Pubmed Central PMCID: 2828961.
33. de Feraudy S, Revet I, Bezrookove V, Feeney L, Cleaver JE. A minority of foci or pan-nuclear apoptotic staining of gammaH2AX in the S phase after UV damage contain DNA double-strand breaks. Proceedings of the National Academy of Sciences of the United States of America. 2010 Apr 13;107(15):6870-5. PubMed PMID: 20351298. Pubmed Central PMCID: 2872460.
34. Ward IM, Minn K, Jorda KG, Chen J. Accumulation of checkpoint protein 53BP1 at DNA breaks involves its binding to phosphorylated histone H2AX. The Journal of biological chemistry. 2003 May 30;278(22):19579-82. PubMed PMID: 12697768.
35. Nicklin P, Bergman P, Zhang B, Triantafellow E, Wang H, Nyfeler B, et al. Bidirectional transport of amino acids regulates mTOR and autophagy. Cell. 2009 Feb 6;136(3):521-34. PubMed PMID: 19203585. Pubmed Central PMCID: 3733119.
36. Xi P, Jiang Z, Zheng C, Lin Y, Wu G. Regulation of protein metabolism by glutamine: implications for nutrition and health. Frontiers in bioscience. 2011 Jan 01;16:578-97. PubMed PMID: 21196190.
37. Son J, Lyssiotis CA, Ying H, Wang X, Hua S, Ligorio M, et al. Glutamine supports pancreatic cancer growth through a KRAS-regulated metabolic pathway. Nature. 2013 Apr 4;496(7443):101-5. PubMed PMID: 23535601. Pubmed Central PMCID: 3656466.
38. Trewick SC, Henshaw TF, Hausinger RP, Lindahl T, Sedgwick B. Oxidative demethylation by Escherichia coli AlkB directly reverts DNA base damage. Nature. 2002 Sep 12;419(6903):174-8. PubMed PMID: 12226667.
39. Fu D, Calvo JA, Samson LD. Balancing repair and tolerance of DNA damage caused by alkylating agents. Nature reviews Cancer. 2012 Feb;12(2):104-20. PubMed PMID: 22237395. Pubmed Central PMCID: 3586545.
40. Gross MI, Demo SD, Dennison JB, Chen L, Chernov-Rogan T, Goyal B, et al. Antitumor activity of the glutaminase inhibitor CB-839 in triple-negative breast cancer. Molecular cancer therapeutics. 2014 Apr;13(4):890-901. PubMed PMID: 24523301.
41. Moreadith RW, Lehninger AL. The pathways of glutamate and glutamine oxidation by tumor cell mitochondria. Role of mitochondrial NAD(P)+-dependent malic enzyme. The Journal of biological chemistry. 1984 May 25;259(10):6215-21. PubMed PMID: 6144677.
42. Davidson SM, Papagiannakopoulos T, Olenchock BA, Heyman JE, Keibler MA, Luengo A, et al. Environment Impacts the Metabolic Dependencies of Ras-Driven Non-Small Cell Lung Cancer. Cell metabolism. 2016 Mar 08;23(3):517-28. PubMed PMID: 26853747. Pubmed Central PMCID: 4785096.

43. Marin-Valencia I, Yang C, Mashimo T, Cho S, Baek H, Yang XL, et al. Analysis of tumor metabolism reveals mitochondrial glucose oxidation in genetically diverse human glioblastomas in the mouse brain in vivo. Cell metabolism. 2012 Jun 06;15(6):827-37. PubMed PMID: 22682223. Pubmed Central PMCID: 3372870.
44. Yuneva MO, Fan TW, Allen TD, Higashi RM, Ferraris DV, Tsukamoto T, et al. The metabolic profile of tumors depends on both the responsible genetic lesion and tissue type. Cell metabolism. 2012 Feb 08;15(2):157-70. PubMed PMID: 22326218. Pubmed Central PMCID: 3282107.
45. Shroff EH, Eberlin LS, Dang VM, Gouw AM, Gabay M, Adam SJ, et al. MYC oncogene overexpression drives renal cell carcinoma in a mouse model through glutamine metabolism. Proceedings of the National Academy of Sciences of the United States of America. 2015 May 26;112(21):6539-44. PubMed PMID: 25964345. Pubmed Central PMCID: 4450371.
46. Lu C, Ward PS, Kapoor GS, Rohle D, Turcan S, Abdel-Wahab O, et al. IDH mutation impairs histone demethylation and results in a block to cell differentiation. Nature. 2012 Feb 15;483(7390):474-8. PubMed PMID: 22343901. Pubmed Central PMCID: 3478770.
47. Wang P, Wu J, Ma S, Zhang L, Yao J, Hoadley KA, et al. Oncometabolite D-2-Hydroxyglutarate Inhibits ALKBH DNA Repair Enzymes and Sensitizes IDH Mutant Cells to Alkylating Agents. Cell reports. 2015 Dec 22;13(11):2353-61. PubMed PMID: 26686626. Pubmed Central PMCID: 4694633.
48. Turkez H, Geyikoglu F, Yousef MI, Celik K, Bakir TO. Ameliorative effect of supplementation with l-glutamine on oxidative stress, DNA damage, cell viability and hepatotoxicity induced by 2,3,7,8-tetrachlorodibenzo-p-dioxin in rat hepatocyte cultures. Cytotechnology. 2012 03/28

01/11/received

03/05/accepted;64(6):687-99. PubMed PMID: PMC3488374.
49. Cao Y, Kennedy R, Klimberg VS. Glutamine protects against doxorubicin-induced cardiotoxicity. The Journal of surgical research. 1999 Jul;85(1):178-82. PubMed PMID: 10383856.
50. De Bont R, van Larebeke N. Endogenous DNA damage in humans: a review of quantitative data. Mutagenesis. 2004 May;19(3):169-85. PubMed PMID: 15123782.
51. Rydberg B, Lindahl T. Nonenzymatic methylation of DNA by the intracellular methyl group donor S-adenosyl-L-methionine is a potentially mutagenic reaction. The EMBO journal. 1982;1(2):211-6. PubMed PMID: 7188181. Pubmed Central PMCID: 553022.
52. Zhang J, Stevens MF, Bradshaw TD. Temozolomide: mechanisms of action, repair and resistance. Current molecular pharmacology. 2012 Jan;5(1):102-14. PubMed PMID: 22122467.
53. Torgovnick A, Schumacher B. DNA repair mechanisms in cancer development and therapy. Frontiers in genetics. 2015;6:157. PubMed PMID: 25954303. Pubmed Central PMCID: 4407582.
54. Wang ES, Frankfurt O, Orford KW, Bennett M, Flinn IW, Maris M, et al. Phase 1 Study of CB-839, a First-in-Class, Orally Administered Small Molecule Inhibitor of Glutaminase in Patients with Relapsed/Refractory Leukemia. Blood. 2015;126(23):2566-.
55. Meric-Bernstam F, Tannir N, Harding J, Voss M, Mier J, DeMichele A, et al. Phase 1 study of CB-839, a small molecule inhibitor of glutaminase, in combination with everolimus in patients (pts) with clear cell and papillary renal cell cancer (RCC). European Journal of Cancer.69:S12-S3.

56. Bunz F, Dutriaux A, Lengauer C, Waldman T, Zhou S, Brown JP, et al. Requirement for p53 and p21 to sustain G2 arrest after DNA damage. Science. 1998 Nov 20;282(5393):1497-501. PubMed PMID: 9822382.
57. Nay SL, Lee DH, Bates SE, O'Connor TR. Alkbh2 protects against lethality and mutation in primary mouse embryonic fibroblasts. DNA repair. 2012 May 01;11(5):502-10. PubMed PMID: 22429847. Pubmed Central PMCID: 3614354.
58. Onyango DO, Howard SM, Neherin K, Yanez DA, Stark JM. Tetratricopeptide repeat factor XAB2 mediates the end resection step of homologous recombination. Nucleic acids research. 2016 Jul 08;44(12):5702-16. PubMed PMID: 27084940. Pubmed Central PMCID: 4937314.
59. Liu X, Ser Z, Locasale JW. Development and quantitative evaluation of a high-resolution metabolomics technology. Analytical chemistry. 2014 Feb 18;86(4):2175-84. PubMed PMID: 24410464. Pubmed Central PMCID: 3983012.

Chapter 4

Metabolic control of Wnt signaling and cellular differentiation in colorectal cancer via epigenetic reprogramming

Summary

Genetic-driven deregulation of the Wnt pathway is crucial but not sufficient for colorectal cancer (CRC) tumorigenesis. Here, we show that environmental glutamine restriction further augments Wnt signaling in APC mutant intestinal organoids to promote stemness and leads to adenocarcinoma formation *in vivo* via decreasing intracellular alpha-ketoglutarate (aKG) levels. aKG supplementation is sufficient to rescue low-glutamine induced stemness and Wnt hyperactivation. Mechanistically, we found that aKG promotes DNA hypomethylation that leads to an upregulation of differentiation-associated genes and Wnt inhibitory genes. Using CRC patient-derived organoids and several *in vivo* CRC tumor models, we show that aKG supplementation suppresses Wnt signaling and promotes cellular differentiation, thereby significantly restricting tumor growth and extending survival. Together, our results reveal how the low glutamine metabolic microenvironment impacts Wnt signaling and identify aKG as a potent antineoplastic metabolite for potential differentiation therapy for CRC patients.

Introduction

Colorectal cancer (CRC) remains the second leading cause of cancer-associated deaths with more than a million people in the United States alone living with the disease (1). Hyperactivation of the Wnt pathway due to adenomatous polyposis coli (APC) mutations occur in 80 % of human CRC and is a crucial initiating step in carcinogenesis that disrupts cellular differentiation and promotes rapid proliferation (2, 3). However, genetic-driven Wnt deregulation only drives the formation of benign polyps and is insufficient to promote colon carcinoma (4, 5). While the accumulation of mutations in other oncogenes and tumor suppressor genes has been implicated in CRC progression, emerging evidences suggest that other non-genetic factors, such as the microenvironment, can contribute to optimal Wnt activation and oncogenic transformation in CRC (6-9).

Colon cancer cells are subjected to diverse metabolic fluctuations in gut microenvironment, yet little is known about the role of metabolism in regulating Wnt signaling and CRC tumorigenesis. It is well established that overactive Wnt signaling through the regulation of metabolic enzymes and transcription factors can directly reprogram metabolic pathways to support rapid proliferation. For examples, LEF/ TCF/ β-catenin transcription complexes through the upregulation of pyruvate dehydrogenase kinase 1 (Pdk1) and lactate transporter (Mct1) can divert glycolytic glucose toward the production of lactate which stimulates angiogenesis at the tumor sites (10, 11). Consequently, the Wnt-mediated aerobic glycolysis can render cancer cells more dependent on glutamine metabolism to meet the elevated bioenergetic demand and support the biosynthesis of macromolecules. Consistently, a recent study demonstrates that human CRC tumors exhibit an increased uptake and catabolism of glutamine compared to healthy tissues (12). Furthermore, around 30 % of circulating glutamine is consumed in the gut, suggesting that

intestinal cells heavily depend on exogenous glutamine as a preferred fuel source to support intestinal regeneration and integrity (13). Therefore, the increased glutamine dependency in CRC tumors, in addition to an already high glutamine demand by normal intestinal cells, may exhaust the local nutrient supply leading to intratumoral glutamine starvation. Glutamine catabolism in proliferative cells in part supports the biosynthesis of alpha ketoglutarate (aKG) to replenish TCA cycle intermediates (14). Importantly, glutamine and aKG levels have been shown to play an important role in metabolic homeostasis, reactive oxygen species (ROS) control and epigenetic regulation in both normal and cancer cells (15, 16). While the Wnt regulation of the metabolic pathways is well established, it remains largely unknown how changing metabolism, such as glutamine levels, modulate oncogenic signaling pathways and cancer progression.

In this study, we measure how changing glutamine and aKG levels affects oncogenic Wnt signaling and cancer cell differentiation primarily using intestinal organoids and CRC mouse models. We demonstrate that while low glutamine concentrations drive Wnt hyperactivation to enhance intestinal stemness and tumorigenicity, the supplementation of a glutamine-derived metabolite, aKG is sufficient to suppress Wnt signaling and promotes terminal differentiation via epigenetic reprogramming. Collectively, we provide compelling evidence for the crucial role of glutamine and aKG homeostasis in regulating oncogenic Wnt signaling and CRC progression and suggest a potential therapeutic direction using aKG supplementation to drive the terminal differentiation of CRC.

Results

Environmental glutamine restriction hyperactivates Wnt signaling and blocks cellular differentiation

Accumulating evidence suggests colon cancer cells rapidly consume glutamine to support cell survival and proliferation (17). To determine potential changes in glutamine levels in CRC *in vivo*, we first measured glutamine concentration in mouse intestinal tumors. We observed that glutamine concentrations were significantly lower in intestinal tumors from APC^{Min} mice compared to healthy tissues (Figure 4-1A). This phenomenon is also observed in human colon tumors and may be due to increased glutamine uptake and utilization in CRC tumors (12, 18). To examine how this environmental glutamine restriction influences CRC progression, we generated heterozygous APC mutant (APC^{Mut}) small intestinal organoids that recapitulate the genetic background of tumor-initiating cells. We found that low glutamine transformed APC^{Mut} organoids with well-defined crypts into cystic organoids, which are less differentiated (Figure 4-1B) (19). Further examination revealed that glutamine-starved organoids exhibited increased expression of a stem cell marker Lgr5 and active β-catenin suggesting an enrichment of intestinal stemness (Figure 4-1C). In contrast, the loss in expression of differentiation marker Krt20 and the decrease in activity of alkaline phosphatase enzyme Alpi upon glutamine deprivation indicated decreased cellular differentiation (Figure 4-1D). Whole exome sequencing revealed no accumulation of genetic alterations in the CRC driver pathways in glutamine-starved organoids, consistent with previous findings that cultured organoids are genetically and phenotypically stable (Figure 4-S1A, B) (4). Furthermore, we detected full-length APC protein in glutamine-starved organoids, further supporting that genetic instability and other mutations did not contribute to the stem-like phenotype observed under low glutamine conditions (Figure 4- S1C).

To better understand how low glutamine alters cellular differentiation, we performed whole transcriptome sequencing in APC^{Mut} organoids. We observed a global reprogramming of gene expression in intestinal organoids in response to glutamine restriction (Figure 4-S2A). Pathway analyses revealed the top upregulated pathways in glutamine-starved organoids are associated with CRC progression or metastasis including Wnt, MAPK, Rho, VEGF, IL1 and IL8 (Figure 4-1E) (20, 21). Interestingly, glutamine-starved organoids displayed upregulation of CRC-associated genes and hyperactivation of Wnt signaling as determined by GSEA analysis and the expression of Wnt target gene *Axin2* (Figure 4-1F and G). In addition, glutamine restriction in SW620 colon cancer cells harboring an APC mutation significantly induced the expression of the Wnt target genes *AXIN2* and *LGR5* in addition to Wnt ligands in a dose-dependent manner (Figure 4-1H). Furthermore, blockade of Wnt signaling with iCRT3 partially reversed cellular differentiation in glutamine-starved APC^{Mut} organoids, as indicated by the ability to re-form crypts (Figure 4-1I). Similarly, other Wnt inhibitors such as IWP2 and XAV393 also blocked the formation of the stem-like cystic organoids upon glutamine deprivation (Figure 4-1J). These results suggest that the glutamine restricted environment promotes Wnt signaling and overall stemness in APC^{Mut} organoids.

Glutamine restriction promotes enhanced self-renewal and niche independence in APC^{Mut} organoids leading to adenocarcinoma formation *in vivo*

It is well-established that APC mutation alone is not sufficient to promote cancer (4). Thus, we wonder whether metabolic inputs could contribute to the oncogenic acceleration in CRC. To test this, we examined the ability of organoids to self-renew from single cells under low glutamine

conditions because the ability to seed new organoids is limited to stem cells and indicative of tumor initiation potential (Figure 4-2A) (22). We found that glutamine-starved organoids exhibited enhanced self-renewal based on the secondary organoids and increased proliferative capacities based on the total cell numbers (Figure 4-2B). Furthermore, glutamine restriction allowed these organoids to survive and grow independent of "stem cell niche" factors such as R-Spondin, Egf and Noggin (Figure 4-2C). However, none of the control organoids survived in the medium lacking these factors suggesting that APC mutation alone is insufficient to drive tumor establishment outside the intestinal microenvironment. Together, these results suggest that exposure to low glutamine promotes stemness and niche independence in these precancerous APC^{Mut} organoids *in vitro*.

To test whether preexposure to glutamine starvation promotes tumorigenicity of APC^{Mut} intestinal organoids *in vivo,* we injected the control organoids and glutamine-starved organoids into the flanks of immunodeficient mice (Figure 4-2D). While paired control APC^{Mut} organoids failed to engraft, glutamine-starved organoids formed visible lesions with features of tubular adenoma in the subcutaneous environment where intestinal niche factors are not found (Figure 4-2E). Remarkably, the tumors, while limited in size, eventually developed into poorly differentiated adenocarcinomas based on histological analysis (Figure 4-2F). These findings suggest that exposure to environmental glutamine limitation enhances the stemness and tumorigenicity of APC mutant cells.

aKG supplementation rescued low glutamine- induced stemness and suppresses Wnt signaling and restores cellular differentiation

In cancer and highly proliferative cells, glutamine metabolism contributes to several biological processes, including the TCA cycle, ROS regulation and epigenetic modifications (Figure 4-S2B) (17). To determine the mechanism by which glutamine metabolism affects organoid differentiation, we supplemented low glutamine medium with N-acetyl cysteine (NAC), an antioxidant; dimethyl succinate, a TCA intermediate; and dimethyl aKG (DM-aKG), a TCA intermediate and an epigenetic modifier. We found both NAC and dimethyl succinate exerted limited potential to restore cellular differentiation, whereas DM-aKG alone was sufficient to inhibit stem-like cystic morphology and partially rescued crypt formation in glutamine-starved APC^{Mut} organoids (Figure 4-3A, B). Consistently, aKG induced expression of the differentiation marker *Krt20* in APC^{Mut} organoids, suggesting an increase in cellular differentiation (Figure 4-S3A). Thus, these results suggest that low glutamine-induced stemness is largely due to the decreased availability of aKG. We next compared the transcriptional change of the organoids under low glutamine and DM-aKG treatment. We found that aKG supplementation antagonized Wnt signaling and promoted the expression of differentiation-related genes, while glutamine limitation displayed an opposite effect (Figure 4-S3 B-C and 3C). GSEA analyses revealed that glutamine starvation and DM-aKG treatment have opposing influences on intestinal stemness and differentiation based on their respective expression profiles (Figure 4-3D). We next tested whether low glutamine and aKG supplementation regulate Wnt signaling by examining β-catenin and *Lgr5* levels in the organoids. Glutamine starvation increased the levels and nuclear localization of β-catenin and elevated *Lgr5* expression (Figure 4-3E, F). In contrast, DM-aKG treatment caused a decrease in nuclear localization of β-catenin and reduced *Lgr5* expression

(Figure 4-3E, F). Together, these findings suggest that glutamine restriction decreases aKG levels and enhances Wnt signaling as well as stemness through transcriptional regulation, whereas supplementation of aKG is able to lower Wnt signaling and increase intestinal differentiation.

aKG supplementation leads to DNA hypomethylation of genes related to intestinal differentiation and Wnt inhibition

aKG is an essential co-factor for various chromatin modifying enzymes including the Ten-eleven translocation (TET) methylcytosine dioxygenase enzymes which demethylate DNA. Notably, aberrant DNA methylation, especially hypermethylation in promoters of tumor suppressor genes and Wnt antagonist genes, has been shown to contribute to CRC oncogenesis (15, 23-25)). We found that inhibition of DNA methylation with Decitabine, a DNA hypomethylating agent, blocked *Axin2* induction in glutamine-starved organoids indicating potential crosstalk between epigenetics and Wnt signaling mediated by intracellular aKG levels (Fig. S4A). Thus, to test whether aKG supplementation remodels the DNA methylome in intestinal organoids, we performed reduced representation bisulfite sequencing (RRBS) to analyze the genome-wide methylation profile. We found that DM-aKG treatment alone resulted in minimal DNA hypermethylation but drastic DNA hypomethylation, indicating a potential hyperactivity of the Tet enzymes (Figure 4-4A). Volcano plot analysis further confirmed this on a gene level revealing that most differentially methylated genes are hypomethylated and a small subset of genes are hypermethylated in response to DM-aKG treatment (Figure 4-4B). Moreover, gene ontology analysis showed that aKG supplementation promotes DNA hypomethylation in genes

involved in cellular differentiation, immune response and metabolism (Figure 4-4C). Strikingly, a global transcriptome remodeling took place with a larger percentage of genes upregulated upon DM-aKG treatment (Figure 4-4D). The integration of the DNA methylation sequencing and the transcriptome profile in a Starburst plot identified 293 genes with DNA hypomethylation and increased gene expression upon DM-aKG treatment (Figure 4-4E). Among these genes are differentiation-associated genes identified by overlapping with an intestinal differentiation signature and genes often hypermethylated in CRC including *Ndrg4* and *Stox2* (26). Moreover, we found genes with tumor suppressive function including *Bbc3* and *Bax* also affected by DM-aKG treatment (Figure 4-4F). Importantly, we found that aKG reshaped epigenetic marks on genes related to Wnt signaling. For example, aKG treatment induced DNA-demethylation and upregulation of *Dkk3* and *Dkk4*, Wnt antagonists that blocks Wnt ligand-receptor interaction, and *Fat1* which interferes with the nuclear localization and transcriptional activity of β-catenin (Figure 4- 4F) (27). Consistently, *DKK4* upregulation was validated in both organoids and colon cancer cells upon aKG or DNA methylation inhibitor treatment (Fig. S4B, C). Similarly, we confirmed that aKG promoted global DNA demethylation on 5-methyl cytosine including the upstream region of *DKK4* in colon cancer cells (Figure 4-4G). We found knocking down the TET1 enzymes blocked *DKK4* induction and inhibited the effect of aKG on the expression of stemness marker *LGR5* (Figure 4-4H, S4D). These data support the notion that aKG-mediated DNA demethylation is in part through TET enzymes. Taken together, these results suggest that aKG supplementation promotes global DNA hypomethylation that in part derepresses the expression of differentiation-related genes and Wnt antagonist genes.

aKG supplementation drives terminal differentiation and suppresses growth of patient-derived colon tumor organoids

As cellular dedifferentiation drives CRC pathogenesis and therapeutic resistance, reinforcement of terminal differentiation is a promising therapeutic approach that has gained success in other cancers that arise similarly from differentiation dysfunction (7, 28, 29). Since aKG supplementation has resulted in remarkable responses in mouse organoids in term of promoting cellular differentiation, we next generated a panel of patient-derived organoids (PDOs) to test the therapeutic potential of aKG supplementation in human CRC cells. We found that DM-aKG treatment inhibited the initiation and growth of a panel of PDOs harboring APC truncated proteins (Figure 4-5A, S5A, B). In addition, DM-aKG treatment significantly reduced organoid size and blocked cystic morphology in PDOs (Figure 4- 5B). Also, aKG-treated PDOs highly expressed intestinal differentiation markers including Krt20 and Muc2 compared to the control organoids (Figure 4- 5C). Rather than inducing cytotoxicity, treatment with aKG arrested the cancer organoids in a terminally differentiated state with a limited proliferative potential that persisted even after the metabolite was washed out (Figure 4-5D). Consistent with the response in mouse intestinal organoids, we found that Wnt signaling was suppressed and differentiation-related genes were induced upon aKG treatment in PDOs (Figure 4-5E). Drug response profiling in PDOs has been shown to accurately predict clinical response in patients with gastrointestinal cancer (30). Therefore, aKG supplementation with the ability to suppress Wnt signaling and induce cellular differentiation in PDOs represent a potential therapeutic opportunity for the treatment of colon cancer.

aKG supplementation inhibits the growth of highly mutated CRC xenograft tumors *in vivo*.

In addition to Wnt dysregulation, CRC tumors commonly acquire mutations in other oncogenic pathways, including KRAS (43% human CRC) and P53 (54% human CRC) that contribute to cancer progression and drug resistance (31). While the effect of aKG supplementation in APC^{Mut} organoids is dramatic, the accumulation of these genetic mutations could render cancer cells insensitive to the metabolite treatment. Thus, we next tested the therapeutic potential for aKG supplementation in CRC tumors with an activating Kras mutation and p53 disruption. In poorly differentiated organoids with Apc knockdown, Kras activation and p53 deletion (AKP), we found that DM-aKG treatment restricted organoid growth and induced cellular differentiation as indicated by the ability of organoids to re-form crypts instead of cystic organoids (Figure 4-6A). Importantly, DM-aKG treatment either by IP injection or in the drinking water suppressed the growth of mouse subcutaneous xenograft tumors generated from AKP organoids (Figure 4-6B). Histological analysis revealed that DM-aKG treated tumors were predominantly occupied by stromal cells while the control AKP organoids grew out as invasive carcinomas (Figure 4-6C). To further validate this result, we tested the effect of aKG on another xenograft tumor model generated from SW620 human colon cancer cells harboring mutations in the *APC, KRAS, TP53 and SMAD4* genes. We found that DM-aKG treatment increased intratumoral aKG levels and limited the tumor growth (Figure 4-6 D, E). Consistently, aKG treatment *in vivo* suppressed the expression of Wnt target genes in the SW620 xenograft tumors (Figure 4-6F). Together, these findings suggest that aKG supplementation is effective for the treatment of CRC tumors bearing other oncogenic mutations in addition to *APC.*

aKG supplementation suppresses Wnt singaling and inhibits tumor initiation in APC^{Min} mice

Combating tumor initiation and preventing recurrence is a clinical challenge in CRC (32). Thus, we evaluated the effects of aKG treatment in intestinal neoplasia using the APC^{Min} mouse, a model that develops spontaneous intestinal tumors due to Wnt deregulation (33). DM-aKG treatment via IP injection raised aKG levels in the intestine without significantly affecting the body weight or intestinal homeostasis in healthy wildtype mice, suggesting DM-aKG is well-tolerable (Figure 4-7A, S6A). Strikingly, DM-aKG treatment in APC^{Min} mice partially protected against tumor-associated weight loss and significantly reduced tumor numbers (Figure 4-7B-D). To gain better insight into how aKG modulates tumor initiation, we performed whole transcriptome sequencing of the intestinal tissue of mice supplemented with DM-aKG. APC^{Min} mice displayed extensive hyperactivation of genes compared to the wild-type mice. Interestingly, DM-aKG treatment in the APC^{Min} mice alone suppressed a significant majority of genes in Cluster 8 (Figure 4-7E). Gene analysis of Cluster 8 revealed gene networks involved in Wnt signaling, angiogenesis, and other oncogenic pathways suggesting that aKG treatment may suppress many cancer-associated genes to inhibit tumor initiation and progression in the APC^{Min} mice (Figure 4-7F). The suppression of Wnt signaling and stemness induced upon DM-aKG treatment was confirmed via GSEA analysis, β-catenin staining and mRNA expression of the Wnt-driven stem cell markers *Lgr5* and *Ascl2* (Figure 4-7G, I, J). Together, our data suggest that aKG represses Wnt signaling and thus restricts tumor initiation. In order to achieve a more direct and continuous delivery of aKG, we tested the therapeutic potential of DM-aKG supplementation in drinking water. We found that supplementation of DM-aKG in drinking water has no noticeable effect on general health of the mice, including body weight, liver

function and kidney function (Figure 4-S6B, C). Strikingly, we found that over 90 % control APC^{Min} mice at day 50 developed rectal bleeding, an indication of intestinal tumors, while only 23% mice with aKG supplementation in drinking water had rectal bleeding (Figure 4-7K). Moreover, Kaplan-Meier survival curve revealed a significant extension in the survival of APC^{Min} mice with DM-aKG supplementation (Figure 4-7L).

Discussion

Despite enormous progress in understanding the molecular carcinogenesis of colon cancer, there is little understanding of the crosstalk between environmental factors and various hallmarks of colon cancer including hyperactivated Wnt signaling and differentiation dysfunction. In this study, we demonstrate that the glutamine-aKG axis is an active determinant of Wnt signaling and cellular differentiation in colon cancer. The depletion of intracellular αKG as the result of environmental glutamine restriction potentiates oncogenic Wnt signaling to promote tumorigenesis. In contrast, we identified aKG as a potent antitumor metabolite that suppresses Wnt signaling to promote cellular differentiation. Thus, these findings shed light on the potential role of the metabolic environment in cancer progression and therapeutic opportunity.

We found that glutamine concentration is dramatically depleted in mouse intestinal tumors compared to healthy tissues, consistent with previous studies using metabolomics analysis compared glutamine levels in colon patient samples with healthy tissues (18). Additionally, the intratumoral glutamine deficiency is also observed in other solid tumors including hepatomas,

melanoma, pancreatic and sarcomas (34, 35). In the case of CRC, constitutive Wnt signaling can directly regulate cellular metabolism to support rapid cell division. One example of this crosstalk is that β-catenin transcriptional complexes target Pdk1 to inhibit pyruvate oxidation in the TCA cycle and favor aerobic glycolysis leading to increased glutamine dependency (10, 36). In addition, Myc, a well-established Wnt target, also drives glutaminolysis which intensifies the demand for exogenous glutamine in Wnt-driven cancer cells (11). Thus, Wnt-driven metabolic reprogramming may contribute to rapid glutamine utilization which eventually depletes the local supply leading to a period of glutamine deprivation observed in CRC tumors.

Glutamine is a vital nutrient that supports metabolic homeostasis and survival of cancer cells, making glutamine metabolism an attractive target for cancer therapy (17). While the complete withdrawal of glutamine may lead to cell cycle arrest and cancer cell death, we found that intestinal organoids can survive and adapt to the low glutamine conditions. Surprisingly, we found that glutamine restriction further activates the Wnt signaling pathway to promote cancer dedifferentiation even in the organoids or cancer cell lines carrying APC mutations. This finding is consistent with the emerging evidence suggesting that other factors contribute to the optimal activation of the Wnt signaling in colon cancer in addition to the genetic alterations. It is important to note that most APC mutations in CRC tumors often generate premature stop codons resulting in stable truncated APC proteins, which still retain partial function to suppress Wnt signaling (37-39). Accordingly, intracellular signaling such as EGF and RAS has been shown to enhance the oncogenic activity of Wnt signaling in colon cancer cells (40, 41). Similarly, microenvironmental factors including the close proximity to neighboring myofibroblasts also induce transcriptional activity of Wnt signaling and the clonogenicity capacity of colon cancer

stem cells (9). Nearly 50 % of people will develop intestinal polyps at some point in their lifetimes, yet only a small fraction of these begin lesions eventually develop into invasive tumors (42). Mutations in other driver pathways including KRAS, P53 or SMAD are implicated in CRC progression, yet some advanced tumors only harbor one or two driver mutations suggesting non-genetic factors also contribute to the oncogenic transformation of CRC (43, 44). We found that exposure to glutamine restriction endows the APC mutant intestinal organoids with the ability to grow independent of intestinal niche factors and form adenocarcinoma tumors *in vivo.* Thus, an altered metabolic microenvironment such as glutamine deficiency by potentiating Wnt signaling and dedifferentiation may contribute to colon cancer progression.

We also found that low glutamine augments Wnt signaling and stemness through the depletion of intracellular aKG. Importantly, increasing intracellular aKG levels antagonize oncogenic Wnt signaling and facilitate terminal differentiation in intestinal organoids and PDOs. While aKG was previously shown to preserve the undifferentiated state of embryonic stem cells (15), the role of aKG in restoring intestinal differentiation suggests the metabolic regulation of cellular fate also depends on the tissue of origin. As a required co-factor for TET enzymes, we found aKG supplementation leads to drastic DNA hypomethylation partially through TET1 activity, which has been previously shown to exhibit tumor suppressive function in cancer (45). We demonstrated that aKG-induced DNA hypomethylation affects genes related to Wnt suppression and cellular differentiation. In line with this finding, DNA hypomethylation was previously shown to induce the expression of differentiation genes to facilitate the stem-differentiation transition during the normal intestinal regeneration process (24, 46). In addition to DNA methylation, aKG fluctuation also affects the activity of many histone demethylases (15, 16).

Since DNA methyltransferase inhibitors in clinical trials have yielded limited clinical efficacy in CRC patients, the regulation of aKG levels on histone methylation also likely contribute to the potent antitumor activity of aKG observed in this study (47).

While the molecular pathogenesis of colorectal cancer is well characterized, clinical effort to inhibit the Wnt pathway remain unsuccessful in clinical settings. As such, treatment regimens for advanced CRC still depend heavily on chemotherapies as they have for decades. Many Wnt signaling inhibitors exert detrimental effects on normal intestinal homeostasis and other tissues where physiological Wnt plays a crucial role in somatic stem cell maintenance (28, 48, 49). Numerous Wnt inhibitors have entered clinical trials in recent years, yet none have reached clinical approval for the treatment of colon cancer mainly due to multiple side deleterious effects in patients including bone breakage (50, 51). Thus, the ability to safely modulate Wnt signaling to a sufficient level to restore terminal differentiation in colon cancer cells presents a promising therapeutic approach for colon cancer. Indeed, cancer therapies that promote terminal cellular differentiation yield impressive clinical outcomes. For example, the all-trans retinoic acid in combination with chemotherapy drives terminal differentiation resulting in a cure rate of more than 80% in patients with promyelocytic leukemia (29). Similarly, our results indicate that aKG could be used as a novel therapeutic agent to suppress Wnt signaling and drive CRC differentiation. This approach could represent a less aggressive therapy for the treatment of colon cancer. Rather than inducing abrupt cell death, aKG drives the cancerous cells to terminally differentiated state with limited proliferative and oncogenic potential. While we show that aKG supplementation in drinking water is relatively safe and significantly improves survival of mice bearing intestinal tumors, the metabolite can be further modified to enhance efficacy and

minimize potential toxicity. In conclusion, our work provides a new therapeutic direction to harness the potency of aKG in driving intestinal differentiation to improve clinical outcome of patients with CRC.

Methods

Mouse intestinal crypt isolation and culture

Intestinal crypts from 6-8 week-old APC^{Min} mice were isolated based on the previous study. Small intestinal shAPC/KRAS/$P53^{-/-}$ organoids were cultured with 500 ng/ml doxycycline, and kindly provided by Dr. Lukas Dow laboratory (Weill Cornell Medicine) (22). Organoids were cultured in organoid media (IntestiCult™ Organoid Growth Medium, Stemcell, 06005 supplemented with penicillin/streptomycin) and mixed 1:1 ratio with Growth Factor Reduced Matrigel (Corning, 356230). 50uL of the organoid mix was plated into a pre-warmed 48-well plate followed by 10-minute incubation at 37 °C to polymerize the matrigel. 200 µL of room temperature intestinal organoids medium was added on the side of the well to cover the Matrigel. For organoid maintenance, the medium was changed every other day, and the organoids were passaged 1:5 every week. To passage the organoids, the culture medium was removed and the matrigel was dissociated in EDTA-PBS and incubated briefly in EDTA-PBS at room temperature for 10 minutes on a rocking platform. For subcloning assays, organoids were dissociated into single cells using TrypLE (ThermoFisher, 12605036). For glutamine starvation experiment, DMEM/F-12 medium- No glutamine (Gibco, 21331020) was used as basal media and L-glutamine (Corning, 25-005) was added back to the desired concentration.

Patient-derived colon isolation and organoid culture. Colonic human tissue was collected following surgical resection with consent at St. Joseph Hospital Orange (Orange, CA). All patients were diagnosed with colorectal cancer and diagnosis was confirmed by a pathologist. Establishment of organoids was performed based on a previous study (van de Wetering et al, Cell, 2015). Tumor Organoids were grown in basement membrane extract (Cultrex PathClear BME Type 2) with medium consisting of: 50 % advanced DMEM/F12 (supplemented with penicillin/streptomycin, 10mM HEPES, Glutamax, and Primocin), 20 % R-Spondin conditioned medium (from Cultrex Rspo1-expressing cells, Trevigen), 10 % Noggin conditioned medium (from HEK293 cells stably transfected with pcDNA3 NEO mouse Noggin insert, kindly provided by Dr. Hans Clevers Laboratory), 20% Expansion medium 5x (final concentrations in medium of the following 1x B27, 1.25 mM n-Acetyl Cysteine, 10 mM Nicotinamide, 50 ng/ml human EGF, 10 nM Gastrin, 500 nM A83-01, 3 μM SB202190, 10 nM Prostaglandine E2). Media was changed every 2-3 days and organoids were passaged about once per week following established protocols.

Cell culture, reagents, proliferation assay, and siRNA transfection

SW620 cells were obtained from American Type Culture Collection (ATCC). Cells were cultured in Dulbecco's Modified Eagle Medium (DMEM, Corning) supplemented with 10 % fetal bovine serum (FBS; Gemini Bio-Products), 100 units/mL of penicillin, and 100 μg/mL of streptomycin (Gemini Bio-Products) at 37 °C with 5 % CO2. For glutamine starvation experiments, DMEM-No glutamine (Corning) and 10 % dialyzed FBS (Gemini Bio-Products) were used to make glutamine-free media. For cell proliferation assays, cells were cultured in a

96-well plate for treatment. Relative cell number was determined by CellTiter-Glo assay (Promega) according to the manufacturer's protocol. For siRNA transfection, ON-TARGET plus Human TET1 siRNA (Dharmacon, L-014635-03-0005) or control siRNA (Dharmacon) was used in the presence of RNAi Max lipofectamine reagent (Invitrogen). DM-aKG treatment was performed two days after transfection.

Reagents: Dimethyl α-ketoglutarate (Sigma, 349631), N-Acetyl-L-cysteine/NAC (Sigma, A7250), Dimethyl-succinate (Sigma), iCRT3 (Millipore, 219332), IWP2 (Stemgent 04-0034), XAV393 (Sigma X3004).

Glutamine, aKG, ALT and AST measurement assay

For glutamine measurement, metabolites were extracted from tissues or tumors as previously described (Pan, NBC). Briefly, 20-40 mg of frozen/fresh tissue was homogenized in ice-cold 70 % ethanol by Precellys 24 homogenizer, and the supernatant was collected and dried using a SpeedVac Vacuum Concentrator. The pellet was collected and suspended in water (1 μL water per mg of fresh tissue). The concentration of glutamine in the solution was then determined by the EnzyChrom Glutamine Assay Kit (BioAssay Systems) according to the manufacturer's protocol. For aKG measurement, Alpha Ketoglutarate Assay Kit (Abcam) was used according to the manufacturer's protocol for colorimetric assay without the deproteinization step. For ALT and AST measurement in mouse serum, EnzyChrom™ Alanine Transaminase Assay Kit and EnzyChromTM Aspartate Transaminase Assay Kit from Bioassays were used according to the manufacturer's protocol.

Immunofluorescence and Immunohistochemistry. Immunofluorescence was performed as described previously (31). Organoids after treatment were fixed with 4 % of formaldehyde for 10 minutes at room temperature followed by blocking with 1 % BSA at 4 °C overnight. The organoids were stained with primary antibodies against KRT20 (Cell Signaling, 13063), Non-phospho (Active) β-catenin (Cell Signaling, 19807), Muc2 (Abcam, 11197) or DAPI (ThermoFisher, D1306) at 4 °C overnight. Secondary antibodies, goat anti-rabbit Alexa Fluor 488 (Invitrogen, 11037) and goat anti-mouse Alexa Fluor 594 (Invitrogen, A11029), were purchased from Millipore-Sigma. Alkaline Phosphatase activity was determined by Red Alkaline Phosphatase Substrate Kit (Vector, SK5100). Images were captured 20x magnification by using a Zeiss LSM 700 Confocal Microscope and the ZEN Blue image acquisition software. IHC staining were performed on sections prepared from formalin fixed and paraffin-embedded tissue by San Diego Pathology Group (San Diego, CA) and UCI-ETR pathology core.

RNA extraction, quantitative real-time PCR

Total RNA was extracted and purified using Trizol (Invitrogen) or RNeasy kit (Qiagen) according to the manufacturer's protocol. qScript cDNA synthesis kit (Quanta Biosciences) was used to make cDNA. Quantitative real-time PCR were performed using SYBR-Green PCR master mix (Quanta Biosciences) and a BioRad real-time PCR machine. Relative gene expression was normalized to rRNA ribosomal 18S or Actin. The primers used in the study are listed below.

m-AXIN2	5'- GCAGCTCAGCAAAAAGGGAAAT-3'	5'- TACATGGGGAGCACTGTCTCGT-3'

m-MYC	5'-CTCAGTGGTCTTTCCCTACCCG -3'	5'- TGTCCAACTTGGCCCTCTTGGC-3'
m-LGR5	5'- CAAGCCATGACCTTGGCCCTG-3'	5'- TTTCCCAGGGAGTGGATTCTATT-3'
m-ASCL2	5'-TAGTGCAGCCTGACCAAATG -3'	5'-AAGTCCTGATGCTGCAACGT -3'
m-DKK4	5'-GTACTGGTGACCTTGCTTGGA-3'	5'-CCGTTCATCGTGAAACGCTAAG-3'
h-WNT3	5'- CTCGCTGGCTACCCA ATTTG -3'	5' -AGGCTG TCA TCT ATG GTG GTG -3'
h-LGR5	5'-CTC CCA GGT CTG GTG TGT TG-3'	5'- GAGGTCTAGGTAGGAGGT GAA G-3'
h-AXIN2	5'-CAA CAC CAG GCG GAA CGA A-3'	5'-GCCCAATAAGGAGTGTAAGGA CT-3'
h-WNT6	5'- GGC AGC CCC TTG GTT ATG G-3'	5'-CTC AGC CTG GCA CAA CTC G-3'
h-CCND2	5’-TTCCCTCTGGCCATGAATTA-3’	5’- TGTAAATGCACAGCTTCTCC-3’
h-MYC	5’- TTCGGGTAGTGGAAAACCAG-3’	5’- CAGCAGCTCGAATTTCTTCC-3’
h-DKK4	5'-ACATGCAGAAGGAACAACTG-3'	5'-CTCCAAAAGGACTGGCTTAC-3'
mKRT20	5'-TTCAGTCGTCAAAGTTTTCACCG-3'	5'-TCCTATGCGAGCCACTCA-3'
h-WNT5a	5'-ATT CTT GGT GGT CGC TAG GTA -3'	5'-CGC CTT CTC CGA TGT ACT GC-3'
h-WNT10a	5'-GGT CAG CAC CCA ATG ACATTC -3'	5'-TGG ATG GCG ATC TGG ATG C-3'
h-MUC2	5'-GAG GGC AGA ACC CGA AAC C-3'	5'-GGC GAAGTT GTA GTC GCA GAG -3'
h-KRT20	5'- GGA CGA CAC CCA GCG TTT AT -3'	5'-CGC TCC CAT AGT TCA CCG TG-3'

h-TET1	5'-CATCAGTCAAGACTTTAAGCCCT -3'	5'- CGG GTG GTT TAG GTT CTG TTT -3'

RNA sequencing

Kapa RNA mRNA HyperPrep kit (Kapa Biosystems, Cat KR1352) was used for RNA sequencing library preparation.100 ng of total RNA from each sample was used for polyA RNA enrichment using magnetic oligo-dT beads. cBot cluster generation system (Illumina) with HiSeq SR Cluster V4 Kit was used to prepare library templates for sequencing. Sequencing run was performed using Illumina HiSeq 2500 with HiSeq SBS V4 Kits. Real time analysis 2.2.38 (RTA) software was used to process the image analysis and base calling. RNA-seq sequences are aligned to mouse genome (mm10) using HISAT2 and RNA-seq expression level were measured as RPKM using Partek Genomic Suite software (v6.6). Different expressed genes were detected using Partek GS's RNA-seq pipeline. The significant different expressed genes were detected using FDR adjusted p-value <0.05 and +/-1.5-fold change as cutoff.

GSEA analysis was based on following gene sets:

Wnt signaling: KEGG_WNT_SIGNALING_PATHWAY (M19428)

Intestinal stem cell signature: adapted from Muñoz et al, EMBO, 2012 and Tong et al, Cell Report, 2017.

Intestinal differentiation signature: adapted from Chong et al, Nature, 2009 and Tong et al, Cell report, 2017.

RRBS-seq sequencing and exome-seq sequencing

The RRBS-seq sequencing libraries were prepared with City of Hope IGC modified protocol. Briefly, 250 ng of genomic DNA was digested with the methylation insensitive restriction enzyme MspI (NEB) at 37 °C overnight, and followed by incubation at 80 °C for 20 minutes to inactivate MspI. In the same reaction tube, Klenow Fragment (3′→5′ exo-minus; NEB) and dNTP was added and incubated at 37 °C for 40 minutes to repair MspI digested DNA and add dAMP to the 3' end. Illumina methylated adapters and T4 DNA ligase (Promega) were added in the same tube for an overnight ligation. 1.6xAmpureXp beads purification was used for the cleanup after the ligation. EZ DNA Methylation-Gold kit (Zymo Resarch, Cat. D5005) was used for the DNA bisulfite conversion. Bisulfite converted DNA was amplified with a 12 cycle of PCR with Pfu Turbo Cx Hotstart DNA Polymerase (Agilent). The final PCR products were run on 6 % TBE acrylamide gels and DNA fragments with size from 160-500 bp (insert size 40-380 bp) were excised and eluted in EB buffer. RRBS-seq library templates were prepared for sequencing with Illumina HiSeq PE Cluster V4 Kit, sequencing runs were performed in the paired end mode of 101cycle on Illumina HiSeq 2500 with HiSeq SBS V4 Kits. Real-time analysis (RTA) 2.2.38 software was used to process the image analysis and base calling. RRBS-seq sequences were aligned to mouse genome using novocraft's Novoalign (V3.08.02). The bisulphite reference sequence was generated based on mm10 genome sequence using Novocraft's novoindex with bisulphite mode. The alignment results were used to detect CpG Methylation site using Novocraft's novomyethyl tool. Each sample type has three biology replications and the results of each biology replication were merged to generate the total methylation sites list. Most of the CpG methylation sites are close to gene region (+/-20 Kbps) and over 80% of the methylation sites are located close to gene regions. Different methylation

pattern between samples are detected using ANOVA with FDR adjusted p-value <0.05 and +/- 1.5-fold change on methylation percentage. To identify the methylation status at the gene level, the average of methylation difference of significant (FDR adjusted p-value) differential methylation sites was calculated.

For Exome-seq sequencing, 250 ng genomic DNA was fragmented using Covaris S220 (Covaris, Woburn, MA) with the 200 bp peak setting. The fragmented DNA was end-repaired and ligated to Illumina adaptor oligonucleotides with Kapa Hyper Prep Kit (KAPA Biosystems, Wilmington, MA; Cat.KK8504). Ligation products were purified and amplified with a 7 cycle of PCR. The enriched PCR products were subject to the exome capture procedure using the SureSelecXT mouse All Exon kit (Agilent, Technologies, Santa Clara, CA; Cat 5190-4641) according to manufacturer's protocols. The captured products were further amplified with an 8-cycle of PCR. Exome-seq library templates were prepared for sequencing with Illumina HiSeq PE Cluster V4 Kit as described in RRBS sequencing. Whole exome capturing and sequencing on target regions designed by Agilent SureSelect Mouse All Exon V1 were performed. The circular binary segmentation (CBS) algorithm was used to identify abnormal copy number change between samples. Read depth of coverage in each exon region was calculated, and log2-based coverage difference was further adjusted by subtracting the mean of log2-based coverage difference between y. The outcome was smoothed and segmented to identify potential copy number change between the samples. Among the potential copy number change, only the segments that span across at least 2 markers and are at least log2 (1.5) distance away from the mean copy number level was retained.

Immunoblotting

Following treatment, organoids and cells were harvested in ice cold PBS, lysed in lysis buffer containing protease and phosphatase inhibitor (Thermo Scientific) and followed by brief sonication. Equal amount of protein, as measured by BCA protein assay, were loaded into precast NuPAGE Bis-Tris gels (Life Technologies) followed by transfer onto nitrocellulose or PVDF membrane. After blocking with 5 % milk-PBS, membranes were incubated with primary antibody overnight at 4 °C with shaking followed by horseradish-peroxidase-conjugated secondary antibodies for 1 hour at room temperature. The signal was visualized by Western Lightning Plus-ECL (PerkinElmer). The antibodies used are LGR5 (Abcam, 75732), Non-phospho/ Active β-Catenin (Cell Signaling, 19807), Histone H3 (Cell Signaling, 4499), APC (Millipore, 2504)

Dot blot assay and MeDIP assay

For Dot blot assay, DNeasy Blood & Tissue Kit (Qiagen) was used to isolate genomic DNA. After incubation at 95 °C for 5 minutes, equal amount of DNA was loaded onto a positively charged nylon membrane (Amersham Hybond-N+; GE Healthcare). The membrane was UV cross-linked and blocked in 5 % milk-PBS followed by incubation with anti-5 methyl-cytosine (Millipore, MABE146) overnight at 4 °C. After the secondary antibody incubation for 1 hour at room temperature, the signal was visualized using Western Lightning Plus-ECL (Perkin-Elmer**).**

For methylated DNA immunoprecipitation (MeDIP), genomic DNA following DM-aKG treatment was isolated using DNeasy Blood & Tissue Kit (Qiagen) and sonicated to yield 300-1000 bp DNA fragments. The sonicated DNA was immunoprecipitated with a monoclonal antibody against 5-methylcytosine (Millipore, MABE146) for 3 hours or IgG at 4 °C with

shaking. DNA complexes was pulled down using Protein A Agarose and purified with PCR purification kit. The DNA was then analyzed by RT-qPCR with the MeDIP-hDKK4 primers: F 5'-TGG CCA GTA TGA TTC ATC CT-3' AND R 5'-AAG TTA GTT CAA AGG GCC AC-3'

Animal study

All studies involving animals were performed according to approved IACUC protocols at the City of Hope Cancer Center and The University of California, Irvine. Sample size was generally chosen based on preliminary data indicating the variance within each group and the differences between groups.

Xenotransplantation of organoids in mice: APC mutant organoids cultured in low glutamine (0.3 mM) condition and paired control organoids with similar passage were cultured for one week. Organoids were expanded in organoid culture DMEM/F12 medium containing (Recombinant Murine EGF 50 ng/ml (Peprotech), Recombinant murine Wnt-3A 100 ng/ml (Millipore GF-160), Recombinant Murine Noggin 50 ng/ml (R&D system), 20% R-Spondin conditioned medium (from Rspo1-expressing cells, Trevigen), penicillin, and streptomycin. Organoids were dissociated into single cell with TrypLE (Thermofisher), and 1 million cells, suspended in cold Matrigel and DMEM/F12 (1:1 ratio), were injected subcutaneously into the flank of 10-week-old NSG mice. Control organoids were injected into the left flank and low glutamine organoids were injected into the right flank. The established tumors were collected and fixed for subsequent histological analysis. To generate xenograft tumors with AKP organoids, 7-week-old athymic nude male mice (Taconic Laboratories, Rensselaer, NY) were injected subcutaneously into the flank with 0.5 x 10^6 cells of AKP organoids in DMEM/F12 media and Matrigel (1:1 ratio). The

mice were treated with doxycycline in drinking water at 0.5 mg/ml with sucrose to turn on APC shRNA. After the tumors were established (around 100 mm^3), the mice were randomized into groups treated with PBS control, 600 mg/kg DM-aKG by intraperitoneal injection, or 25 mg/ml DM-aKG in drinking water. SW620 xenograft tumors were generated with 1 x 10^6 cells in 8-week-old athymic nude male mice. After tumor engraftment, the mice were randomized into groups treated with control PBS or with 600 mg/kg DM-aKG by intraperitoneal injection four times per week. SW620 xenograft tumors were generated with 1 x 10^6 cells in 8-week-old athymic nude male mice. After tumor engraftment, the mice were randomized into groups treated with PBS control or DM-aKG by intraperitoneal injection.

DM-aKG treatment in APC^{Min} mice: 5-8 week-old C57BL/6J-ApcMin/J mice were obtained from Jackson laboratory (MIN-002020). Some APC^{Min} mice were bred by crossing the Male APC^{Min} mice with female wild-type C57BL/6J mice, APC mutant genotyping was determined by Transnetyx Inc. 8-9 week APC min mice were treated with 400 mg/kg DM-aKG by intraperitoneal injection or in drinking water supplemented with 15 mg/ml of DM-aKG (Sigma-349631 or TCI Chemical-K0013). DM-aKG supplemented water was replaced every other day. Survival endpoint was determined by established parameters including 25 % of body weight loss, pale extremities, hunching, poor body condition/dehydration, lethargy and/or irreversible rectal relapse. For 18F-FDG PET imaging of Apc^{Min}, mice were fasted overnight and 100μCi FDG was i.v. injected and PET images were taken 1-hour post injection.

Statistical analysis

Results are shown as averages; most error bars represent standard deviation (SD) (or standard error of the mean (SEM) if indicated). Unpaired Student t-test was calculated by Graphpad or Excel was used to determine the statistical significance of differences between means (* $p < 0.05$, ** $p < 0.01$, *** $p < 0.001$). p-value for mice survival study was determined by Graphpad.

Reference

1. Torre LA, Bray F, Siegel RL, Ferlay J, Lortet-Tieulent J, Jemal A. Global cancer statistics, 2012. CA: a cancer journal for clinicians. 2015 Mar;65(2):87-108. PubMed PMID: 25651787. Epub 2015/02/06. eng.
2. Fearon ER. Molecular Genetics of Colorectal Cancer. Annual Review of Pathology: Mechanisms of Disease. 2011 2011/02/28;6(1):479-507.
3. Schepers A, Clevers H. Wnt signaling, stem cells, and cancer of the gastrointestinal tract. Cold Spring Harbor perspectives in biology. 2012 Apr 1;4(4):a007989. PubMed PMID: 22474007. Pubmed Central PMCID: 3312683.
4. Drost J, van Jaarsveld RH, Ponsioen B, Zimberlin C, van Boxtel R, Buijs A, et al. Sequential cancer mutations in cultured human intestinal stem cells. Nature. 2015 May 7;521(7550):43-7. PubMed PMID: 25924068.
5. Kinzler KW, Vogelstein B. Lessons from hereditary colorectal cancer. Cell. 1996 Oct 18;87(2):159-70. PubMed PMID: 8861899.
6. Fearon ER, Vogelstein B. A genetic model for colorectal tumorigenesis. Cell. 1990 Jun 1;61(5):759-67. PubMed PMID: 2188735.
7. de Sousa e Melo F, Kurtova AV, Harnoss JM, Kljavin N, Hoeck JD, Hung J, et al. A distinct role for Lgr5(+) stem cells in primary and metastatic colon cancer. Nature. 2017 Mar 29;543(7647):676-80. PubMed PMID: 28358093.
8. Medema JP. Targeting the Colorectal Cancer Stem Cell. The New England journal of medicine. 2017 Aug 31;377(9):888-90. PubMed PMID: 28854096.
9. Vermeulen L, De Sousa EMF, van der Heijden M, Cameron K, de Jong JH, Borovski T, et al. Wnt activity defines colon cancer stem cells and is regulated by the microenvironment. Nature cell biology. 2010 May;12(5):468-76. PubMed PMID: 20418870.
10. Pate KT, Stringari C, Sprowl-Tanio S, Wang K, TeSlaa T, Hoverter NP, et al. Wnt signaling directs a metabolic program of glycolysis and angiogenesis in colon cancer. The EMBO journal. 2014 Jul 1;33(13):1454-73. PubMed PMID: 24825347. Pubmed Central PMCID: 4194089.
11. Gao P, Tchernyshyov I, Chang TC, Lee YS, Kita K, Ochi T, et al. c-Myc suppression of miR-23a/b enhances mitochondrial glutaminase expression and glutamine metabolism. Nature. 2009 Apr 9;458(7239):762-5. PubMed PMID: 19219026. Pubmed Central PMCID: 2729443.
12. Huang F, Zhang Q, Ma H, Lv Q, Zhang T. Expression of glutaminase is upregulated in colorectal cancer and of clinical significance. Int J Clin Exp Pathol. 2014;7(3):1093-100. PubMed PMID: 24696726. Pubmed Central PMCID: 3971313.
13. Kim MH, Kim H. The Roles of Glutamine in the Intestine and Its Implication in Intestinal Diseases. International journal of molecular sciences. 2017 May 12;18(5). PubMed PMID: 28498331. Pubmed Central PMCID: 5454963.
14. Le A, Lane AN, Hamaker M, Bose S, Gouw A, Barbi J, et al. Glucose-independent glutamine metabolism via TCA cycling for proliferation and survival in B cells. Cell metabolism. 2012 Jan 4;15(1):110-21. PubMed PMID: 22225880. Pubmed Central PMCID: 3345194.
15. Carey BW, Finley LW, Cross JR, Allis CD, Thompson CB. Intracellular alpha-ketoglutarate maintains the pluripotency of embryonic stem cells. Nature. 2015 Feb 19;518(7539):413-6. PubMed PMID: 25487152. Pubmed Central PMCID: 4336218.
16. Pan M, Reid MA, Lowman XH, Kulkarni RP, Tran TQ, Liu X, et al. Regional glutamine deficiency in tumours promotes dedifferentiation through inhibition of histone demethylation.

Nature cell biology. 2016 Oct;18(10):1090-101. PubMed PMID: 27617932. Pubmed Central PMCID: 5536113.
17. Altman BJ, Stine ZE, Dang CV. From Krebs to clinic: glutamine metabolism to cancer therapy. Nature reviews Cancer. 2016 Nov;16(11):749. PubMed PMID: 28704361.
18. Denkert C, Budczies J, Weichert W, Wohlgemuth G, Scholz M, Kind T, et al. Metabolite profiling of human colon carcinoma--deregulation of TCA cycle and amino acid turnover. Molecular cancer. 2008 Sep 18;7:72. PubMed PMID: 18799019. Pubmed Central PMCID: 2569965.
19. Schuijers J, Junker JP, Mokry M, Hatzis P, Koo BK, Sasselli V, et al. Ascl2 acts as an R-spondin/Wnt-responsive switch to control stemness in intestinal crypts. Cell stem cell. 2015 Feb 5;16(2):158-70. PubMed PMID: 25620640.
20. Gregorieff A, Clevers H. Wnt signaling in the intestinal epithelium: from endoderm to cancer. Genes & development. 2005 Apr 15;19(8):877-90. PubMed PMID: 15833914.
21. Voronov E, Apte RN. IL-1 in Colon Inflammation, Colon Carcinogenesis and Invasiveness of Colon Cancer. Cancer microenvironment : official journal of the International Cancer Microenvironment Society. 2015 Dec;8(3):187-200. PubMed PMID: 26686225. Pubmed Central PMCID: 4715003.
22. Sato T, Vries RG, Snippert HJ, van de Wetering M, Barker N, Stange DE, et al. Single Lgr5 stem cells build crypt–villus structures in vitro without a mesenchymal niche. Nature. 2009 03/29/online;459:262.
23. Tse JWT, Jenkins LJ, Chionh F, Mariadason JM. Aberrant DNA Methylation in Colorectal Cancer: What Should We Target? Trends Cancer. 2017 Oct;3(10):698-712. PubMed PMID: WOS:000425971000005. English.
24. Kim R, Sheaffer KL, Choi I, Won KJ, Kaestner KH. Epigenetic regulation of intestinal stem cells by Tet1-mediated DNA hydroxymethylation. Genes & development. 2016 Nov 1;30(21):2433-42. PubMed PMID: 27856615. Pubmed Central PMCID: 5131782.
25. Tse JWT, Jenkins LJ, Chionh F, Mariadason JM. Aberrant DNA Methylation in Colorectal Cancer: What Should We Target? Trends Cancer. 2017 Oct;3(10):698-712. PubMed PMID: 28958388.
26. Ashktorab H, Brim H. DNA Methylation and Colorectal Cancer. Current colorectal cancer reports. 2014;10(4):425-30. PubMed PMID: 25580099. Epub 08/31.
27. Morris LG, Kaufman AM, Gong Y, Ramaswami D, Walsh LA, Turcan S, et al. Recurrent somatic mutation of FAT1 in multiple human cancers leads to aberrant Wnt activation. Nature genetics. 2013 Mar;45(3):253-61. PubMed PMID: 23354438. Pubmed Central PMCID: 3729040.
28. Ring A, Kim YM, Kahn M. Wnt/catenin signaling in adult stem cell physiology and disease. Stem cell reviews. 2014 Aug;10(4):512-25. PubMed PMID: 24825509. Pubmed Central PMCID: 4294579.
29. Degos L, Wang ZY. All trans retinoic acid in acute promyelocytic leukemia. Oncogene. 2001 Oct 29;20(49):7140-5. PubMed PMID: 11704842.
30. Vlachogiannis G, Hedayat S, Vatsiou A, Jamin Y, Fernandez-Mateos J, Khan K, et al. Patient-derived organoids model treatment response of metastatic gastrointestinal cancers. Science. 2018 Feb 23;359(6378):920-6. PubMed PMID: 29472484. Pubmed Central PMCID: 6112415.
31. Dow LE, O'Rourke KP, Simon J, Tschaharganeh DF, van Es JH, Clevers H, et al. Apc Restoration Promotes Cellular Differentiation and Reestablishes Crypt Homeostasis in

Colorectal Cancer. Cell. 2015 Jun 18;161(7):1539-52. PubMed PMID: 26091037. Pubmed Central PMCID: 4475279.
32. De Rosa M, Pace U, Rega D, Costabile V, Duraturo F, Izzo P, et al. Genetics, diagnosis and management of colorectal cancer (Review). Oncology reports. 2015 Sep;34(3):1087-96. PubMed PMID: 26151224. Pubmed Central PMCID: 4530899.
33. Moser AR, Luongo C, Gould KA, McNeley MK, Shoemaker AR, Dove WF. ApcMin: a mouse model for intestinal and mammary tumorigenesis. European journal of cancer. 1995 Jul-Aug;31A(7-8):1061-4. PubMed PMID: 7576992.
34. Kamphorst JJ, Nofal M, Commisso C, Hackett SR, Lu W, Grabocka E, et al. Human pancreatic cancer tumors are nutrient poor and tumor cells actively scavenge extracellular protein. Cancer research. 2015 Feb 1;75(3):544-53. PubMed PMID: 25644265. Pubmed Central PMCID: 4316379.
35. Roberts E, Caldwell AL, et al. Amino acids in epidermal carcinogenesis in mice. Cancer research. 1949 Jun;9(6):350-3. PubMed PMID: 18144236.
36. Miyo M, Konno M, Nishida N, Sueda T, Noguchi K, Matsui H, et al. Metabolic Adaptation to Nutritional Stress in Human Colorectal Cancer. Scientific reports. 2016 Dec 7;6:38415. PubMed PMID: 27924922. Pubmed Central PMCID: 5141444
(http://www.taiho.co.jp/english/), the Evidence Based Medical (EBM) Research Center (http://ebmrce.co.jp/index.html), Chugai Co., Ltd. (http://www.chugai-pharm.co.jp/english/index.html), Yakult Honsha Co., Ltd. (http://www.yakult.co.jp/english/index.html), and Merck Co., Ltd. (http://www.merck.co.jp/en/index.html). Those funders had no role in the main experimental equipment, supply expenses, study design, data collection and analysis, decision to publish, or preparation of the manuscript for this work.
37. Miyoshi Y, Nagase H, Ando H, Horii A, Ichii S, Nakatsuru S, et al. Somatic mutations of the APC gene in colorectal tumors: mutation cluster region in the APC gene. Human molecular genetics. 1992 Jul;1(4):229-33. PubMed PMID: 1338904.
38. Voloshanenko O, Erdmann G, D Dubash T, Augustin I, Metzig M, Moffa G, et al. Wnt secretion is required to maintain high levels of Wnt activity in colon cancer cells2013. 2610 p.
39. Schneikert J, Grohmann A, Behrens J. Truncated APC regulates the transcriptional activity of beta-catenin in a cell cycle dependent manner. Human molecular genetics. 2007 Jan 15;16(2):199-209. PubMed PMID: 17189293.
40. Pai R, Soreghan B, Szabo IL, Pavelka M, Baatar D, Tarnawski AS. Prostaglandin E2 transactivates EGF receptor: a novel mechanism for promoting colon cancer growth and gastrointestinal hypertrophy. Nature medicine. 2002 Mar;8(3):289-93. PubMed PMID: 11875501.
41. Janssen KP, Alberici P, Fsihi H, Gaspar C, Breukel C, Franken P, et al. APC and oncogenic KRAS are synergistic in enhancing Wnt signaling in intestinal tumor formation and progression. Gastroenterology. 2006 Oct;131(4):1096-109. PubMed PMID: 17030180.
42. Jemal A, Bray F, Center MM, Ferlay J, Ward E, Forman D. Global cancer statistics. CA: a cancer journal for clinicians. 2011 Mar-Apr;61(2):69-90. PubMed PMID: 21296855.
43. Seshagiri S, Stawiski EW, Durinck S, Modrusan Z, Storm EE, Conboy CB, et al. Recurrent R-spondin fusions in colon cancer. Nature. 2012 Aug 30;488(7413):660-4. PubMed PMID: 22895193. Pubmed Central PMCID: 3690621.

44. Cancer Genome Atlas N. Comprehensive molecular characterization of human colon and rectal cancer. Nature. 2012 Jul 18;487(7407):330-7. PubMed PMID: 22810696. Pubmed Central PMCID: 3401966.
45. Thienpont B, Galle E, Lambrechts D. TET enzymes as oxygen-dependent tumor suppressors: exciting new avenues for cancer management. Epigenomics. 2016 Nov;8(11):1445-8. PubMed PMID: 27733058.
46. Sheaffer KL, Kim R, Aoki R, Elliott EN, Schug J, Burger L, et al. DNA methylation is required for the control of stem cell differentiation in the small intestine. Genes & development. 2014 Mar 15;28(6):652-64. PubMed PMID: 24637118. Pubmed Central PMCID: 3967052.
47. Weisenberger DJ, Liang G, Lenz HJ. DNA methylation aberrancies delineate clinically distinct subsets of colorectal cancer and provide novel targets for epigenetic therapies. Oncogene. 2017 10/09/online;37:566.
48. Lyou Y, Habowski AN, Chen GT, Waterman ML. Inhibition of nuclear Wnt signalling: challenges of an elusive target for cancer therapy. British journal of pharmacology. 2017 Dec;174(24):4589-99. PubMed PMID: 28752891. Pubmed Central PMCID: 5727325.
49. Kahn M. Can we safely target the WNT pathway? Nature reviews Drug discovery. 2014;13(7):513-32. PubMed PMID: PMC4426976.
50. Krishnamurthy N, Kurzrock R. Targeting the Wnt/beta-catenin pathway in cancer: Update on effectors and inhibitors. Cancer treatment reviews. 2018 Jan;62:50-60. PubMed PMID: 29169144. Pubmed Central PMCID: 5745276.
51. Jimeno A, Gordon M, Chugh R, Messersmith W, Mendelson D, Dupont J, et al. A First-in-Human Phase I Study of the Anticancer Stem Cell Agent Ipafricept (OMP-54F28), a Decoy Receptor for Wnt Ligands, in Patients with Advanced Solid Tumors. Clin Cancer Res. 2017 Dec 15;23(24):7490-7. PubMed PMID: 28954784. Epub 2017/09/29. eng.

Figures

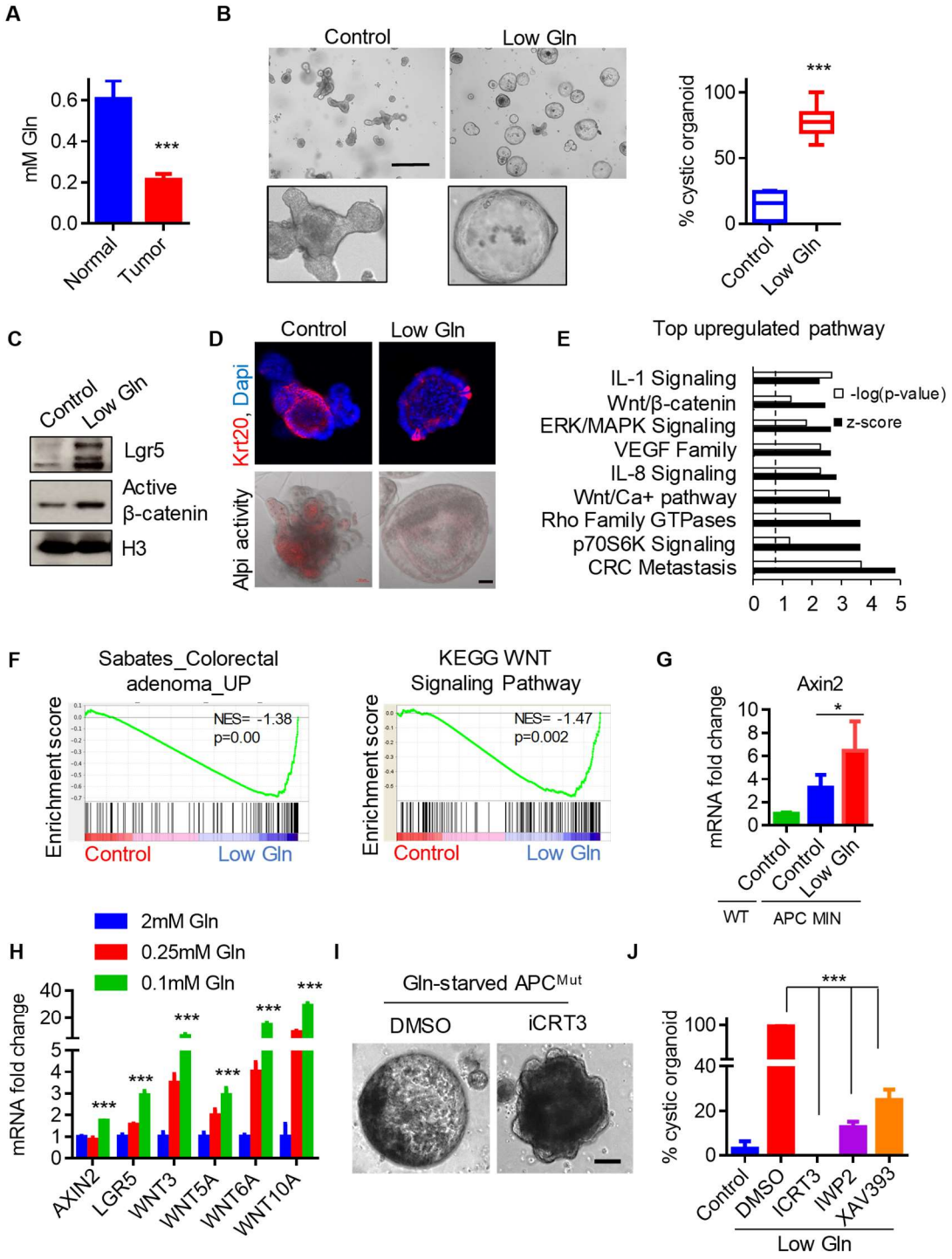

<u>Figure 4-1</u>. Environmental glutamine restriction hyperactivates Wnt signaling and blocks cellular differentiation. (**A**) Glutamine levels in intestinal tumors from APC^{Min} mice (n=10) and

normal intestinal tissues of wildtype mice (n=6), data represent mean ± SEM. (**B**) Bright-field images and percentage of cystic morphology in APC^{Mut} small intestine organoids cultured in control (3mM) or low glutamine (0.3 mM) medium after 4-6 passages (n=8 biological replicates from two organoid lines). (**C**) Immunoblots for stem cell marker LGR5 and active β-catenin, (**D**) Immunofluorescent images for intestinal differentiation markers Krt20 and Alpi enzyme activity in APC^{Mut} organoids cultured in control or low glutamine medium. (**E**) IPA analysis of top upregulated pathways and (**F**) GSEA analysis between control organoids versus glutamine-starved APC^{Mut} organoids from RNA sequencing data. Dotted lines indicate threshold of significance ($p = 0.05$). (**G**) qPCR analysis of Wnt target gene, Axin2, in APC^{WT} organoids and APC^{Mut} organoids cultured in control and low glutamine (0.3 mM) medium (n= 6 replicates). (**H**) qPCR analysis of the indicated genes in SW620 colon cancer cells cultured in medium with the indicated glutamine concentration for 3 days. (**I**) Representative bright-field images of glutamine-starved APC^{Mut} organoids treated with 5 μM iCRT3 for 1 week. (**J**) Percentage of cystic organoids of control and glutamine-starved APC^{Mut} organoids treated with 10 μM of indicated Wnt inhibitors for 4 days (n=3 biological replicates). Scale bars, 400 μm (B), 50 μm (D), 100 μm (I). * $p < 0.005$, *** $p < 0.001$

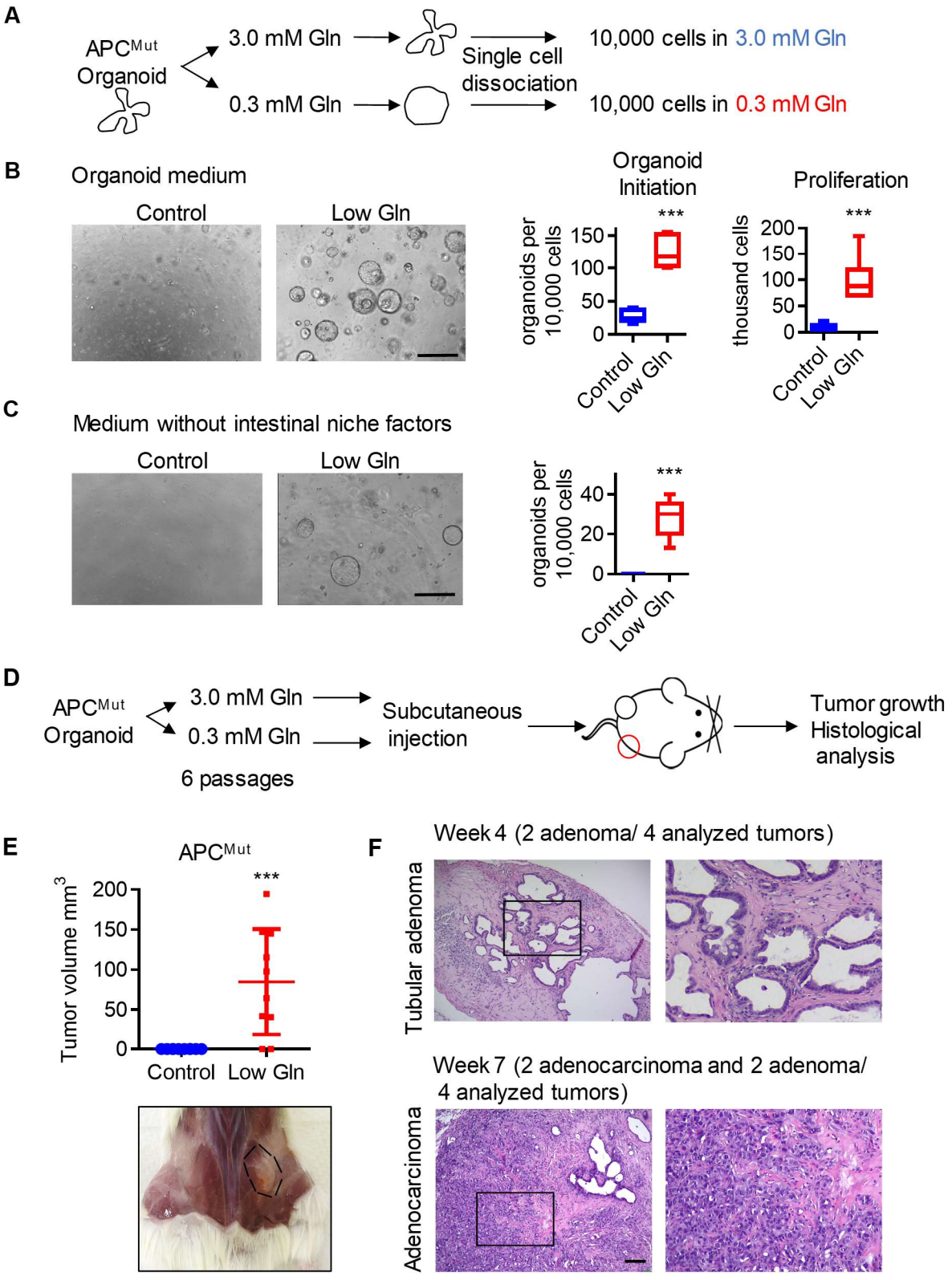
A
APCMut Organoid
3.0 mM Gln
0.3 mM Gln
Single cell dissociation
10,000 cells in 3.0 mM Gln
10,000 cells in 0.3 mM Gln
B
Organoid medium
Control
Low Gln
Organoid Initiation
organoids per 10,000 cells
***
Proliferation
thousand cells
C
Medium without intestinal niche factors
D
APCMut Organoid
3.0 mM Gln
0.3 mM Gln
6 passages
Subcutaneous injection
Tumor growth
Histological analysis
E
APCMut
Tumor volume mm3
F
Week 4 (2 adenoma/ 4 analyzed tumors)
Tubular adenoma
Week 7 (2 adenocarcinoma and 2 adenoma/ 4 analyzed tumors)
Adenocarcinoma

Figure 4-2. Glutamine restriction promotes self-renewal and niche independence in APC^{Mut} organoids leading to adenocarcinoma formation *in vivo*. (**A, B**) Control and glutamine-starved APC^{Mut} organoids were dissociated into single cell, and equal number of organoid-derived cells were cultured in organoid medium with 3 mM or 0.3mM glutamine. Secondary organoid formation and cell proliferation after 1 week are shown (n= 6 biological replicates). (**C**) Equal number of organoid-derived cells from control and glutamine starved organoids were cultured in FBS-supplemented DMEM/F12 medium without R-Spondin, Egf and Noggin. Secondary organoid formation after 1 week are shown (n= 5 biological replicates). (**D**) Experimental procedure to establish subcutaneous xenograft tumors with APC^{Mut} organoids. (**E, F**) Tumor volume 2 weeks after injection and H&E staining of subcutaneous xenografts generated with control organoids or glutamine-starved organoids (n=10 mice). Scale bars, 400 μm (B, C), 40 μm (F). *** $p < 0.001$

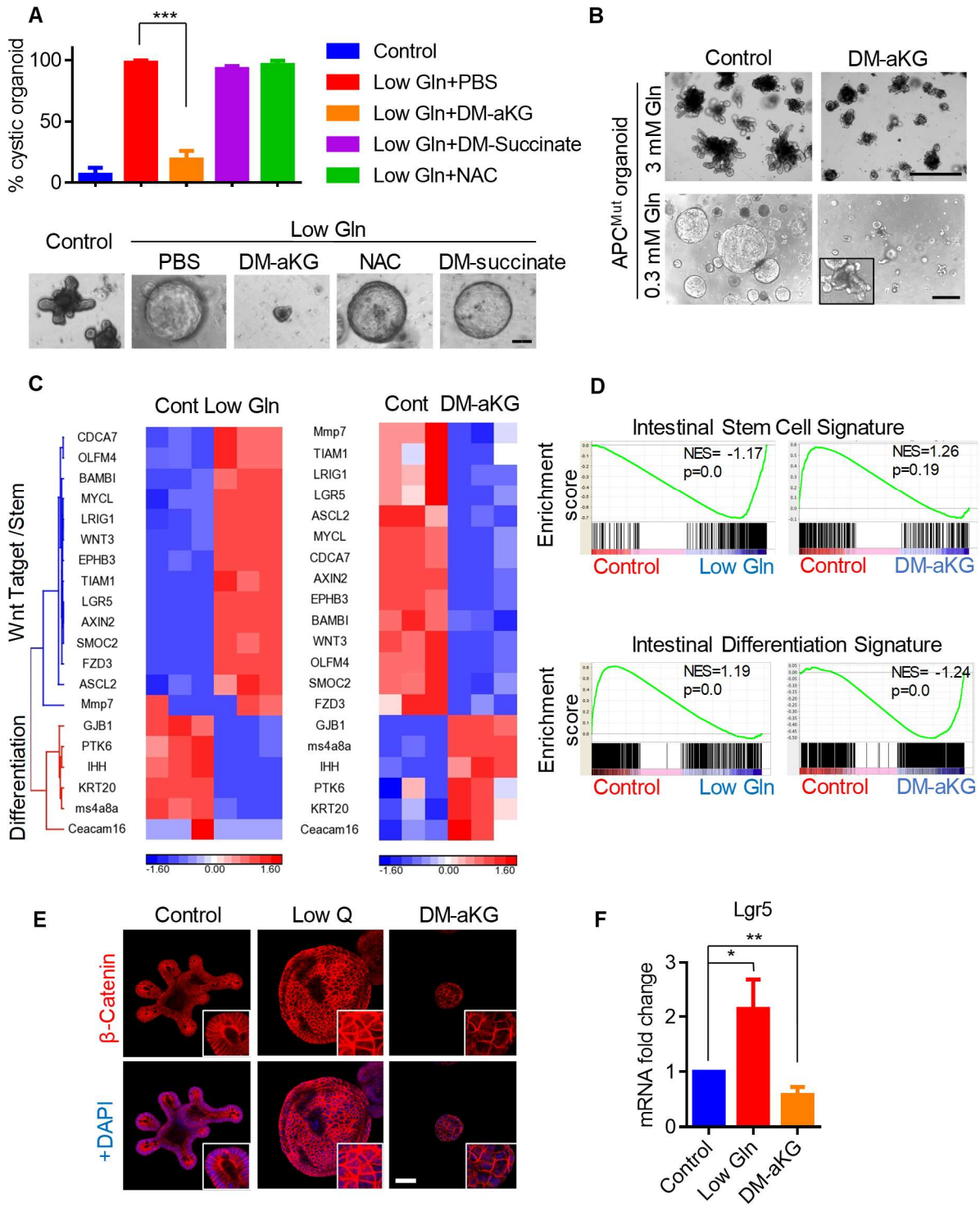

<u>Figure 4-3</u>. aKG supplementation rescued low-glutamine induced stemness and suppresses Wnt signaling. (**A**) Percentage of cystic organoid morphology in control organoids and

glutamine-starved APC^{Mut} organoids supplemented with PBS control, 3 mM DM-αKG, 3 mM DM-succinate, or 5 mM NAC for 3 days (n=3 biological replicates). (**B**) Representative bright-field images of control organoids and glutamine-starved APC^{Mut} organoids treated with 3.5 mM DM-aKG for 3 days. (**C**) Heat map of gene expression profile from RNA sequencing data and (**D**) GSEA analysis between control APC^{Mut} organoids (3 mM glutamine) and organoids cultured in 0.3 mM glutamine conditions or organoids treated with 3.5 mM DM-aKG. (**E**) Representative immunofluorescence for active β-catenin and (**F**) qPCR analysis for *Lgr5* expression in APC^{Mut} organoids cultured in low glutamine conditions or treated with 3.5 mM DM-aKG (n=3 biological replicates). Scale bars, 100 μm (A), 400 μm (B), 50 μm (E). * $p < 0.05$, ** $p < 0.01$, *** $p < 0.001$

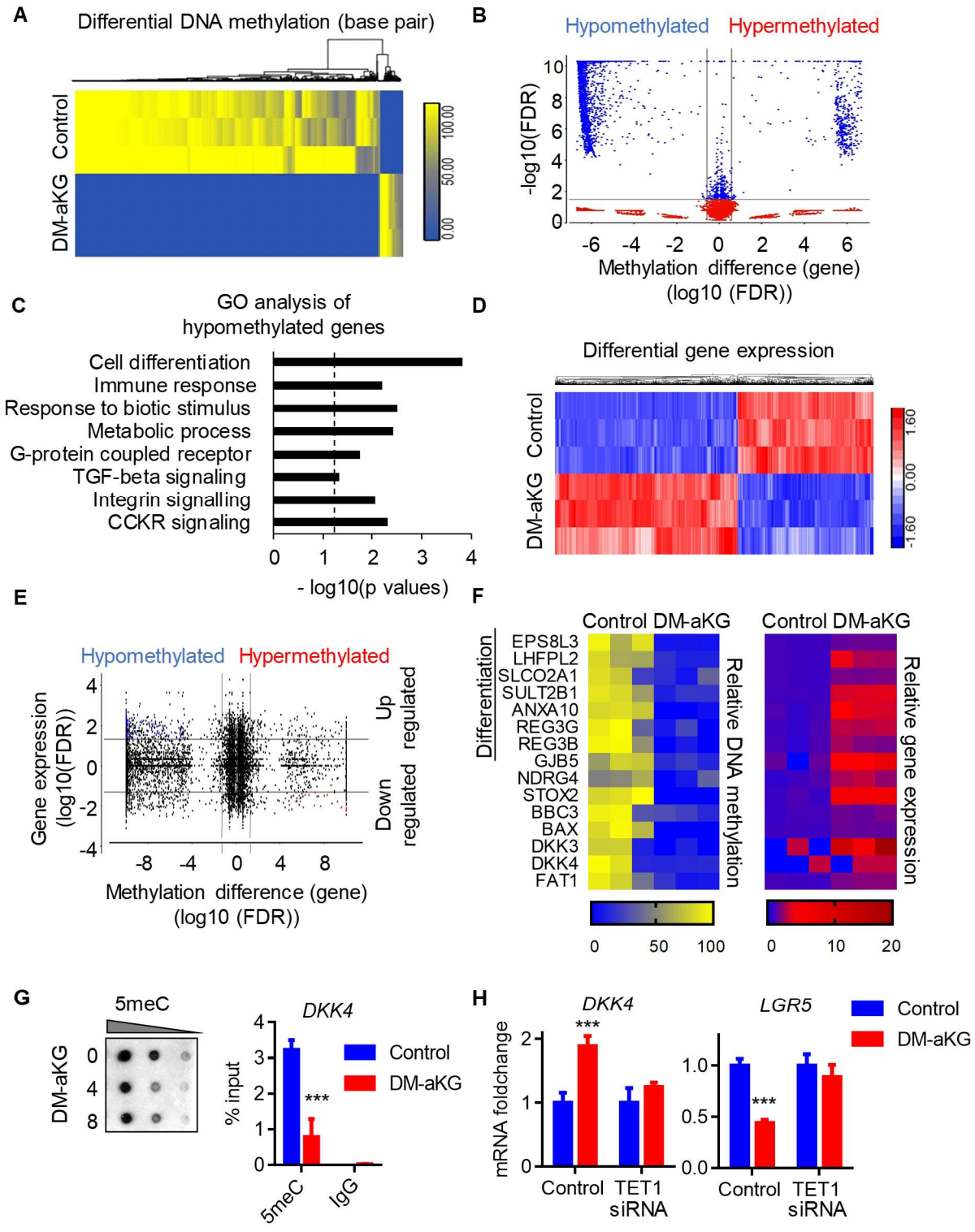

Figure 4-4. aKG supplementation leads to DNA hypomethylation of genes related to differentiation and Wnt inhibition. (**A**) Heatmap showing base pairs with differential DNA

methylation based on RRBS sequencing (n=3 biological replicates). (**B**) Volcano plot showing genes with affected DNA methylation between the control and DM-aKG (3.5mM) treated APC^{Mut} organoids, DNA methylation difference is plotted on the x-axis and p values are plotted on the y-axis. (**C**) Panther gene ontology analysis of hypomethylated genes in DM-aKG treated organoids. Dotted lines indicate threshold of significance (p = 0.05). (**D**) Hierarchical clustering of differential gene expression in control and DM-aKG treated APC^{Mut} organoids (n=3 biological replicates). (**E**) Starburst plot for comparison between DNA methylation and gene expression. The black line represents the cutoff of FDR adjusted p values < 0.05. Blue dots represent genes with DNA hypomethylation and upregulated expression, red dots represent genes with DNA hypermethylation and downregulated expression between control and DM-aKG treated APC^{Mut} organoids. (**F**) Heatmap showing selected genes with decreased DNA methylation at upstream regions and upregulated expression in APC^{Mut} organoids upon DM-aKG treatment. (**G**) Dot blot analysis of 5meC levels in SW620 cells treated with DM-aKG (Left), representative MeDIP experiment with 5meC antibody for *DKK4* promoter in SW620 cells upon DM-aKG treatment (Right) (n=4 replicates). (**H**) Representative qPCR analysis of Wnt antagonist (*DKK4*) and Wnt target gene (*LGR5*) expression in control SW620 cells or TET1 knockdown cells following DM-aKG treatment (n=3 replicates). *** $p < 0.001$

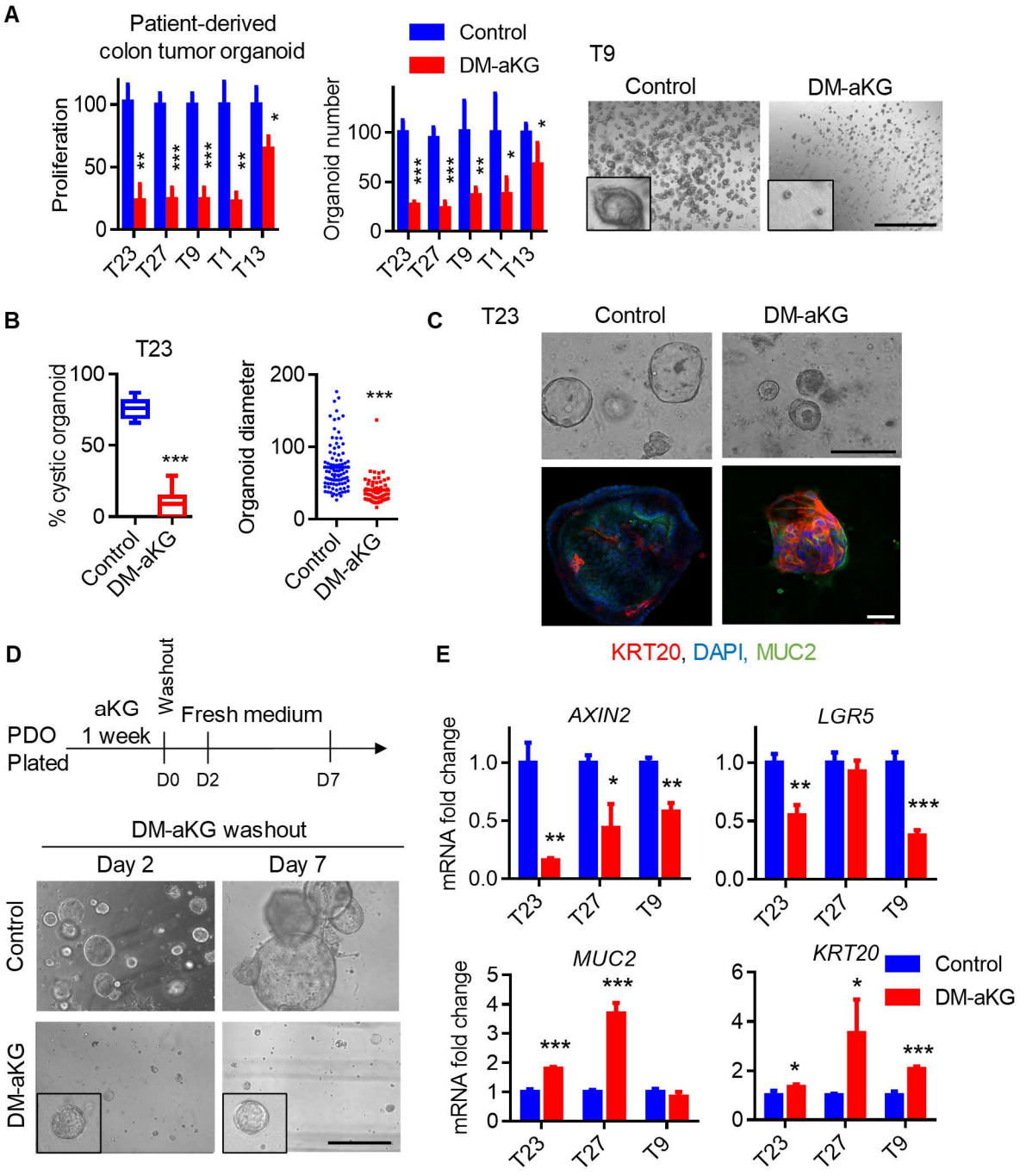

Figure 4-5. aKG supplementation drives terminal differentiation and suppresses growth of patient-derived colon tumor organoids. (A) Titer-Glo proliferation assay and relative organoid number of a panel of PDOs treated with 6 mM DM-aKG for 7 days (n=3 biological replicates). Representative bright-field images of T9 PDOs after DM-aKG treatment are shown. (**B**)

Percentage of cystic organoids (n= 8 biological replicates) and relative organoid size of T23 PDOs treated with DM-aKG. (**C**) Bright-field images and immunofluorescent staining for the indicated differentiation markers of T23 PDOs following 6 mM DM-aKG treatment for 7 days. (**D**) Representative images of T23 PDOs treated with 6 mM DM-aKG for 7 days, followed by the metabolite wash-out and subsequent culture for 7 days. (**E**) qPCR analysis of the indicated genes in different PDOs treated with 6mM DM-aKG for 7 days (n=3 replicates). Scale bars, 1000 μm (A), 200 μm and 50 μm (C), 400 μm (D). * $p < 0.05$, ** $p < 0.01$, *** $p < 0.001$

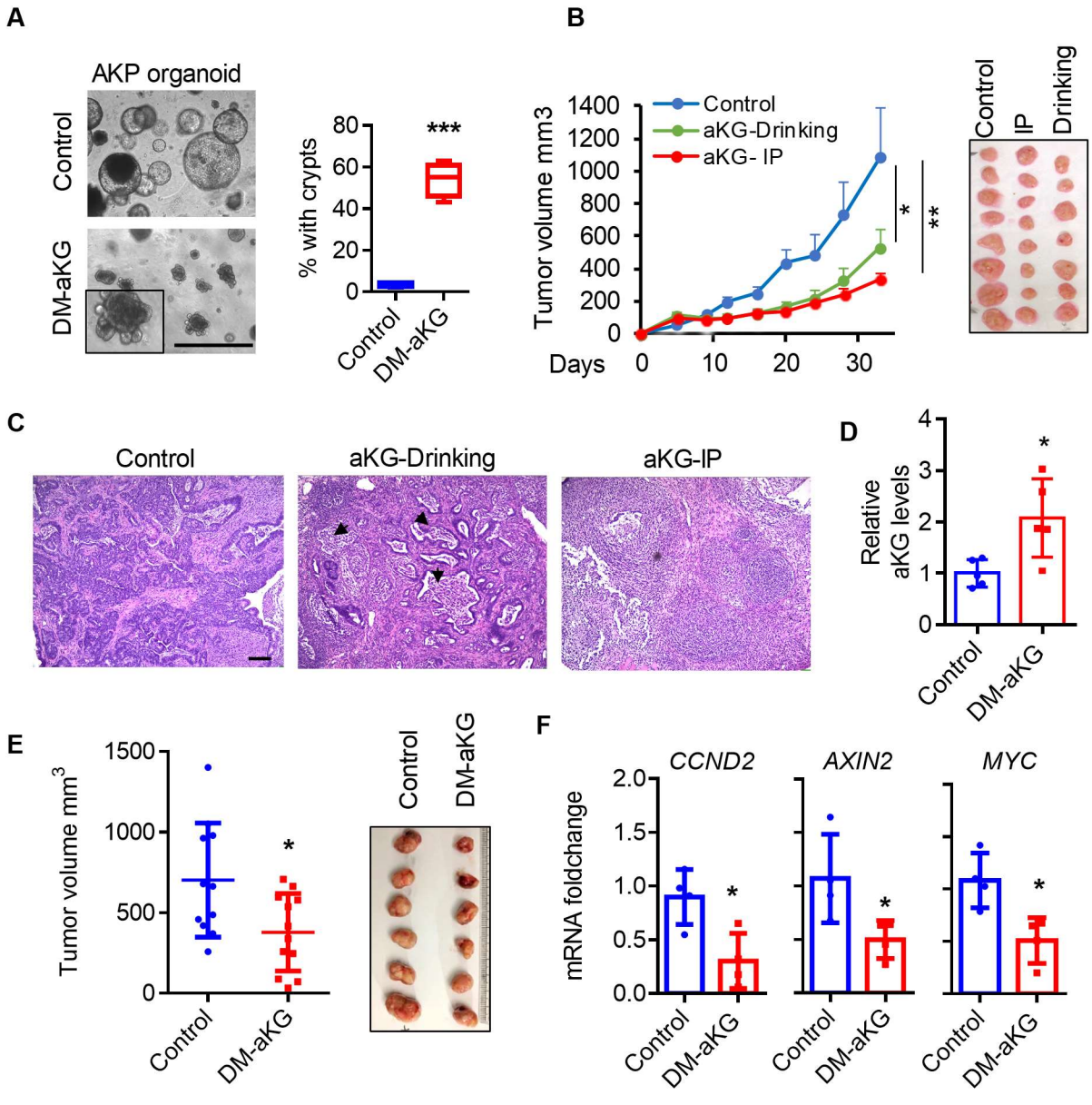

Figure 4-6. aKG supplementation inhibits the growth of highly mutated CRC tumors *in vivo*. **(A)** Bright-field images of shApc /Kras^{G12D}/p53$^{fl/fl}$ (AKP) small intestine organoids treated with 3 mM DM-aKG for 3 days (n=4 biological replicates). (**B**) Tumor volume of xenograft tumors established with AKP organoids treated with 600 mg/kg DM-aKG intravenously (IP) daily or 25 mg/ml in drinking water (n=8 tumors, SEM), p-values at day 20 are shown. (**C**) H&E

staining of control AKP tumor and DM-aKG treated tumors. (**D**) Relative aKG levels in xenograft tumors established with SW620 colon cancer cells treated with 400 mg/kg DM-aKG intravenously daily (n=5 tumors). (**E**) Tumor volume 23 days after the first treatment (n=11 tumors). (**F**) qPCR analysis of Wnt target genes in SW620 xenograft tumors treated with DM-aKG or vehicle control (n=4 tumors). Scale bars, 1000 μm (C), 100 μm (E). * $p < 0.05$, ** $p < 0.01$, *** $p < 0.001$

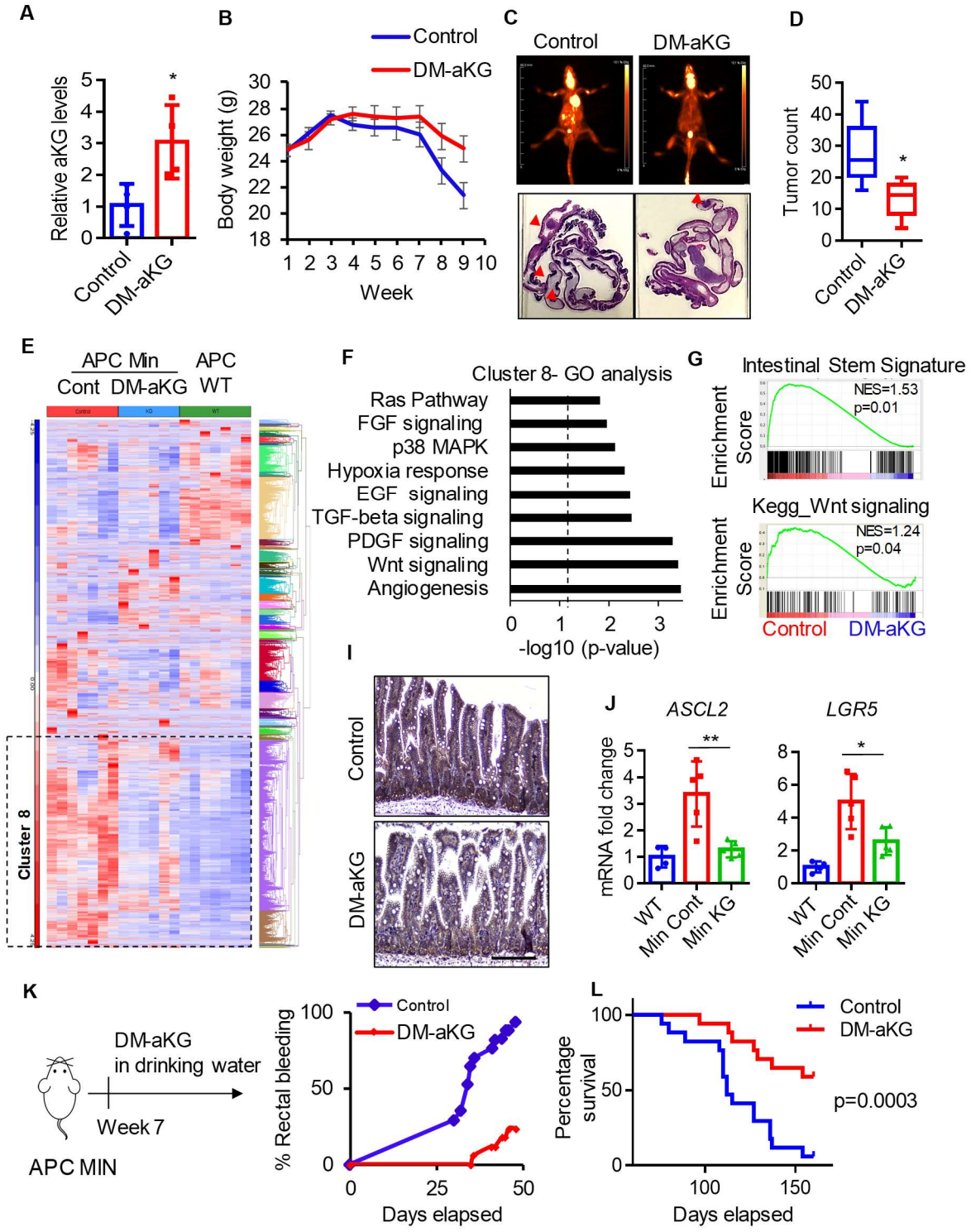

Figure 4-7. aKG supplementation is an effective therapeutic intervention in a mouse model of intestinal cancer. (**A**) Relative aKG levels in intestinal tissues of APC^{Min} mice treated with DM-aKG via IP injection or vehicle control (n=4 mice). (**B**) Body weight of APC^{Min} mice treated

with DM-aKG or vehicle control (n=8 mice, SEM). (**C**) PET scan images at day 70 after treatment and H&E images in APC^{Min} treated with 400 mg/kg of DM-aKG intravenously, 4 times per week. (**D**) Number of visible intestinal tumor (n=6 mice) in APC^{Min} mice treated with DM-aKG or vehicle control. (**E**) Hierarchical clustering of gene expression from RNA sequencing data in tumor-free intestinal tissues of wildtype B6 mice, APC^{Min} mice and APC^{Min} mice treated with DM-aKG. (**F**) Panther gene ontology enrichment analysis of cluster 8 and GSEA analysis for the indicated gene signatures between control APC^{Min} mice and DM-aKG treated mice. (**I**) IHC staining for β-catenin of APC^{Min} mice treated with vehicle control or DM-aKG. (**J**) qPCR analysis of stem/Wnt target genes. (**K**) Percentage of rectal bleeding, an indication of intestinal tumors, and (**L**) percentage survival of APC^{Min} mice supplemented with 15 mg/ml DM-aKG in the drinking water (n=17 mice). Scale bars, 200 μm and 50 μm (B), 1000 μm (C), 100 μm (E, I). * $p < 0.05$, ** $p < 0.01$, *** $p < 0.001$

SUPPLEMENTAL FIGURES

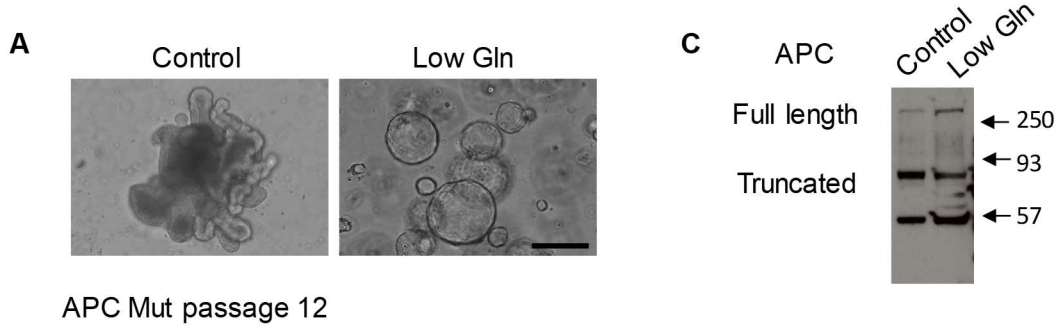

B

Exome sequencing: Control vs Low Gln

Chr	Start	End	Ref	Alt	Func.ref Gene	Gene.ref Gene	ExonicFunc.ref Gene	Other info
chr2	44844614	44844614	T	A	exonic	Zeb2	nonsynonymous SNV	heterozygous
chr5	24824820	24824820	T	G	exonic	Kmt2c	nonsynonymous SNV	heterozygous
chr17	37450924	37450924	T	G	exonic	Olfr100, Olfr102	nonsynonymous SNV	heterozygous

Figure 4-S1. Genetic alterations do not contribute to morphological changes upon glutamine starvation. (A) Representative brightfield images of control and glutamine-starved APC^{Mut} organoids after 12 passages. Scale bars, 200µm. (**B**) Identified genetic alterations in glutamine-starved APC^{Mut} organoids compared to paired control organoids as determined by exome sequencing are shown. (**C**) Immunoblots for APC protein in control and glutamine-starved APCMut organoids after 8 passages.

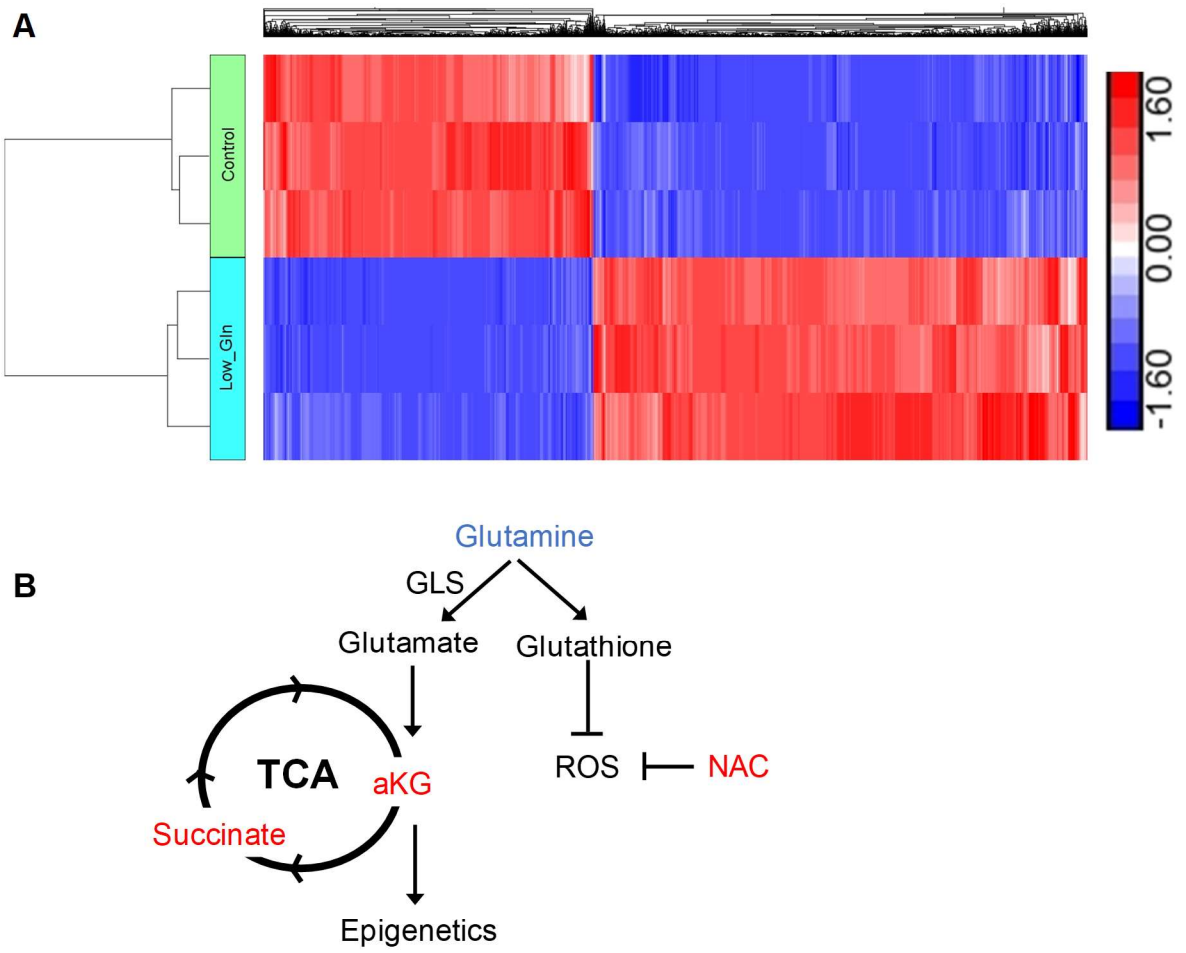

Figure 4-S2. Exposure to glutamine restriction reprograms transcriptional profile in APC^{Mut} organoids. (**A**) Hierarchical clustering of significant differentiated gene expression of APC^{Mut} organoids cultured in control or low-glutamine medium. (**B**) Diagram of glutamine metabolism in cancer.

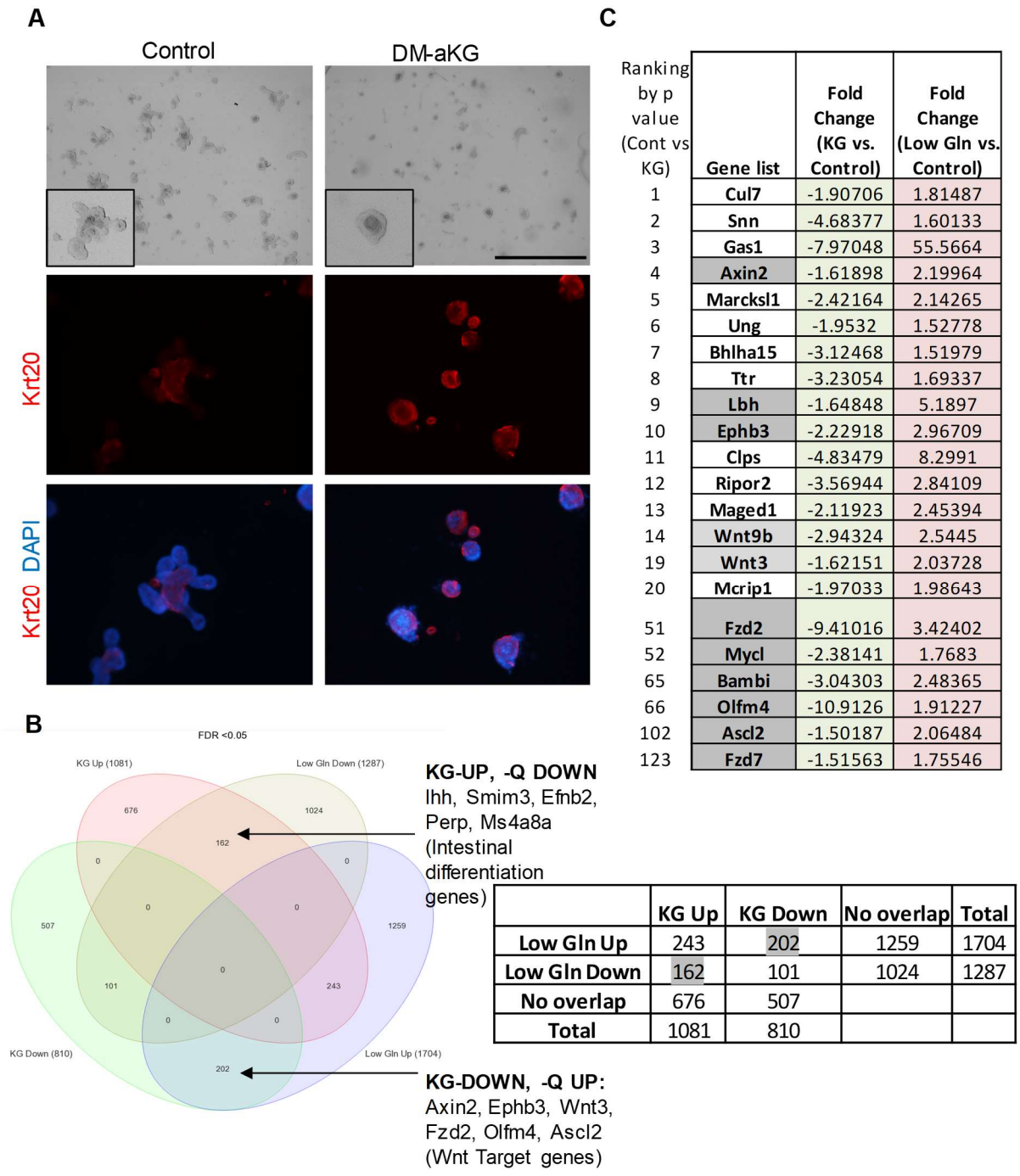

Ranking by p value (Cont vs KG)	Gene list	Fold Change (KG vs. Control)	Fold Change (Low Gln vs. Control)
1	Cul7	-1.90706	1.81487
2	Snn	-4.68377	1.60133
3	Gas1	-7.97048	55.5664
4	Axin2	-1.61898	2.19964
5	Marcksl1	-2.42164	2.14265
6	Ung	-1.9532	1.52778
7	Bhlha15	-3.12468	1.51979
8	Ttr	-3.23054	1.69337
9	Lbh	-1.64848	5.1897
10	Ephb3	-2.22918	2.96709
11	Clps	-4.83479	8.2991
12	Ripor2	-3.56944	2.84109
13	Maged1	-2.11923	2.45394
14	Wnt9b	-2.94324	2.5445
19	Wnt3	-1.62151	2.03728
20	Mcrip1	-1.97033	1.98643
51	Fzd2	-9.41016	3.42402
52	Mycl	-2.38141	1.7683
65	Bambi	-3.04303	2.48365
66	Olfm4	-10.9126	1.91227
102	Ascl2	-1.50187	2.06484
123	Fzd7	-1.51563	1.75546

	KG Up	KG Down	No overlap	Total
Low Gln Up	243	202	1259	1704
Low Gln Down	162	101	1024	1287
No overlap	676	507		
Total	1081	810		

Figure 4-S3. aKG suppresses Wnt signaling and drives intestinal differentiation. (**A**) Representative bright field images and immunofluorescent staining of differentiation marker (Krt20) in APC^{Mut} organoids treated with 3mM DM-aKG for 3 days. (**B**) Overlapping gene expression profile of APC Mut organoids cultured in low glutamine medium or treated with aKG

reveals opposing regulation on Wnt target genes and intestinal differentiation related genes. (**C**) Top gene list with downregulation upon aKG treatment and upregulation upon glutamine starvation. Scale bars, 1000μm (Brightfield), 200μm (Immunofluorescence).

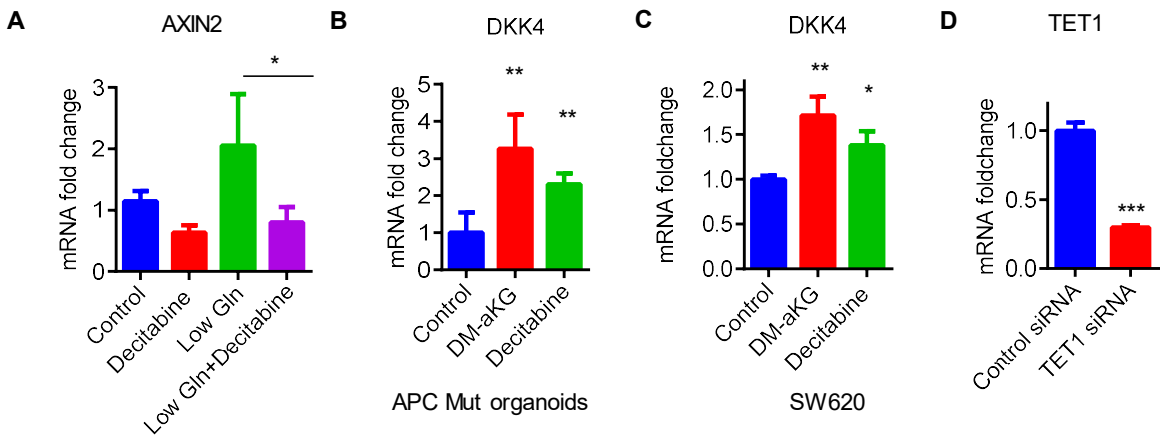

<u>Figure 4-S4</u>. aKG upregulates Wnt antagonists through DNA hypomethylation. (**A**) Representative qPCR analysis of Axin2, a canonical Wnt target, in control and glutamine-starved organoids treated with 1uM decitabine for 3 days. (**B**) qPCR analysis of DKK4 in APCmut organoids treated with 4mM DM-aKG or 1uM decitabine. (**C**) qPCR analysis of DKK4 in SW620 colon cancer cells treated with 8mM aKG or 5μM Decitabine. (**D**) qPCR analysis of TET1 in SW620 cells transfected with control siRNA or TET1 siRNA (n=3 replicates).

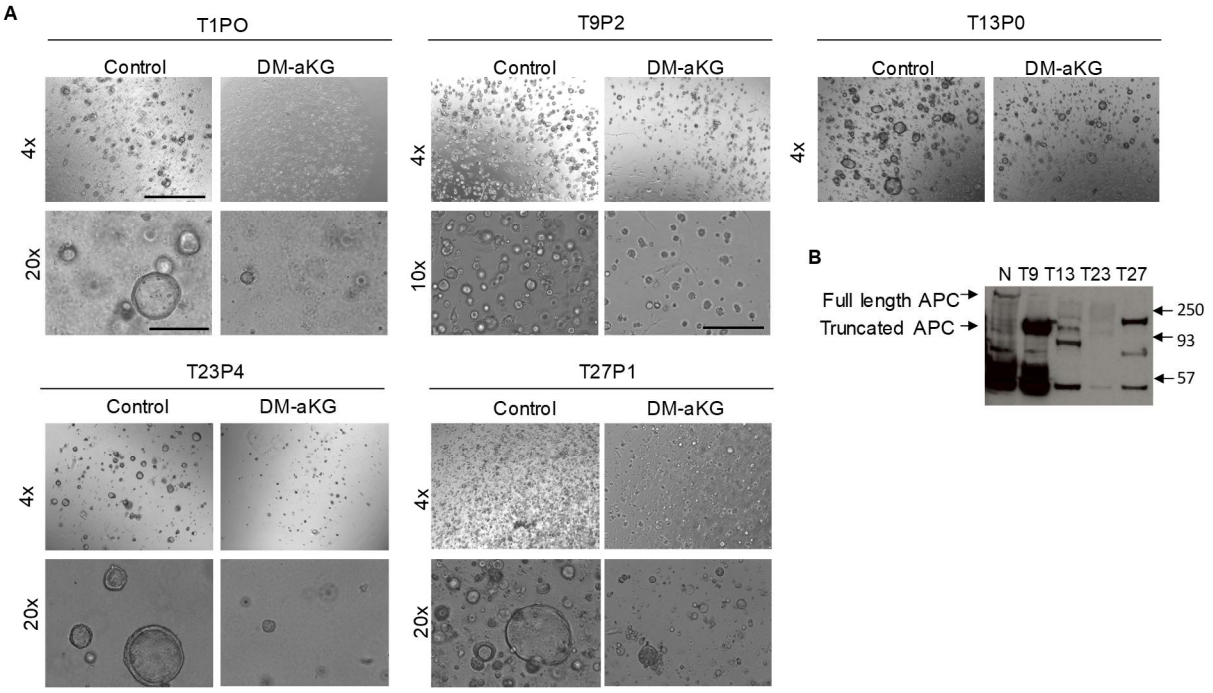

<u>Figure 4-S5</u>. DM-aKG treatment inhibits initiation and growth of PDOs. (**A**) Representative image of PDOs treated with 6mM DM-aKG for 7 days. (**B**) Immunoblot probed for APC protein in PDOs.

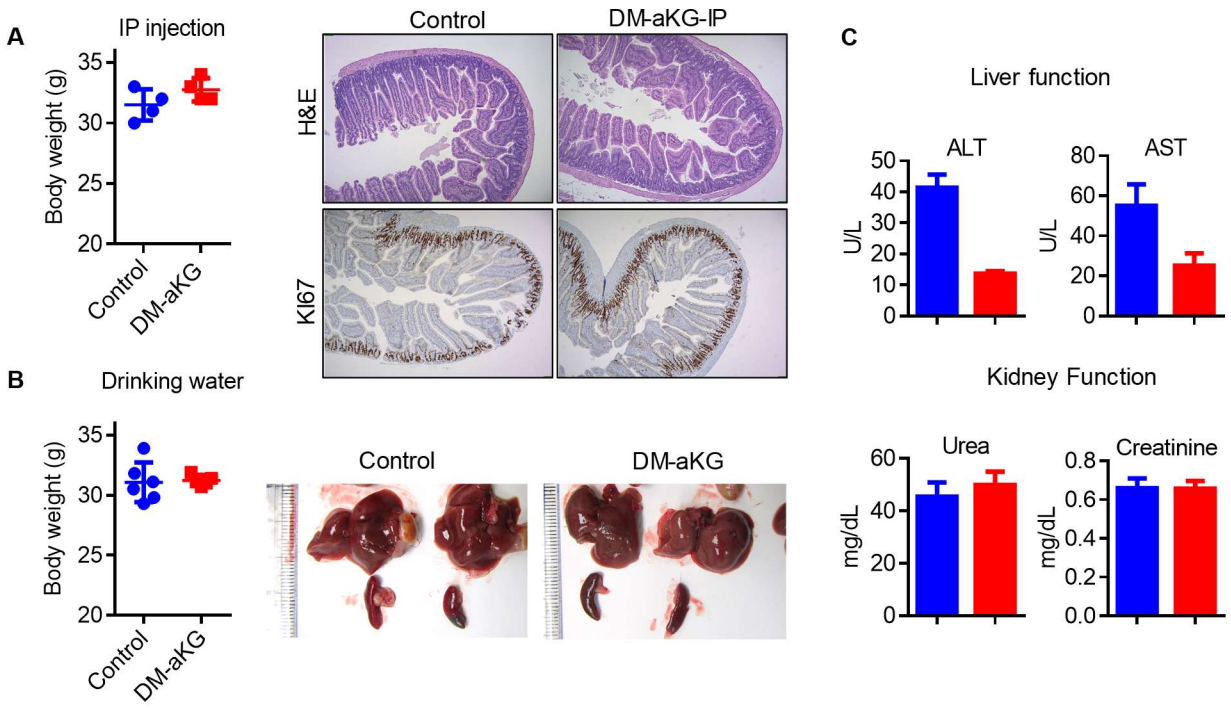

Figure 4-S6. Toxicity study of DM-aKG treatment in mice. (**A**) Body weight and histological analysis of wildtype mice treated with 400mg/kg DM-aKG via IP injection for more than 2 months (n=4 mice). (**B**) Body weight changes and organ images of APC^{Min} mice treated with DM-aKG via IP injection (n=5 mice). (**C**) Liver and kidney function of wildtype mice treated with 15mg/ml DM-aKG supplemented in drinking water for more than 4 months (n=5 mice, SEM).

Chapter 5

Part I: Metabolic control of epigenetics and gene expression in cancer

Part II: Summary and concluding remarks

This chapter is partly derived from an article published in Clinical Cancer Research, entitled "Molecular Pathways: Metabolic control of histone methylation and gene expression in cancer." DOI: 10.1158/1078-0432.CCR-16-2506

Part I: Metabolic control of epigenetics and gene expression in cancer

Genetic and epigenetic alterations contribute to tumor development, progression, and therapeutic response. Many epigenetic enzymes and DNA repair enzymes use metabolic intermediates as cofactors and sometimes as critical substrates to carry out their functions. Emerging evidence suggests that fluctuation in metabolite levels may regulate activities of these chromatin-modifying enzymes. Metabolic changes due to dietary inputs, genetic mutations, tumor microenvironment, and therapeutic interventions can affect these enzymes leading to modulation in gene expression profiles and tumorigenesis. The interaction between metabolism and epigenetic control of gene expression in cancer allows the crosstalk between the microenvironment and the tumor fitness.

Epigenetic regulations by histone and DNA methylation

Genetic alterations play a prominent role in tumorigenesis. DNA mutations or chromosomal translocation in cancer cells trigger aberrant gene expression that contributes to chronic proliferation, resistance to cell death, and metastasis (1, 2). Emerging evidence reveals many tumors also exhibit distinct epigenetic patterns (3, 4). These epigenetic modifications dictate chromatin accessibility, adding another means by which gene transcription is intricately regulated throughout tumor development (5).

Histone modifications are post translational modifications made on core histone proteins (6). Histone acetylation results in more accessible DNA contributing to active transcription. Histone methyltransferase (HMT) facilitates histone methylation on specific histone residues which can

recruit different transcription associated proteins to regulate transcription (7). In particular, trimethylation of histone at lysine 9, 27 and 20 (H3K9, H3K27, H4K20) is often associated with repressed transcription, while methylation of H3K4, H3K36, and H3K79 correlates with active transcription (8). Interestingly, a variety of chromatin modifying enzymes including histone methyltransferases MLL2, EZH2 and histone demethylase UTX are mutated in cancer, leading to abnormal histone methylation and altered gene expression (9-11). In addition to histone methylation, DNA methylation also contribute to gene regulation in mammals. Methylation of DNA bases occurred on cytosine in CpG islands often results in more compact chromatin structure leading gene silencing (12). DNA methylation facilitates stable gene silencing of more differentiated cells during normal development. In cancer cells, deregulation in DNA methylation has been implicated in the suppression of many tumor suppressor genes, the expression of previously quiescent oncogenes and the induction of genomic instability (13).

The crosstalk between metabolism and epigenetics

Many chromatin modifying enzymes often require a specific metabolite cofactor to function (14, 15). For example, HMT requires S-adenosylmethionine (SAM), an intermediate metabolite in one-carbon metabolism, to methylate histone and DNA (16). Similarly, Jumonji-domain containing histone demethylase (JmjC-KDM) and the Ten-eleven translocation (TET) enzymes use a TCA-cycle intermediate alpha-ketoglutarate (αKG) to remove methyl groups from histones and DNA respectively (17). Interestingly, the availability of a given metabolite may fluctuate in response to metabolic rewiring caused by genetic alterations or the result of a dynamic tumor microenvironment. Cell metabolism is comprised of dynamic reactions induced by *de novo* synthesis, but also heavily influenced by exogenous sources like diet. In cancer cells, metabolic

networks are further complicated by oncogenic stimuli, genetic alterations of metabolic enzymes, and the tumor microenvironment, such as hypoxia and nutrient depletion (18). Emerging evidence suggests that changing metabolite levels can regulate enzymatic activity of chromatin modifying proteins, indicating potential crosstalk between cellular metabolism and epigenetics (14, 15). Therefore, besides mutation of epigenetic enzymes, modulation of metabolite levels provides an additional layer of epigenetic control and transcriptional regulation in cancer cells.

Methionine metabolism in cancer and histone methylation

SAM serves as a major methyl donor for the methylation of DNA and histone. SAM is primarily generated from methionine in the one-carbon metabolism pathway. Under normal conditions, cells acquire endogenous methionine from either the methionine salvage cycle or the folate cycle (19). Interestingly, a key enzyme in the methionine salvage cycle, methylthioadenosine phosphorylase (MTAP), is deleted across a wide range of cancers (20). Loss of MTAP expression impairs methionine biosynthesis and may render cancer cells dependent on exogenous methionine (20). Moreover, defects in folate metabolism also promote methionine dependence in cancer cells (21). Methionine is shown to be highly consumed in tumor cells compared to normal cells, and some cancer cells are not able to grow in the absence of methionine (21, 22). Recent studies have demonstrated that defects in methionine metabolism reduce intracellular SAM levels, affecting histone methylation dynamics (23-25). Deficiency in methionine or folate leads to reduced SAM levels and reduced H3K4 methylation in both yeast and human cells (23). Knockdown of SAM synthase *SAMS-1* in *C. Elegans* inhibits H3K4 methylation and suppresses the expression of H3K4-associated genes during *Pseudomonas* infection (26). In addition, methionine metabolism also plays an important role in cellular

differentiation of mouse embryonic stem cells. Depletion of methionine in stem cells diminishes H3K4 levels and reduces the expression of the pluripotent marker, NANOG, leading to enhanced differentiation potency (25). This evidence suggests that H3K4-specific HMT activity is sensitive to fluctuating intracellular SAM levels. In fact, a methionine restriction diet in mice triggers a rapid decrease in H3K4 methylation by modulating intracellular SAM levels. Importantly, ChIP-sequencing analysis of H3K4me3 reveals that methionine restriction decreases H3K4 methylation, affecting cell fate genes and cancer-associated genes including *AKT1*, *MYC*, and *MAPK* (24) (Figure 1). Therefore, it is speculated that elevated methionine metabolism through the induction of H3K4 methylation drives the expression of many cancer-associated genes and contributes to tumor progression.

Targeting methionine metabolism with dietary restriction

Elevated SAM levels can modulate epigenetic control of gene expression which may contribute to the progression of cancer. Recent studies also suggest that methionine restriction (MR) diets can be an effective approach to lower intracellular SAM levels and reduce histone methylation (22, 24) (Figure 5). MR diets have demonstrated anticancer effects in addition to prolonging life in animal models (27-29). Cumulative evidence demonstrates that a low methionine diet inhibits xenograft tumor growth, prevents metastasis, and enhances the efficacy of chemotherapy drug treatment in different animal models (30-32). Moreover, methionine metabolism may contribute to oncogenesis as MR diets inhibit colonic tumor development in carcinogen-treated rats (33). Data from a phase 1 clinical trial suggests that a MR diet is effective in reducing plasma methionine levels and is safe for 18 weeks (34). However, the effect of an extended MR diet may not be tolerable and remains to be determined. Alternatively, administration of the methioninase

enzyme can serve as an alternative approach to reduce methionine levels. Methioninase, originally purified from bacteria, breaks down methionine to α-ketobutyrate, methanethiol and ammonia (35). Treatment with recombinant methioninase enzyme is well-tolerated and displays better anti-cancer properties than a MR diet (36-38). However, the effect of methioninase treatment on SAM levels and histone methylation remains unknown.

Genetic mutation of metabolic enzymes and histone methylation

Histone demethylase enzymes use αKG as the co-substrate to remove methyl groups on histones and to release succinate and formaldehyde. While histone αKG is essential for histone demethylation, increased succinate or fumarate levels inside the cell can antagonize the activity of the histone demethylases. In fact, accumulation of succinate or depletion of αKG promotes cellular differentiation in both mouse embryonic stem cells and human pluripotent stem cells (39, 40). In contrast, the elevated intracellular αKG in naive stem cells through the modulation of histone methylation induces the expression of pluripotency-associated genes (e.g. *NANOG*) and favors self-renewal (39). Thus, genetic mutations that lead to alteration of succinate, fumarate or αKG levels often result in changes in histone methylation and gene expression. For example, loss of function mutations in the succinate dehydrogenase (SDH) gene and the fumarate hydratase (FH) gene are found in a number of human cancers that lead to rapid accumulation of succinate or fumarate (41, 42). In SDH and FH deficient cancer cells, the accumulation of succinate and fumarate respectively inhibits various KDM enzymes leading to histone hypermethylation and altered gene expression (43) (Figure 5). Recent studies also demonstrate that fumarate accumulation in FH deficient cells, through epigenetic modulation, activates the

expression of EMT-related transcription factors and vimentin to promote epithelial-to-mesenchymal-transition (44).

In normal cells, the isocitrate dehydrogenase (IDH) converts isocitrate to αKG in the TCA cycle. Multiple whole-genome sequencing experiments reveal heterogeneous mutations on the IDH gene in different cancers including, glioblastoma, acute myeloid leukemia and T cell lymphoma (45). The mutated IDH1 and IDH2 not only fail to synthesize αKG, but also gain additional function to produce 2 hydroxyglutarate (2HG). 2HG, a structural analog of αKG, competitively inhibits many αKG-dependent enzymes including histone demethylases, leading to histone hypermethylation and inhibition of cellular differentiation (46, 47). In fact, 2HG treatment in 3T3-L1 cells inhibits H3K9-specific demethylase KDM4C activity and represses the expression of adipogenesis-associated factors *CEBPA*, *PPARG* and *ADIPOQ*, ultimately blocking adipocyte differentiation (48) (Figure 5). A recent study also demonstrates that IDH1 mutation promotes H3K9 hypermethylation and downregulates ATM expression, resulting in increased DNA damage and impaired cell renewal in hematopoietic stem cells (49).

Tumor microenvironment and histone methylation

Hypoxia and histone methylation. In addition to metabolic stress, cancer cells in the microenvironment of solid tumors also experience a profound shortage in oxygen. Hypoxia can contribute to cancer progression, metastasis and drug resistance (50). Recently, different studies have demonstrated that hypoxic conditions in cancer cells induce significant changes in the epigenetic landscape (51, 52). Specifically, hypoxia induces histone dimethylated H3K9 by inducing the activity of methyl transferase G9a , and potentially inhibiting the demethylation

activity (53). The hypoxia-mediated H3K9 methylation often leads to repression of tumor suppressors including *BRCA1, RUNX3, RAD51*, and *MLH1* (49, 54, 55) (Figure 5). Interestingly, oxygen is required by all αKG dependent JmjC-KDM enzymes to facilitate the demethylation process. In vitro enzymatic activity assays suggest that JmjC-HDMs have weak binding affinities for oxygen when at levels near the cellular oxygen concentration , leading to the sensitivity of demethylation activities to changes in oxygen availability (56). Earlier reports also indicate that hypoxia inhibits Jumonji histone demethylase activity leading to induction of repressive histone markers, H3K9 and H3K36, and down regulation of chemokines (e.g. Ccl2) and chemokine receptors (e.g. Ccr1 and Ccr5) in macrophages (57). Similarly, hypoxic conditions attenuate the activity of the H3K4-specific demethylase JARID1A, but do not affect protein levels. Hypoxia induced hyper methylation of H3K4 increases the expression of *HMOX1* and *DAF* genes in Beas-2B (58). While indicated evidence suggests that hypoxia inhibits demethylase activity to alter epigenetics, further studies are needed to determine whether the histone demethylase activity depends on oxygen availability, and if oxygen depletion directly impairs demethylase activity *in vivo*. Lastly, lactate dehydrogenase A enzyme, under hypoxic conditions, can produce oncometabolite 2-HG, independent of IDH enzymes (59, 60). Importantly, hypoxia-mediated 2HG also inhibits KDM4C activity to promote H3K9 methylation and alter gene expression (59) (Figure 5).

Targeting epigenetic modifications to reverse deregulation in gene expression. Metabolic alterations in cancer cells affect epigenetic modifications leading to abnormal gene expressions. Thus, the metabolic control of epigenetic also contributes to tumor progression of human cancer. Different from genetic alteration, epigenetic modifications by methylation and acetylation are

intrinsically reversible. Therefore, chromatin modifying enzymes can be potential targets to reverse the change in gene expression mediated by epigenetic modifications. Indeed, some inhibitors targeting epigenetic machinery exhibits potent anticancer properties and have been approved by the FDA for the treatment of many cancers (61). Elevated methionine metabolism in cancer is associated with H3K4 hypermethylation which is accountable for the active transcription of many cancer-associated genes. Beside MR, targeting the H3K4 histone methylstransferase may provide some therapeutic advantage to reverse abnormal gene expression and block tumor progression. The H3K4 specific inhibitor, MM-401, directly inhibits the MML1 histone methylatransferase, blocking H3K4 methylation and suppressing the expression of *MYC* and dedifferentiation genes (62, 63) (Figure 5). MM-401 treatment can promote cell cycle arrest, cell death and myeloid differentiation in mixed-lineage leukemia cells (62). Thus, it will be of interest to determine whether MM-401 or other H3K4-specific inhibitors can be used to target H3K4 hypermethylation in methionine dependent cells.

Cancer cells in the regions of solid tumors with poorly developed vasculature are subjected to hypoxia and glutamine depletion due to poor tumor vasculature (50, 64). The distinct tumor microenvironment may promote cancer cell dedifferentiation and drug resistance, contributing to poor clinical outcome (65). In particular, glutamine deficiency in melanoma has been shown to promote H3K27 methylation resulting in cell dedifferentiation and drug resistance (64). While it remains challenging to modulate glutamine levels in the tumors, targeting the H3K27 histone methyltransferase (e.g. EZH2) may underscore a therapeutic advantage. The potent and selective EZH2 inhibitors (i.e. EPZ005687 and GSK126) directly block H3K27 methylation and reactivates transcription of target genes (66, 67). Importantly, treatment using specific

(EPZ005687) or global histone methylation inhibitors suppress the expression of dedifferentiation markers in melanoma cells and reverses the drug resistance phenotype mediated by glutamine deficiency (64). Thus, targeting epigenetic machinery is a promising approach to impair the oncogenic effect of metabolic changes in cancer.

Limited oxygen in the tumor microenvironment facilitates the emergence of cancer stem cells and promotes resistance to chemotherapy (68-70). Moreover, hypoxia-induced H3K9 methylation represses expression of different tumor suppressors, and consequently contributes to tumor progression (71). Therefore, targeting H3K9 methylation in cancer may reverse the change of gene expression and diminish the oncogenic effect of hypoxia in cancer. Chaetocin is an inhibitor that inhibits methyltransferase Suv39h1 and reduces H3K9 repressive markers (72). Chaetocin treatment in human leukemia cells inhibits H3K9 methylation and reactivates the expression of E-cadherin and tumor suppressor p15 (73, 74). Further studies are needed to investigate the effect of H3K9-specific methyltransferase inhibitors on gene expression and the therapeutic response of cancer cells during hypoxia.

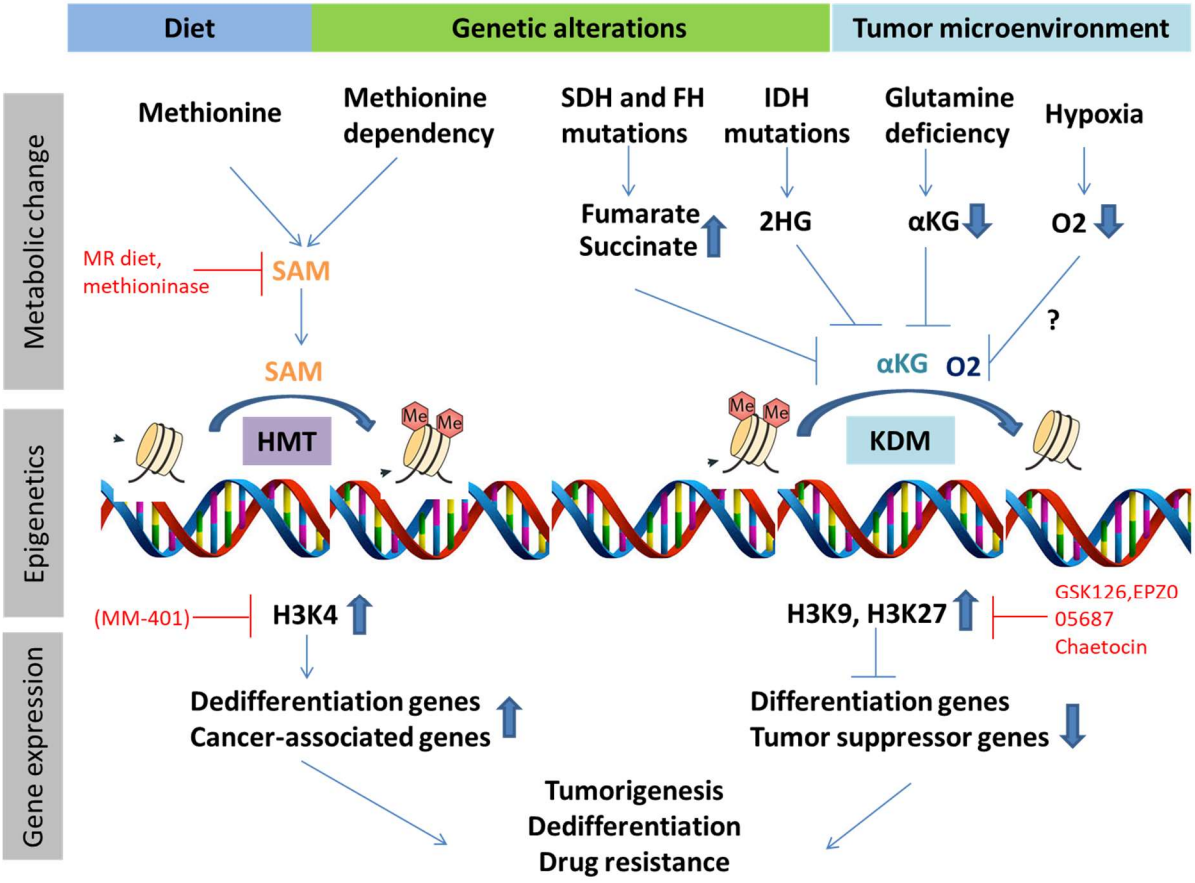

Figure 5: The crosstalk between metabolism and epigenetic control of gene expression in cancer. (Left) Elevated methionine dietary intake or methionine metabolism leads to accumulation of S-adenosylmethionine (SAM) which promotes histone methylation catalyzed by histone methyltransferase (HMT). Subsequently, hypermethylation at active marker H3K4 induces transcription of dedifferentiation genes and cancer-associated genes. (Right) Fumarate or succinate accumulation due to the loss-of-function mutant fumarate hydratase (FH) or succinate dehydrogenase (SDH), 2-hydroxyglutarate (2HG) from mutant isocitrate dehydrogenase (IDH), depletion of α-ketoglutarate (α-KG) due to glutamine deficiency, or hypoxia inhibits histone demethylation process catalyzed by histone demethylases (HMD).

Subsequently, hyper-methylation at suppressive histone makers H3K9 or H3K27 inhibits transcription of differentiation genes and tumor suppressor genes. Together, these metabolic regulations of epigenetics and genes expression may contribute to cell dedifferentiation, tumor progression and drug resistance in cancer.

Glutamine deficiency and DNA methylation in colon cancer

Glutamine metabolism and oncogenic Wnt signaling. Glutamine is consumed rapidly in the intestine and plays a significant role in intestinal regeneration. As intestinal epithelial cells have the highest turnover rate in the human body, and glutamine demand is elevated in this tissue (75). In addition to being a key metabolic fuel for cell proliferation, previous studies suggest that glutamine may also play a regulatory role in the regeneration of intestinal lining (76, 77). In Chapter 4, we found that mice with intestinal tumors experience glutamine shortage in both blood and intestinal tissue compared to wildtype mice. In correlation, it was observed in human colon tumors wherein glutamine was significantly depleted compared to healthy tissues (4). Importantly, we found that glutamine shortage facilitates the tumorigenic transformation of intestinal organoids by driving stemness and suppressing differentiation.

The hypothesis that CRC tumors arise from the intestinal stem cells at the bottoms of the crypts are well supported in the field (78). While many adult stem cells are dormant, intestinal stem cells proliferate rapidly to generate transition amplifying cells which are converted to differentiated cells including enterocytes, goblet cells, Paneth cells, and enterocytes (78, 79). While the crypt regeneration process is tightly regulated, stem cells and/or transition cells that fail to differentiate can retain their highly proliferative feature. This deregulation in intestinal differentiation can lead to uncontrolled cell growth and development of colon adenoma (79). We found that glutamine restriction exacerbates the differentiation dysfunction in APC mutation in

APC mutant cells to further potentiate stemness and block differentiation. Thus, glutamine deprivation by interfering with the normal intestinal differentiation can contribute to the progression of colon cancer.

It appears that chronic glutamine depletion in the intestine can drive the elevated activity of the Wnt signaling to drive stemness and potentiate colon cancer development, even in APC mutant cells. Wnt pathway plays a critical role in intestinal function and regeneration (80) (81). Almost 80% of CRC patients develop tumors with hyperactive Wnt signaling through mutation of the adenomatous polyposis coli (APC) gene (82). However, heterozygous APC mutant exhibited in human tumors only leads to partial Wnt activation due to the activity of the remaining wildtype-APC protein. Moreover, a recent study also demonstrated that truncated APC proteins still retain partial function to suppress Wnt signaling (83). Thus, we identified that environmental glutamine restriction is one of the extracellular inputs that contribute to the oncogenic potential of the Wnt signaling in APC mutant tumors to facilitate colon cancer progression. While oncogenic signaling such as Wnt or mTOR have been previously shown to directly remodel metabolic pathways to support tumorigenesis, our study is the first one to identify the potential regulation of metabolic microenvironment on Wnt signaling pathway in colon cancer.

DNA methylation and Wnt regulation. How does the depletion of exogenous glutamine lead to Wnt activation and enhanced stemness? Since glutamine is essential for the survival and proliferation of malignant cells, most cancer cells become dependent on exogenous glutamine (84, 85). In highly proliferative cells, glutamine can be converted into alpha ketoglutarate (α-KG) to replenish TCA cycle intermediates to ensure sufficient energy production under the effect of aerobic glycolysis (86). Interestingly, emerging studies demonstrate that αKG in addition to its

role in central metabolism exerts regulatory roles in gene expression through the regulation of different enzymes. For examples, αKG can bind and block TOR and ATP synthase activity that leads to prolonged lifespan in *C. elegans (87).* Important, αKG also serves as a cofactor for many epigenetic modifying enzymes including histone and DNA demethylases. In addition, it was shown that intracellular αKG levels plays a critical role in maintaining the pluripotency of embryonic stem cells via regulation of these demethylases and ultimately the epigenetic landscape (88, 89). Therefore, fluctuation in glutamine availability in the environment directly influence the intracellular levels of αKG, thereby modulating the activity of different chromatin modifying enzymes. We propose that the depletion of intracellular αKG due to intestinal glutamine depletion reprograms the epigenetic landscape in the intestinal organoids and leads to the hyperactivation of Wnt and suppression of intestinal differentiation. Consistently, in Chapter 4, we found that inhibition of DNA methylation with small molecule rescued the low-glutamine's effect on both Wnt hyperactivation and stemness, suggesting that DNA methylation plays a crucial role for the crosstalk between glutamine deficiency and Wnt signaling. DNA hypermethylation, especially in the many tumor suppressor genes and Wnt antagonists, are prevalent in colorectal cancer. Thus, we propose that that the DNA hypermethylation induced by the low glutamine conditions silences the expression of many tumor suppressor genes and many Wnt antagonist genes contributing to tumor progression and aggressiveness. However, further studies are required to support this hypothesis that depletion in intracellular aKG as a result of glutamine deficiency inhibits the activity of the DNA demethylase enzyme TET leading to DNA hypermethylation and Wnt activation. Collectively, this study reinforces the notion that metabolic alterations can bring about significant changes to epigenetics and gene expression in cancer.

αKG supplementation as a novel therapy for colorectal cancer. In the United States, there are more than a million people living with colon cancer which remains the second leading cause of cancer death (90). With a five-year survival rate of 65 percent, early diagnosis and detection play a significant role in disease outcome (91). However, distant metastasis and recurrence remain challenges in CRC treatment. Molecular pathogenesis of colorectal cancer is one of the most clearly understood among cancers, yet clinical effort to inhibit the Wnt pathway remain unsuccessful in clinical settings (92, 93). Many Wnt inhibitors that directly interfere with the Wnt signaling pathway may have detrimental effects on normal intestinal homeostasis and other tissues such as mammary gland and bone marrow where physiological Wnt plays a crucial role in somatic stem cell maintenance (92, 94, 95). Cell permeable version of αKG, a TCA cycle intermediate, was found to block hyper-proliferation and drives intestinal differentiation in both patient-derived colon organoids and K-Ras, P53-/- driven tumors. Mechanistically, we found that an increase in intracellular aKG levels facilitate the activity of the TET enzymes to demethylate DNA globally. Interestingly, the DNA hypomethylation occurs in the upstream regions of many tumor suppressor genes and many Wnt inhibitor genes. These results suggest that the αKG supplementation through DNA methylation induces the expression of genes that suppress Wnt signaling and facilitate cellular differentiation. Other Wnt inhibitors may completely block the Wnt signaling and result in cell death and acute toxicity. Thus, αKG supplementation represents a less aggressive therapy for the treatment of colon cancer since our preliminary result suggests αKG, rather than inducing apoptosis, drives the cancerous cells to terminally differentiated cells which will spontaneously go under apoptosis during the crypt regeneration process. Indeed, clinical drugs that prime cancer cell differentiation have impressive clinical outcomes. For

example, retinoic acid therapy in promyelocytic leukemia can drive leukemic cells into differentiated cells which results in more than 80% cure rate observed in patients (96).

Remaining questions and future direction

Despite tremendous progress in the field of cancer metabolism and epigenetics, many fundamental questions remain to be addressed. Many studies suggest that the metabolic control of epigenetics often leads to global changes in epigenetic and genes expression. However, it remains unclear how certain metabolic conditions exerts tumor-promoting effects while other metabolic changes would result in tumor suppression. For examples, different studies in various cancer models demonstrate that the increase in intracellular aKG often results in cellular differentiation and tumor regression, while the depletion of aKG leading to enhanced stemness and cancer progression (Chapter 4). Furthermore, we found that glutamine restriction in intestinal organoids is not only able to activate the oncogenic Wnt signaling but also many other hallmarks of cancer including other inflammation cascades and metastasis. It remains to be determined if there is any selectivity on the epigenetic alterations of certain genes or group of genes in response to a specific metabolic alteration. There could be some potential unknown mechanisms that modulate the specificity, such as adaptor proteins or additional enzymes that facilitate the specificity of epigenetic alterations in response to a certain metabolic condition. For example, there could be a nutrient sensor protein, in response to certain metabolic stimuli, can directly bind to a chromatin-modifying enzyme to selectively alter epigenetic marks on targeted regions of the genome. Alternatively, chromatin state may also influence the effect of metabolic fluctuation on epigenetics. For example, open chromatin at DNA regions with active

transcription may be more susceptible to metabolic inputs than close chromatin at the non-coding DNA regions.

In order to further address these questions, we will need more advanced research tools to study the interaction between metabolism and epigenetics. Since most of the findings described above are based on cell culture studies, it is important to utilize the systematic approach to dissect the interaction between cancer metabolism and epigenetics *in vivo*. Moving forward, we will need to perform metabolic flux experiments that can determine the rate of turnover of metabolites through metabolic pathways in different tissues in response to certain conditions including tumor burden, oncogene activation, or dietary changes in real time. In addition to determining whole-body metabolism, novel chromatin biology tools need to be developed to study epigenetic in a dynamic and systematic fashion, especially in response to microenvironmental changes. In addition to chromatin immunoprecipitation sequencing, it would be helpful to have research tools to study epigenetic changes in high-resolution and in real-time. The ability to dissect epigenetic changes in response to metabolic fluctuation at a single-cell level is also important in addressing the remaining biological questions because of the cellular heterogenicity exhibited in tumors. Lastly, with a better understanding of the regulation of metabolism on epigenetics and gene expression, it is possible to develop novel compounds that can modulate epigenetics in a specific and controlled manner to selectively inhibit or activate a certain group of genes for therapeutic purposes.

Part II: Summary and concluding remarks

Summary

Cancer is a major global health problem and remains the second leading cause of death in the United States. Despite tremendous progress in understanding the pathogenesis of different cancers, most frontline therapies are limited to chemotherapy, surgery, and radiation. Physicians traditionally make treatment decisions heavily based on the type of cancer and the stage of the disease. Currently, there is a strong push for personalized/precision medicine in cancer treatment. To improve the survival outcome and minimize toxicity, physicians use genetic and epigenetic information of each individual to identify more effective treatment strategies. Understanding the unique molecular and genetic profile of each individual will allow better biomarkers and targeted therapies to be developed with a great promise to transform cancer treatment (97).

In addition to genetic alteration, the environment also plays an important role in tumor biology, yet the effect of environmental inputs is largely ignored when deciding treatment for cancer patients. These environmental factors can be on the organismal level and includes diet, lifestyle, and exposure to certain chemicals from the environment. Furthermore, cancer cells are constantly exposed to metabolic fluctuations as well as inputs from the microbiome and the immune cells in the tumor microenvironment (98). The continuous crosstalk between the tumors and its microenvironment can affect tumor progression as well as tumor response to certain therapies.

The crosstalk between genetic alterations and metabolic microenvironment in tumors

Metabolic changes are a critical component of the tumor microenvironment, since nutrient availability can greatly impact tumor growth. Cancer cells display fundamental changes in their core metabolism compared to normal cells. Our laboratory and other researchers have reported that the metabolic reprogramming in cancer with the increased glutamine dependency often create a glutamine depleted microenvironment (99). However, the effect of this metabolic microenvironment on tumor progression and drug response is largely unexplored. In this dissertation, I highlight different connections between metabolic microenvironment and tumor biology and discuss the impact of these connections on both tumor progression and therapeutic response. Specifically, this dissertation explores how metabolic fluctuation affects the genetic and epigenetic states of cancer cells. I will demonstrate how certain genetic alterations can be beneficial for cancer cells in poor-nutrient microenvironment conditions and reveal how the metabolic microenvironment itself could serve as an understudied novel driver of tumorigenesis.

Genetic alterations protect cancer cells from metabolic stress in the tumor microenvironment

Genomic instability is a hallmark of cancer that plays an important role in tumorigenesis. More than half of human tumors carry mutations in the tumor suppressor p53 (100). Mutant p53 has been shown to drive tumorigenesis and drive drug resistance due to the loss of tumor suppressor function. In chapter 2, I demonstrate that tumor-associated mutant p53 can protect cancer cells from depleted glutamine conditions in the tumor microenvironment. Specifically, cancer cells expressing mutant p53 survived better in the nutrient-poor microenvironment compared to p53

null cells or cells expressing wild-type p53. Mechanistically, we found that mutant p53 abrogated its pro-death activity, while enhancing the pro-survival function of wild-type p53 in response to metabolic stress. The ability of mutant p53 to hyper-activate cell cycle arrest target genes and reprogram metabolism allowed cancer cells to adapt to glutamine starvation.

This study highlights that certain genetic dispositions (e.g. mutant p53) in tumors can protect cancer cells from metabolic stress and promote tumor progression. Developing tumors in poorly vascularized microenvironments often create severe glutamine deficiency, with glutamine dropping to almost undetectable levels in the tumor core. Most human tumors carry a somatic mutation in the TP53 gene. Emerging tumors often contain a heterogeneous population of cells carrying mutant p53 or wild-type p53. Our data suggest that metabolic stress within the tumor microenvironment selectively favors the emergence of clones carrying the mutant p53. This finding supports the idea that genetic predispositions are further exploited by the metabolic microenvironment in cancer. Therefore, it will be of interest in future studies to identify other genetic alterations that can protect cancer cells from metabolic stress.

Metabolic stress in the tumor microenvironment can drive other hallmarks of cancer to promote tumorigenesis

Normal cells have to acquire a sufficient number of biological capacities to transform into malignant cells. To become fully transformed and invasive, precancerous cells acquire the following hallmarks of cancer: “genome instability, sustained proliferative signaling, evasion of growth suppressors, resistance to cell death, replicative immortality, induction of angiogenesis,

invasion and metastasis properties, immune avoidance, tumor-promoting inflammation, and deregulation of cellular energetics" (1). Genetic alterations in tumor suppressor genes and oncogenes are often the initiating drivers of tumorigenesis in a vast majority of cancers. Thus, genomic instability not only promotes tumor initiation but also facilitates the emergence of other hallmarks of cancer. While intensive preclinical research focuses on targeting these hallmarks of cancer for therapeutic purposes, many drugs that target only one of these hallmarks typically yield poor clinical activity. For example, the inhibitor of VEGF, which blocks angiogenesis, initially causes a tumor to regress, but tumors often become resistant to the treatment (95).

Emerging evidence suggests the hallmarks of cancer are rather interdependent, and the tumor microenvironment plays a vital role in these interactions. These hallmarks of cancer often interact and even rely on each other to ensure ensuring tumor fitness, especially in response to environmental stress and drug treatment. For example, while many genotoxic agents can inhibit tumor growth, some chemotherapy drugs like alkylating agents can induce certain genomic alterations which selectively upregulate other hallmarks of cancer in the surviving cells, leading to drug resistance and cancer relapse. Thus, understanding the crosstalk between different hallmarks of cancer will not only provide significant insights on tumor pathogenesis but also allow better therapies to be developed.

Cancer cell metabolism is considered an "emerging" hallmark of cancer. Well-studied metabolic pathways are rewired to meet the elevated demand for energy and macromolecule biosynthesis in malignant cells. Metabolic reprogramming is frequently driven by oncogenes versus genetic

mutations of metabolic enzymes. Recent findings suggest that the metabolic microenvironment, which is influenced by dietary intake, plays a crucial role in remodeling different cellular processes of cancer cells. Importantly, these environmental factors modulate intracellular levels of different metabolites, including aKG, acetyl-CoA, and SAM, which serve as cofactors for different enzymes involved in DNA damage repair and epigenetic regulation. Therefore, the changing metabolic microenvironment in tumors—through epigenetic and genetic alterations—affects gene expression and cellular functions of cancer cells.

In chapter 3, I identified novel crosstalk between metabolic stress and genomic instability in cancer. Specifically, I demonstrated that glutamine restriction in cancer cells through the depletion of aKG can inhibit the activity of the DNA repair enzyme, Alkbh, to repair alkylation damage. We found that cancer cells grown in a glutamine-starved environment display extensive DNA damage, a hallmark of genomic instability. This finding suggests that metabolic stress can potentially promotes genetic alterations in tumors, implicating crosstalk between metabolic stress and genomic instability. Furthermore, genetic alterations caused by metabolic stress can impact regions of genes that define other hallmarks of cancer, such as angiogenesis and metastasis. Therefore, metabolic stress through genetic alterations can have a far-reaching impact on tumorigenesis by enhancing genetic changes. It would be of interest in future studies to determine whether glutamine deficiency in tumors can directly promote genetic alterations that directly drive tumorigenesis.

In chapter 4, I provide compelling evidence for the crosstalk between metabolic stress and epigenetic regulation in cancer. We observe that changing glutamine or aKG levels in colorectal cancer cells can influence DNA methylation, leading to a dramatic change in gene expression. Specifically, I found that glutamine deficiency not only induces the upregulation of genes in the Wnt signaling pathway but also alters the expression of genes involved in other hallmarks of cancer including inflammation and metastasis. Therefore, the metabolic regulation of epigenetics provides an additional layer that allows environmental changes, like hypoxia and nutrient restriction, to modulate the epigenetic landscape to select for "other hallmarks" in cancer cells. These environmental and metabolic disruptions, by promoting abnormal restrictive or permissive chromatin on both histone methylation and DNA methylation levels, can globally reprogram the transcriptional profile. Importantly, these epigenetic alterations can lead to upregulation of proto-oncogenes or suppression of tumor suppressor genes that in turn promote tumorigenesis.

The crosstalk between the tumor microenvironment and epigenetic plasticity in cancer appears to play a critical role in cellular differentiation potential (Chapter 4). It has been shown that changing metabolic conditions can drive or inhibit cellular differentiation in cancer cells. Thus, the impact of the metabolic environment, through epigenetic modulation, plays an important role in cancer progression. Whether it is of greater impact than genetic alterations is yet to be determined. Moreover, metabolic alterations often induce a global change in epigenetic landscapes resulting in a dramatic change in gene expression profile. Thus, it would be important to study how metabolically induced epigenetic modifications impact other hallmarks of cancer. The impact of the microenvironment on metabolism and epigenetics on tumor-associated cells

including macrophage, fibroblast and other immune cells are areas of interest since these cells often play an important role in tumor fitness and therapeutic response.

Metabolic microenvironment modulates cellular response to cancer therapy

In addition to the role of metabolic stress in driving cancer development, we also found that changes to the metabolic microenvironment can modulate the cancer response to drug treatments. Chemotherapy with alkylating agents remain the frontline therapy for different types of aggressive cancer. In chapter 2, we found that the metabolic microenvironment can dictate cancer cell response to alkylating agents, a common chemotherapy drug for aggressive tumors(101). Specifically, glutamine depletion can diminish intracellular aKG levels to inhibit the activity of Alkbh enzyme to repair DNA damage induced by alkylating agent treatment. Therefore, a combination treatment with glutaminase inhibitor and an alkylating agent can be more efficacious than single drug treatment. In contrast, supplementation of aKG can protect cancer cells from DNA damage and cell death after alkylating agent treatment. These results suggest that metabolism plays a significant role in determining cellular response to cancer drug treatment.

Modulating glutamine metabolism for cancer treatment: opportunities and challenges

Over the past ten years, many efforts have been done to cut the fuel supply or "starve" cancer cells, including blocking glutamine usage. Due to cancer cell dependency on exogenous glutamine, glutamine metabolism has become an attractive target for cancer therapy. There is a

strong push to use the glutamine-restriction diet for cancer patients. In addition, a glutaminase inhibitor aimed at starving cancer cells of glutamine is currently in clinical trials for cancer patients, including colorectal cancer. Inhibition of glutamine metabolism, especially in combination with other therapies, have shown promising results in preclinical and clinical studies(102). However, our findings in chapter 4 suggest that chronic and moderate glutamine depletion can drive cancer stemness and enhance tumorigenesis in colorectal cancer. Thus, glutaminase inhibitors should be used with caution as cancer cells that manage to survive glutaminase treatment may become more aggressive. To effectively eradicate the cancer cells and avoid drug resistance, different combination therapies and biomarkers should be considered when using glutaminase inhibitor in clinical settings.

In contrast to glutamine deprivation, we found that "feeding" colorectal cancers with the TCA cycle metabolite aKG will "tame" the aggressive tumors and induce differentiation. Chapter 4 specifically highlights the potential use of aKG supplementation as a novel therapeutic direction for colorectal cancer. While this therapeutic approach is in conflict with glutaminase inhibitor treatment, we found that aKG supplementation, especially in drinking water, is a safe and effective strategy to suppress the growth of colorectal tumors and prolong survival in different animal models. Despite the impressive effect of aKG in suppressing tumor growth, one of the major concerns is whether the nutrient supplementation may fuel cancer cell growth by boosting the TCA cycle. While we found that aKG did not enhance proliferation in colorectal cancer cells, the effect of aKG supplementation on other types of cancer remains unclear. Our results suggest that the antitumor properties of aKG in colorectal cancer is attributed to the ability of the metabolite to drive terminal differentiation of highly dedifferentiated cancer cells and cancer stem cells. Therefore, it is important to consider the tissue of origin and differentiation

dysfunction of the tumors when using aKG supplementation as a therapeutic strategy. Cancer with deregulation in Wnt signaling and differentiation (e.g., colorectal cancer) are more vulnerable to aKG treatment. However, tumors originating from more terminally differentiated cells (e.g., pancreatic cancer) are less likely to respond to the metabolite treatment. In conclusion, aKG supplementation should be considered only in cancers with Wnt-driven dedifferentiation phenotypes such as colorectal, breast, and melanoma cancers.

Concluding remarks

Substantial progress has been made in understanding the molecular pathogenesis of different cancers along with the development of new therapeutic strategies. Environmental factors in addition to genetic alterations directly influence tumor fitness and therapeutic response. In this dissertation, I highlight the potential oncogenic roles of glutamine deficiency in driving tumor progression including 1) favoring the emerging of cancer cells harboring a mutant p53 protein, 2) blocking the activity of DNA repair *ALKBH* enzymes leading to accumulation of DNA damage and genomic instability, and 3) hyper-activating Wnt signaling pathway and cellular dedifferentiation in colon cancer. Importantly, understanding the effect of glutamine deficiency on tumorigenesis also leads to new therapeutic opportunities including a combinational therapy with glutaminase inhibitor and aKG supplementation for the treatment of cancer.

Reference

1. Hanahan D, Weinberg RA. Hallmarks of cancer: the next generation. Cell. 2011 Mar 4;144(5):646-74. PubMed PMID: 21376230.
2. Negrini S, Gorgoulis VG, Halazonetis TD. Genomic instability [mdash] an evolving hallmark of cancer. Nature reviews Molecular cell biology. 2010 03//print;11(3):220-8.
3. Feinberg AP, Vogelstein B. Hypomethylation distinguishes genes of some human cancers from their normal counterparts. Nature. 1983 Jan 06;301(5895):89-92. PubMed PMID: 6185846.
4. Rivenbark AG, Coleman WB, Stahl BD. Histone methylation patterns in human breast cancer. The FASEB Journal. 2009 April 1, 2009;23(1 Supplement):38.1.
5. Feil R, Fraga MF. Epigenetics and the environment: emerging patterns and implications. Nat Rev Genet. 2012 02//print;13(2):97-109.
6. Bernstein BE, Mikkelsen TS, Xie X, Kamal M, Huebert DJ, Cuff J, et al. A bivalent chromatin structure marks key developmental genes in embryonic stem cells. Cell. 2006 Apr 21;125(2):315-26. PubMed PMID: 16630819.
7. Greer EL, Shi Y. Histone methylation: a dynamic mark in health, disease and inheritance. Nat Rev Genet. 2012 Apr 03;13(5):343-57. PubMed PMID: 22473383. Pubmed Central PMCID: 4073795.
8. Kaelin WG, Jr., McKnight SL. Influence of metabolism on epigenetics and disease. Cell. 2013 Mar 28;153(1):56-69. PubMed PMID: 23540690. Pubmed Central PMCID: 3775362.
9. van Haaften G, Dalgliesh GL, Davies H, Chen L, Bignell G, Greenman C, et al. Somatic mutations of the histone H3K27 demethylase gene UTX in human cancer. Nature genetics. 2009 May;41(5):521-3. PubMed PMID: 19330029. Pubmed Central PMCID: 2873835.
10. Morin RD, Mendez-Lago M, Mungall AJ, Goya R, Mungall KL, Corbett RD, et al. Frequent mutation of histone-modifying genes in non-Hodgkin lymphoma. Nature. 2011 Jul 27;476(7360):298-303. PubMed PMID: 21796119. Pubmed Central PMCID: 3210554.
11. Nikoloski G, Langemeijer SM, Kuiper RP, Knops R, Massop M, Tonnissen ER, et al. Somatic mutations of the histone methyltransferase gene EZH2 in myelodysplastic syndromes. Nature genetics. 2010 Aug;42(8):665-7. PubMed PMID: 20601954.
12. Kulis M, Esteller M. DNA methylation and cancer. Advances in genetics. 2010;70:27-56. PubMed PMID: 20920744.
13. Wajed SA, Laird PW, DeMeester TR. DNA methylation: an alternative pathway to cancer. Ann Surg. 2001 Jul;234(1):10-20. PubMed PMID: 11420478. Pubmed Central PMCID: 1421942.
14. Lempradl A, Pospisilik JA, Penninger JM. Exploring the emerging complexity in transcriptional regulation of energy homeostasis. Nat Rev Genet. 2015 Nov;16(11):665-81. PubMed PMID: 26460345.
15. Kinnaird A, Zhao S, Wellen KE, Michelakis ED. Metabolic control of epigenetics in cancer. Nature reviews Cancer. 2016 11//print;16(11):694-707.
16. Locasale JW. Serine, glycine and one-carbon units: cancer metabolism in full circle. Nature reviews Cancer. 2013 Aug;13(8):572-83. PubMed PMID: 23822983. Pubmed Central PMCID: 3806315.
17. Kooistra SM, Helin K. Molecular mechanisms and potential functions of histone demethylases. Nature reviews Molecular cell biology. 2012 05//print;13(5):297-311.
18. Ward PS, Thompson CB. Metabolic Reprogramming: A Cancer Hallmark Even Warburg Did Not Anticipate. Cancer cell. 2012;21(3):297-308. PubMed PMID: PMC3311998.

19. Locasale JW. Serine, glycine and one-carbon units: cancer metabolism in full circle. Nat Rev Cancer. 2013 08//print;13(8):572-83.
20. Schmid M, Malicki D, Nobori T, Rosenbach MD, Campbell K, Carson DA, et al. Homozygous deletions of methylthioadenosine phosphorylase (MTAP) are more frequent than p16INK4A (CDKN2) homozygous deletions in primary non-small cell lung cancers (NSCLC). Oncogene. 1998 Nov 19;17(20):2669-75. PubMed PMID: 9840931.
21. Cavuoto P, Fenech MF. A review of methionine dependency and the role of methionine restriction in cancer growth control and life-span extension. Cancer treatment reviews. 2012 Oct;38(6):726-36. PubMed PMID: 22342103.
22. Cellarier E, Durando X, Vasson MP, Farges MC, Demiden A, Maurizis JC, et al. Methionine dependency and cancer treatment. Cancer treatment reviews. 2003 Dec;29(6):489-99. PubMed PMID: 14585259.
23. Sadhu MJ, Guan Q, Li F, Sales-Lee J, Iavarone AT, Hammond MC, et al. Nutritional control of epigenetic processes in yeast and human cells. Genetics. 2013 Nov;195(3):831-44. PubMed PMID: 23979574. Pubmed Central PMCID: 3813867.
24. Mentch SJ, Mehrmohamadi M, Huang L, Liu X, Gupta D, Mattocks D, et al. Histone Methylation Dynamics and Gene Regulation Occur through the Sensing of One-Carbon Metabolism. Cell metabolism. 2015 Nov 03;22(5):861-73. PubMed PMID: 26411344. Pubmed Central PMCID: 4635069.
25. Shiraki N, Shiraki Y, Tsuyama T, Obata F, Miura M, Nagae G, et al. Methionine metabolism regulates maintenance and differentiation of human pluripotent stem cells. Cell metabolism. 2014 May 06;19(5):780-94. PubMed PMID: 24746804.
26. Ding W, Smulan Lorissa J, Hou Nicole S, Taubert S, Watts Jennifer L, Walker Amy K. s-Adenosylmethionine Levels Govern Innate Immunity through Distinct Methylation-Dependent Pathways. Cell metabolism. 2015 10/6/;22(4):633-45.
27. Orentreich N, Matias JR, DeFelice A, Zimmerman JA. Low methionine ingestion by rats extends life span. The Journal of nutrition. 1993 Feb;123(2):269-74. PubMed PMID: 8429371.
28. Lee BC, Kaya A, Ma S, Kim G, Gerashchenko MV, Yim SH, et al. Methionine restriction extends lifespan of Drosophila melanogaster under conditions of low amino-acid status. Nature communications. 2014 Apr 07;5:3592. PubMed PMID: 24710037. Pubmed Central PMCID: 4350766.
29. Hens JR, Sinha I, Perodin F, Cooper T, Sinha R, Plummer J, et al. Methionine-restricted diet inhibits growth of MCF10AT1-derived mammary tumors by increasing cell cycle inhibitors in athymic nude mice. BMC cancer. 2016 Jun 03;16:349. PubMed PMID: 27255182. Pubmed Central PMCID: 4891836.
30. Hoshiya Y, Guo H, Kubota T, Inada T, Asanuma F, Yamada Y, et al. Human tumors are methionine dependent in vivo. Anticancer research. 1995 May-Jun;15(3):717-8. PubMed PMID: 7645948.
31. Poirson-Bichat F, Goncalves RA, Miccoli L, Dutrillaux B, Poupon MF. Methionine depletion enhances the antitumoral efficacy of cytotoxic agents in drug-resistant human tumor xenografts. Clinical cancer research : an official journal of the American Association for Cancer Research. 2000 Feb;6(2):643-53. PubMed PMID: 10690550.
32. Breillout F, Hadida F, Echinard-Garin P, Lascaux V, Poupon MF. Decreased rat rhabdomyosarcoma pulmonary metastases in response to a low methionine diet. Anticancer research. 1987 Jul-Aug;7(4B):861-7. PubMed PMID: 3674775.

33. Komninou D, Leutzinger Y, Reddy BS, Richie JP, Jr. Methionine restriction inhibits colon carcinogenesis. Nutrition and cancer. 2006;54(2):202-8. PubMed PMID: 16898864.
34. Epner DE, Morrow S, Wilcox M, Houghton JL. Nutrient intake and nutritional indexes in adults with metastatic cancer on a phase I clinical trial of dietary methionine restriction. Nutrition and cancer. 2002;42(2):158-66. PubMed PMID: 12416254.
35. Kreis W, Hession C. Isolation and purification of L-methionine-alpha-deamino-gamma-mercaptomethane-lyase (L-methioninase) from Clostridium sporogenes. Cancer research. 1973 Aug;33(8):1862-5. PubMed PMID: 4720797.
36. Kreis W, Hession C. Biological effects of enzymatic deprivation of L-methionine in cell culture and an experimental tumor. Cancer research. 1973 Aug;33(8):1866-9. PubMed PMID: 4720798.
37. Tan Y, Xu M, Hoffman RM. Broad selective efficacy of recombinant methioninase and polyethylene glycol-modified recombinant methioninase on cancer cells In Vitro. Anticancer research. 2010 Apr;30(4):1041-6. PubMed PMID: 20530407.
38. Tan Y, Xu M, Guo H, Sun X, Kubota T, Hoffman RM. Anticancer efficacy of methioninase in vivo. Anticancer research. 1996 Nov-Dec;16(6C):3931-6. PubMed PMID: 9042315.
39. Carey BW, Finley LWS, Cross JR, Allis CD, Thompson CB. Intracellular [agr]-ketoglutarate maintains the pluripotency of embryonic stem cells. Nature. 2015 02/19/print;518(7539):413-6.
40. TeSlaa T, Chaikovsky Andrea C, Lipchina I, Escobar Sandra L, Hochedlinger K, Huang J, et al. α-Ketoglutarate Accelerates the Initial Differentiation of Primed Human Pluripotent Stem Cells. Cell metabolism. 2016 9/13/;24(3):485-93.
41. Tomlinson IP, Alam NA, Rowan AJ, Barclay E, Jaeger EE, Kelsell D, et al. Germline mutations in FH predispose to dominantly inherited uterine fibroids, skin leiomyomata and papillary renal cell cancer. Nature genetics. 2002 Apr;30(4):406-10. PubMed PMID: 11865300.
42. Pollard PJ, Briere JJ, Alam NA, Barwell J, Barclay E, Wortham NC, et al. Accumulation of Krebs cycle intermediates and over-expression of HIF1alpha in tumours which result from germline FH and SDH mutations. Human molecular genetics. 2005 Aug 01;14(15):2231-9. PubMed PMID: 15987702. Epub 2005/07/01. eng.
43. Xiao M, Yang H, Xu W, Ma S, Lin H, Zhu H, et al. Inhibition of α-KG-dependent histone and DNA demethylases by fumarate and succinate that are accumulated in mutations of FH and SDH tumor suppressors. Genes & development. 2012 03/07/received

05/09/accepted;26(12):1326-38. PubMed PMID: PMC3387660.
44. Sciacovelli M, Gonçalves E, Johnson TI, Zecchini VR, da Costa ASH, Gaude E, et al. Fumarate is an epigenetic modifier that elicits epithelial-to-mesenchymal transition. Nature. 2016 09/22/print;537(7621):544-7.
45. Losman J-A, Kaelin WG. What a difference a hydroxyl makes: mutant IDH, (R)-2-hydroxyglutarate, and cancer. Genes & development. 2013;27(8):836-52. PubMed PMID: PMC3650222.
46. Xu W, Yang H, Liu Y, Yang Y, Wang P, Kim S-H, et al. Oncometabolite 2-Hydroxyglutarate Is a Competitive Inhibitor of α-Ketoglutarate-Dependent Dioxygenases. Cancer cell. 2011 1/18/;19(1):17-30.
47. Chowdhury R, Yeoh KK, Tian YM, Hillringhaus L, Bagg EA, Rose NR, et al. The oncometabolite 2-hydroxyglutarate inhibits histone lysine demethylases. EMBO reports. 2011;12(5):463-9.

48. Lu C, Ward PS, Kapoor GS, Rohle D, Turcan S, Abdel-Wahab O, et al. IDH mutation impairs histone demethylation and results in a block to cell differentiation. Nature. 2012 03/22/print;483(7390):474-8.
49. Inoue S, Li WY, Tseng A, Beerman I, Elia AJ, Bendall SC, et al. Mutant IDH1 Downregulates ATM and Alters DNA Repair and Sensitivity to DNA Damage Independent of TET2. Cancer cell. 2016 Aug 08;30(2):337-48. PubMed PMID: 27424808. Pubmed Central PMCID: 5022794.
50. Wilson WR, Hay MP. Targeting hypoxia in cancer therapy. Nature reviews Cancer. 2011 Jun;11(6):393-410. PubMed PMID: 21606941.
51. Johnson AB, Denko N, Barton MC. Hypoxia induces a novel signature of chromatin modifications and global repression of transcription. Mutation research. 2008 Apr 02;640(1-2):174-9. PubMed PMID: 18294659. Pubmed Central PMCID: 2346607.
52. Chen H, Yan Y, Davidson TL, Shinkai Y, Costa M. Hypoxic stress induces dimethylated histone H3 lysine 9 through histone methyltransferase G9a in mammalian cells. Cancer research. 2006 Sep 15;66(18):9009-16. PubMed PMID: 16982742.
53. Chen H, Yan Y, Davidson TL, Shinkai Y, Costa M. Hypoxic Stress Induces Dimethylated Histone H3 Lysine 9 through Histone Methyltransferase G9a in Mammalian Cells. Cancer research. 2006;66(18):9009-16.
54. Lee SH, Kim J, Kim WH, Lee YM. Hypoxic silencing of tumor suppressor RUNX3 by histone modification in gastric cancer cells. Oncogene. 2009 Jan 15;28(2):184-94. PubMed PMID: 18850007. Epub 2008/10/14. eng.
55. Lu Y, Chu A, Turker MS, Glazer PM. Hypoxia-induced epigenetic regulation and silencing of the BRCA1 promoter. Molecular and cellular biology. 2011 Aug;31(16):3339-50. PubMed PMID: 21670155. Pubmed Central PMCID: PMC3147797. Epub 2011/06/15. eng.
56. Cascella B, Mirica LM. Kinetic Analysis of Iron-Dependent Histone Demethylases: α-Ketoglutarate Substrate Inhibition and Potential Relevance to the Regulation of Histone Demethylation in Cancer Cells. Biochemistry. 2012 2012/11/06;51(44):8699-701.
57. Tausendschön M, Dehne N, Brüne B. Hypoxia causes epigenetic gene regulation in macrophages by attenuating Jumonji histone demethylase activity. Cytokine. 2011 2//;53(2):256-62.
58. Zhou X, Sun H, Chen H, Zavadil J, Kluz T, Arita A, et al. Hypoxia induces trimethylated H3 lysine 4 by inhibition of JARID1A demethylase. Cancer research. 2010 May 15;70(10):4214-21. PubMed PMID: 20406991. Pubmed Central PMCID: 3007597.
59. Intlekofer Andrew M, Dematteo Raymond G, Venneti S, Finley Lydia WS, Lu C, Judkins Alexander R, et al. Hypoxia Induces Production of L-2-Hydroxyglutarate. Cell metabolism. 2015 8/4/;22(2):304-11.
60. Oldham William M, Clish Clary B, Yang Y, Loscalzo J. Hypoxia-Mediated Increases in l-2-hydroxyglutarate Coordinate the Metabolic Response to Reductive Stress. Cell metabolism. 2015 8/4/;22(2):291-303.
61. Jones PA, Issa J-PJ, Baylin S. Targeting the cancer epigenome for therapy. Nat Rev Genet. 2016 10//print;17(10):630-41.
62. Cao F, Townsend EC, Karatas H, Xu J, Li L, Lee S, et al. Targeting MLL1 H3K4 methyltransferase activity in mixed-lineage leukemia. Molecular cell. 2014 Jan 23;53(2):247-61. PubMed PMID: 24389101. Pubmed Central PMCID: 3965208.
63. Karatas H, Townsend EC, Cao F, Chen Y, Bernard D, Liu L, et al. High-affinity, small-molecule peptidomimetic inhibitors of MLL1/WDR5 protein-protein interaction. Journal of the

American Chemical Society. 2013 Jan 16;135(2):669-82. PubMed PMID: 23210835. Pubmed Central PMCID: 5180416.
64. Pan M, Reid MA, Lowman XH, Kulkarni RP, Tran TQ, Liu X, et al. Regional glutamine deficiency in tumours promotes dedifferentiation through inhibition of histone demethylation. Nature cell biology. 2016 Oct;18(10):1090-101. PubMed PMID: 27617932. Pubmed Central PMCID: 5536113.
65. Junttila MR, de Sauvage FJ. Influence of tumour micro-environment heterogeneity on therapeutic response. Nature. 2013 09/19/print;501(7467):346-54.
66. Knutson SK, Wigle TJ, Warholic NM, Sneeringer CJ, Allain CJ, Klaus CR, et al. A selective inhibitor of EZH2 blocks H3K27 methylation and kills mutant lymphoma cells. Nature chemical biology. 2012 Nov;8(11):890-6. PubMed PMID: 23023262.
67. McCabe MT, Ott HM, Ganji G, Korenchuk S, Thompson C, Van Aller GS, et al. EZH2 inhibition as a therapeutic strategy for lymphoma with EZH2-activating mutations. Nature. 2012 12/06/print;492(7427):108-12.
68. Mao Q, Zhang Y, Fu X, Xue J, Guo W, Meng M, et al. A tumor hypoxic niche protects human colon cancer stem cells from chemotherapy. Journal of cancer research and clinical oncology. 2013 Feb;139(2):211-22. PubMed PMID: 23052691. Epub 2012/10/12. eng.
69. Conley SJ, Gheordunescu E, Kakarala P, Newman B, Korkaya H, Heath AN, et al. Antiangiogenic agents increase breast cancer stem cells via the generation of tumor hypoxia. Proceedings of the National Academy of Sciences of the United States of America. 2012 Feb 21;109(8):2784-9. PubMed PMID: 22308314. Pubmed Central PMCID: PMC3286974. Epub 2012/02/07. eng.
70. Muz B, de la Puente P, Azab F, Luderer M, Azab AK. Hypoxia promotes stem cell-like phenotype in multiple myeloma cells. Blood cancer journal. 2014 Dec 05;4:e262. PubMed PMID: 25479569. Pubmed Central PMCID: PMC4315888. Epub 2014/12/06. eng.
71. Ramachandran S, Ient J, Gottgens EL, Krieg AJ, Hammond EM. Epigenetic Therapy for Solid Tumors: Highlighting the Impact of Tumor Hypoxia. Genes. 2015 Sep 25;6(4):935-56. PubMed PMID: 26426056. Pubmed Central PMCID: 4690023.
72. Greiner D, Bonaldi T, Eskeland R, Roemer E, Imhof A. Identification of a specific inhibitor of the histone methyltransferase SU(VAR)3-9. Nature chemical biology. 2005 08//print;1(3):143-5.
73. Ramachandran S, Ient J, Gottgens EL, Krieg AJ, Hammond EM. Epigenetic Therapy for Solid Tumors: Highlighting the Impact of Tumor Hypoxia. Genes. 2015 Dec;6(4):935-56. PubMed PMID: WOS:000367013300001. English.
74. Huong TTT, Kim HN, Lee IK, Nguyen-Pham TN, Ahn JS, Kim YK, et al. Improved Therapeutic Effect against Leukemia by a Combination of the Histone Methyltransferase Inhibitor Chaetocin and the Histone Deacetylase Inhibitor Trichostatin A. J Korean Med Sci. 2013 Feb;28(2):237-46. PubMed PMID: WOS:000314528000011. English.
75. Umar S. Intestinal stem cells. Current gastroenterology reports. 2010 Oct;12(5):340-8. PubMed PMID: 20683682. Pubmed Central PMCID: 2965634.
76. Moore SR, Guedes MM, Costa TB, Vallance J, Maier EA, Betz KJ, et al. Glutamine and alanyl-glutamine promote crypt expansion and mTOR signaling in murine enteroids. American journal of physiology Gastrointestinal and liver physiology. 2015 May 15;308(10):G831-9. PubMed PMID: 25792564. Pubmed Central PMCID: 4437023.

77. Rhoads JM, Argenzio RA, Chen W, Rippe RA, Westwick JK, Cox AD, et al. L-glutamine stimulates intestinal cell proliferation and activates mitogen-activated protein kinases. The American journal of physiology. 1997 May;272(5 Pt 1):G943-53. PubMed PMID: 9176200.
78. Beumer J, Clevers H. Regulation and plasticity of intestinal stem cells during homeostasis and regeneration. Development. 2016 Oct 15;143(20):3639-49. PubMed PMID: 27802133.
79. Schwitalla S, Fingerle AA, Cammareri P, Nebelsiek T, Goktuna SI, Ziegler PK, et al. Intestinal tumorigenesis initiated by dedifferentiation and acquisition of stem-cell-like properties. Cell. 2013 Jan 17;152(1-2):25-38. PubMed PMID: 23273993.
80. Clevers H. Wnt/beta-catenin signaling in development and disease. Cell. 2006 Nov 3;127(3):469-80. PubMed PMID: 17081971.
81. Fevr T, Robine S, Louvard D, Huelsken J. Wnt/beta-catenin is essential for intestinal homeostasis and maintenance of intestinal stem cells. Molecular and cellular biology. 2007 Nov;27(21):7551-9. PubMed PMID: 17785439. Pubmed Central PMCID: 2169070.
82. Rowan AJ, Lamlum H, Ilyas M, Wheeler J, Straub J, Papadopoulou A, et al. APC mutations in sporadic colorectal tumors: A mutational "hotspot" and interdependence of the "two hits". Proceedings of the National Academy of Sciences of the United States of America. 2000 Mar 28;97(7):3352-7. PubMed PMID: 10737795. Pubmed Central PMCID: 16243.
83. Voloshanenko O, Erdmann G, Dubash TD, Augustin I, Metzig M, Moffa G, et al. Wnt secretion is required to maintain high levels of Wnt activity in colon cancer cells. Nature communications. 2013 10/28/online;4:2610.
84. DeBerardinis RJ, Lum JJ, Hatzivassiliou G, Thompson CB. The biology of cancer: metabolic reprogramming fuels cell growth and proliferation. Cell metabolism. 2008 Jan;7(1):11-20. PubMed PMID: 18177721.
85. Tannock IF, Steele D, Roberts J. Influence of reduced concentration of L-glutamine on growth and viability of cells in monolayer, in spheroids, and in experimental tumours. British journal of cancer. 1986 Nov;54(5):733-41. PubMed PMID: 3801270. Pubmed Central PMCID: 2001537.
86. Le A, Lane AN, Hamaker M, Bose S, Gouw A, Barbi J, et al. Glucose-independent glutamine metabolism via TCA cycling for proliferation and survival in B cells. Cell metabolism. 2012 Jan 4;15(1):110-21. PubMed PMID: 22225880. Pubmed Central PMCID: 3345194.
87. Chin RM, Fu X, Pai MY, Vergnes L, Hwang H, Deng G, et al. The metabolite alpha-ketoglutarate extends lifespan by inhibiting ATP synthase and TOR. Nature. 2014 Jun 19;510(7505):397-401. PubMed PMID: 24828042. Pubmed Central PMCID: 4263271.
88. Carey BW, Finley LW, Cross JR, Allis CD, Thompson CB. Intracellular alpha-ketoglutarate maintains the pluripotency of embryonic stem cells. Nature. 2015 Feb 19;518(7539):413-6. PubMed PMID: 25487152. Pubmed Central PMCID: 4336218.
89. TeSlaa T, Chaikovsky AC, Lipchina I, Escobar SL, Hochedlinger K, Huang J, et al. alpha-Ketoglutarate Accelerates the Initial Differentiation of Primed Human Pluripotent Stem Cells. Cell metabolism. 2016 Sep 13;24(3):485-93. PubMed PMID: 27476976. Pubmed Central PMCID: 5023506.
90. Haggar FA, Boushey RP. Colorectal cancer epidemiology: incidence, mortality, survival, and risk factors. Clinics in colon and rectal surgery. 2009 Nov;22(4):191-7. PubMed PMID: 21037809. Pubmed Central PMCID: 2796096.

91. Siegel RL, Miller KD, Fedewa SA, Ahnen DJ, Meester RGS, Barzi A, et al. Colorectal cancer statistics, 2017. CA: a cancer journal for clinicians. 2017 May 6;67(3):177-93. PubMed PMID: 28248415.
92. Lyou Y, Habowski AN, Chen GT, Waterman ML. Inhibition of nuclear Wnt signalling: challenges of an elusive target for cancer therapy. British journal of pharmacology. 2017 Dec;174(24):4589-99. PubMed PMID: 28752891. Pubmed Central PMCID: 5727325.
93. Novellasdemunt L, Antas P, Li VSW. Targeting Wnt signaling in colorectal cancer. A Review in the Theme: Cell Signaling: Proteins, Pathways and Mechanisms. American Journal of Physiology-Cell Physiology. 2015;309(8):C511-C21. PubMed PMID: 26289750.
94. Kahn M. Can we safely target the WNT pathway? Nature reviews Drug discovery. 2014;13(7):513-32. PubMed PMID: PMC4426976.
95. Ring A, Kim YM, Kahn M. Wnt/catenin signaling in adult stem cell physiology and disease. Stem cell reviews. 2014 Aug;10(4):512-25. PubMed PMID: 24825509. Pubmed Central PMCID: 4294579.
96. Degos L, Wang ZY. All trans retinoic acid in acute promyelocytic leukemia. Oncogene. 2001 Oct 29;20(49):7140-5. PubMed PMID: 11704842.
97. Baudino TA. Targeted Cancer Therapy: The Next Generation of Cancer Treatment. Current drug discovery technologies. 2015;12(1):3-20. PubMed PMID: 26033233.
98. Wang M, Zhao J, Zhang L, Wei F, Lian Y, Wu Y, et al. Role of tumor microenvironment in tumorigenesis. Journal of Cancer. 2017;8(5):761-73. PubMed PMID: 28382138. Pubmed Central PMCID: 5381164.
99. Wellen KE, Thompson CB. Cellular metabolic stress: considering how cells respond to nutrient excess. Molecular cell. 2010;40(2):323-32. PubMed PMID: 20965425. eng.
100. Yue X, Zhao Y, Xu Y, Zheng M, Feng Z, Hu W. Mutant p53 in Cancer: Accumulation, Gain-of-Function, and Therapy. Journal of molecular biology. 2017 Jun 2;429(11):1595-606. PubMed PMID: 28390900. Pubmed Central PMCID: 5663274.
101. DeVita VT, Jr., Chu E. A history of cancer chemotherapy. Cancer research. 2008 Nov 1;68(21):8643-53. PubMed PMID: 18974103.
102. Choi YK, Park KG. Targeting Glutamine Metabolism for Cancer Treatment. Biomolecules & therapeutics. 2018 Jan 1;26(1):19-28. PubMed PMID: 29212303. Pubmed Central PMCID: 5746034.